University
of Ljubljana
Faculty
for Civil and Geodetic Engineering

MARCOS JULIEN ALEXOPOULOS

USE OF THE REANALYSIS PRODUCTS FOR THE HYDROLOGICAL RAINFALL-RUNOFF MODELLING: SLOVENIAN CASE STUDIES

MASTER'S THESIS

MASTER STUDY PROGRAMME FLOOD RISK MANAGEMENT

Univerza *v Ljubljani*

Ljubljana, 2021

University
of Ljubljana
Faculty
for Civil and Geodetic
Engineering

Candidate
MARCOS JULIEN ALEXOPOULOS

USE OF THE REANALYSIS PRODUCTS FOR THE HYDROLOGICAL RAINFALL-RUNOFF MODELLING: SLOVENIAN CASE STUDIES

Master's thesis no .

Mentor:
Assist. Prof. Nejc Bezak, PhD

Co-mentor:
Assoc. Prof. Mojca Šraj, PhD

Commision member:
Prof. Matjaž Mikoš, PhD
Assoc. Prof. Schalk Jan Van Andel, PhD

Chairman of the Commission:
Assoc. Prof. Nataša Atanasova, PhD

Ljubljana, 23 December 2021

Univerza *v Ljubljani*

"This page is intentionally blank"

ERRATA

Error page	Error bar	Instead	Let it be

ACKNOWLEDGEMENTS

I would like to personally thank my main mentor, Assist. Prof. Nejc Bezak, for giving me the opportunity to actively participate in the present study, for the crucial remarks which shaped the outcome of this dissertation, and the continuous support which was evident during the whole period of this thesis.

I am personally thankful to my co-mentor, Assoc. Prof. Mojca Šraj, for sharply pinpointing any errors that occurred during the development of the present study, for her insights on the technical work, as well as the structure of the present thesis, which ensured the final product was kept to high standards.

A special thanks to Patrick Nistahl, for extracting and providing the datasets needed, in order to test and evaluate the main hypotheses of this study.

BIBLIOGRAPHIC-DOCUMENTALISTIC INFORMATION AND ABSTRACT

UDC: **556.512:004.41(043.3)**
Author: **MARCOS JULIEN ALEXOPOULOS**
Supervisor: **Assist. Prof. Nejc Bezak, PhD**
Co-supervisor: **Assoc. Prof. Mojca Šraj, PhD**
Title: **Use of the reanalysis products for the hydrological rainfall-runoff modelling: Slovenian case studies**
Document type: **Master thesis**
Scope and tools: **61 p., 15 tab., 51 fig., 2 ann.**
Keywords: **Reanalysis, Slovenia, ERA5, REA6, Hydrological application**

Abstract:

The need for hydrological modeling in ungauged basins has always been a major challenge. Efforts have been made in recent years to address it via the implementation of ex-situ technologies. An attractive option that is becoming increasingly popular are reanalysis products, which provide modeled data for atmospheric variables, based on observations assimilated from various sources, such as satellites and radar stations.

The present study is focusing on the evaluation of two reanalysis precipitation and temperature datasets, namely ERA5 and COSMO-REA6, over a selection of drainage basins located in Slovenia. The two products are available at the hourly temporal scale, and at the time of writing, their quality has not been evaluated in rainfall-runoff applications over European borders. To measure their efficiency, the GR4H and GR4H Cema Neige lumped conceptual rainfall-runoff models were used. Different reanalysis configurations were tested by using the initial model parameters, calibrated using observed data. In addition, it was investigated whether the parameters ingrained within the model are able to make up for low rainfall and temperature data quality, by recalibrating them on every reanalysis configuration.

Initial model runs proved to be adequate only for a few catchments out of the total selection. However, the recalibration process was effective in increasing hydrological performance, increasing the total number of watersheds that were modeled accurately. The study concluded that the two products are partially in agreement with observations, suggesting their use as a proxy when observed data is scarce.

BIBLIOGRAFSKO – DOKUMENTACIJSKA STRAN IN IZVLEČEK

UDK:	**556.512:004.41(497.4)**
Avtor:	**Marcos Julien Alexopoulos**
Mentor:	**doc. dr. Nejc Bezak**
Somentor:	**izr. prof. dr. Mojca Šraj**
Naslov:	**Uporaba produktov reanaliz za namen hidrološkega modeliranja: izbrani primeri v Sloveniji**
Tip dokumenta:	**magistrsko delo**
Obseg in oprema:	**61 str., 15 pregl., 51 sl., 2 pril.**
Ključne besede:	**Reanalize, Slovenija, ERA5, REA6, hidrološko modeliranje**

Izvleček:

Hidrološko modeliranje nemerjenih porečij je še vedno velik izziv, saj za taka porečja ni na voljo ali podatkov o pretokih ali podatkov o padavanih in temperaturi zraka. V zadnjih letih je bilo na tem področju narejenih veliko raziskav. Ena izmed metod, ki jih lahko uporabimo namesto točkovno merjenih podatkov, so podatki reanaliz, ki združujejo modelske izračune, točkovne meritve ter tudi satelitske in radarske podatke.

Magistrska naloga analizira ustreznost dveh produktov reanaliz z vidika ustreznosti podatkov o padavinah in temperaturi zraka. Izbrana sta dva produkta, in sicer ERA5 in COSMO-REA6, ki sta v nalogi testirana na izbranih porečjih na območju Slovenije. Oba produkta imata na voljo podatke z urnim časovnim korakom in do sedaj z vidika hidrološkega modeliranja površinskega odtoka še nista bila preverjena. Za modeliranje sta uporabljena enovita konceptualna modela GR4H in CemaNeigeGR4H. Testirane so različne konfiguracije modelov (npr. s ponovnim umerjanjem ali brez le-tega).

Ugotovljeno je bilo, da so podatki reanaliz primerni za uporabo samo za nekatera porečja, in sicer v primeru da hidrološki model ni ponovno umerjen na podatke reanaliz, ampak se privzame parametre, določene glede na točkovno izmerjene podatke. Ponovno umerjanje modela pa je izboljšalo rezultate modeliranja. Rezultati so pokazali, da se izbrana produkta reanaliz delno ujemata s točkovno izmerjenimi podatki, kar pomeni da ju lahko upoorabimo kot grobo oceno dejanskega stanja v primeru, da podatkov o padavinah in temperaturi zraka ni na razpolago.

TABLE OF CONTENTS

LIST OF FIGURES

LIST OF TABLES

ABBREVIATIONS

PUB	Predictions in ungauged basins
DWR	Doppler Weather Radar
QPE	Quantitative Precipitation Estimation
GCM	Global Climate Models
CFSR	Climate Forecast System Reanalysis
JRA	Japanese Reanalysis
CMADS	China Meteorological Assimilation Driving Datasets
ECMWF	European Centre for Medium-Range Weather Forecasts
POD	Probability of Detection
VHI	Volumetric Hit Index
FAR	False Alarm Ratio
PBIAS	Percent Bias
BR	Bias Ratio
IOA	Index of Agreement
SWAT	Soil & Water Assessment Tool
KGE	Kling-Gupta Efficiency
NSE	Nash-Sucliffe Efficiency
ARSO	Slovenian Environment Agency
PP	Precipitation Product
TP	Temperature Product
P	Precipitation
T	Temperature
Qs	Simulated discharge
Conf.	Configuration
cc	correlation coefficient
No.	number

mm	millimeter
m^3	cubic meter
s	seconds
km	kilometer
km^2	square kilometer

1 INTRODUCTION

Information extracted from rainfall-runoff models provides key insights for water resources management. Accurate prediction of catchment behavior can be beneficial in the context of urban planning, flood mitigation or security of water supply. For gauged basins, modeling catchment response is a relatively easy task, given that an adequate number of historical records is available for model calibration and evaluation. In many cases however, stream flow simulations need to be performed in sites where gauged discharge data availability is scarce or completely absent.

For such studies, different approaches have been developed to deal with complications and uncertainty, which are classified as predictions in ungauged basins (PUB) (Sivapalan *et al.*, 2003; Hrachowitz *et al.*, 2013). In cases where discharge observations are absent, model parameter estimation without calibration is usually achieved by regionalization, a method of extrapolation of response information from gauged to ungauged catchments (James, 1972; Magette, Shanholtz and Carr, 1976; Gottschalk *et al.*, 1979; Skop, 1996; Merz, Blöschl and Parajka, 2006). This is typically performed by transforming parameters from gauged basins (commonly referred to as donor basins) and applying them to the basin of interest. Selection of donor basins can be based on spatial proximity (Egbuniwe and Todd, 1976; Nathan and McMahon, 1990; Vandewiele, Xu and Huybrechts, 1991; Yu and Yang, 2000), physical similarity (Burn and Boorman, 1993; Sefton and Howarth, 1998; Merz and Blöschl, 2003; McIntyre *et al.*, 2005; Oudin *et al.*, 2010), or the most popular regression methods (Magette, Shanholtz and Carr, 1976; Kokkonen *et al.*, 2003; Young, 2006; Yang *et al.*, 2018). Research conducted during the PUB decade (2003-2013) concluded that no approach performs universally better: results depend heavily on model selection and study area characteristics (Parajka, Merz and Blöschl, 2005; Oudin *et al.*, 2008; Reichl *et al.*, 2009; He, Bárdossy and Zehe, 2011; Samuel, Coulibaly and Metcalfe, 2011; Bao *et al.*, 2012; Razavi and Coulibaly, 2013; Salinas *et al.*, 2013; Viglione *et al.*, 2013), which appears to be in agreement with more recent findings (Arsenault *et al.*, 2019; Yang, Magnusson and Xu, 2019).

In catchments where model calibration is possible but data is scarce for atmospheric variables (e.g., precipitation), remote sensing information such as satellite and Doppler Weather Radar (DWR) products can be used for simulating catchment response. The potential of DWR use has been investigated in various hydrological contexts, including pattern and frequency analysis for rainfall events (Ruiz-Villanueva *et al.*, 2012; Goudenhoofdt, Delobbe and Willems, 2017), urban simulations (Tilford, Fox and Collier, 2002; Smith *et al.*, 2007; Josephine, Mudgal and Thampi, 2014; Wang *et al.*, 2015; Cecinati *et al.*, 2017; Thorndahl *et al.*, 2017; Barszcz, 2019; Grimley, Quintero and Krajewski, 2020), operational forecasts (Berenguer *et al.*, 2005; Germann *et al.*, 2006; Heuvelink *et al.*, 2020) and derivation of Intensity-Duration-Frequency curves (Marra and Morin, 2015; Marra *et al.*, 2017). Research indicates that although corrected radar observations tend to underestimate Quantitative Precipitation Estimation (QPE) (Josephine, Mudgal and Thampi, 2014; Gao *et al.*, 2016), results are reliable and their quality is superior to that derived from other remote sensing methods, e.g., satellite observations (Amitai *et al.*, 2012; Tapiador *et al.*, 2012; Chen *et al.*, 2013; Gilewski and Nawalany, 2018).

However, because of its significant areal coverage, satellite precipitation has been tested for rainfall-runoff applications. Although temporal resolution can be high (e.g., hourly timestep) (Kubota *et al.*, 2020), most satellite rainfall products tend to overestimate low rates, underestimate extreme events (Islam and Cartwright, 2020; Runo *et al.*, 2020; Wang *et al.*, 2020) and mean observations (Ghaju and Alfredsen, 2016), and consequently, peak flows (Pakoksung and Takagi, 2016). Calculations performed at the sub-daily timestep can have relatively poor performance but tend to improve with further aggregation onto daily/monthly scales (Runo *et al.*, 2020), providing more reliable results when reproducing stream flow dynamics at these intervals (Tramblay *et al.*, 2016; Wang *et al.*, 2020). The kilometer-range spatial resolution in these products (Hou *et al.*, 2008; Kubota *et al.*, 2020) can sometimes lead to sub-optimal performance: some studies suggest that its application is limited when applied over smaller drainage areas (less than 100,000 km^2) (Zubieta *et al.*, 2015), and areas characterized by high elevation that accounts for orographic and shadow hill effects (Novella and Thiaw, 2009; Ghaju and Alfredsen, 2016; Tramblay *et al.*, 2016). This is especially true when the dataset is calibrated at the global or regional scale (Dinku *et al.*, 2007). In such cases they can be used as a proxy, e.g., for filling missing values in observed time-series (Oyerinde, Fademi and Denton, 2017).

Another option that has been increasingly evaluated in recent years is the use of reanalysis products, gridded datasets, and more rarely, general circulation models (GCM). GCMs operate at coarse horizontal resolutions due to the inevitable computational costs associated when attempts are made to perform simulations at excessively refined grids. This coarse resolution and its inherent biases hardly qualify GCMs as a candidate to study water balance dynamics at the watershed scale. To do so, it would require the recruitment of downscaling methods, which can be classified into two main categories: means of statistical downscaling techniques i.e., the establishment of statistical relationships between physical variables at the local scale (e.g., temperature) and large-scale predictors (e.g., pressure field) and applying them at the areas of interest. Their application can be limited since they often violate core physical principles (Maraun and Widmann, 2018). Another means consists of a dynamical approach, where Regional Climate Models (RCM) are nested within the GCM domain. The GCM acts as the parental model that defines the boundary conditions and the initial state for the variables to be refined. Biases still remain present once simulations are scaled down (Yang *et al.*, 2013; Seguinot *et al.*, 2014), which are usually removed by the implementation of bias-correction methods (Maraun *et al.*, 2010; Berg, Feldmann and Panitz, 2012; Lafon *et al.*, 2013; Fang *et al.*, 2015; Teng *et al.*, 2015; Velasquez, Messmer and Raible, 2020). Depending on the choice of the correction algorithm (especially if the temporal resolution is high) (Shrestha, Acharya and Shrestha, 2017), flow simulations show significant improvement for mean flows; however, for flood extremes, their use is discouraged since correction factors tend to smoothen out precipitation events at the far end of the cumulative distribution function (Willkofer *et al.*, 2018).

Gridded observational products provide grid-box averages for meteorological variables, derived from instrumental observations that undergo assimiliation schemes, and are spatially and temporally interpolated from gauge stations (Xie *et al.*, 2007; Haylock *et al.*, 2008;

Yasutomi, Hamada and Yatagai, 2011; Becker *et al.*, 2013; Isotta *et al.*, 2014) or satellite measurements (Huffman *et al.*, 2007, 2010; Novella and Thiaw, 2013; Ashouri *et al.*, 2015; Maidment *et al.*, 2017; Xie *et al.*, 2017; Ciabatta *et al.*, 2018). For hydrological studies at the catchment scale, research is mostly focused on the evaluation of precipitation datasets. Depending on study area and product choice, it is argued that gridded data can be a viable alternative to observed data (Jeffrey *et al.*, 2001; Vaze *et al.*, 2011; Essou, Brissette and Lucas-Picher, 2017; Ledesma and Futter, 2017). Performance differs significantly depending on the selected temporal scale; satellite-based precipitation provides reliable results only when adjusted at the sub-daily scale, compared to station-based (Satgé *et al.*, 2020). Gridded datasets do not match the quality of observations in densely-gauged areas (Vu, Raghavan and Liong, 2012). However, the quality of gridded records is non-linearly proportional to the number of active stations that contribute to it (Haylock *et al.*, 2008), thus making them more valuable when applied in regions that may not be ideally gauged, but data is neither too scarce. This makes their applicability less feasible in areas characterized by steep elevation gradients, where station density is usually low or completely absent.

A sub-category of gridded products that has been increasingly popular in environmental science (Essou *et al.*, 2016; Giuseppe *et al.*, 2016; Beck *et al.*, 2017; Emerton *et al.*, 2017; Ruffault *et al.*, 2017; Chen, Brissette and Chen, 2018) are reanalysis products (Onogi *et al.*, 2007; Saha *et al.*, 2010, 2014; Dee *et al.*, 2011; Rienecker *et al.*, 2011; Kobayashi *et al.*, 2015; Gelaro *et al.*, 2017; Hersbach *et al.*, 2020), which are based on meteorological models that combine surface observations, but mostly remote sensing data. That is, remote sensing observations are assimilated in the dynamic model to guide the simulation of the reanalysis data. This gives the advantage of producing information at multiple vertical atmospheric levels (Marques *et al.*, 2009; Ruane, Goldberg and Chryssanthacopoulos, 2015; Vousdoukas *et al.*, 2016; Muñoz-Sabater *et al.*, 2021), in addition to providing coverage regardless of the status of the surface observational network.

Several attempts have been made in research to make intercomparisons between different reanalysis products in order to identify the most suitable dataset for a particular region. Lauri, Räsänen and Kummu (2014) made an evaluation of bias-corrected ERA-Interim and Climate Forecast System Reanalysis (CFSR) precipitation and temperature in the Mekong basin in southeast Asia, for the period 1999-2005. The spatial pattern of Era-Interim temperature has greater resemblance to observations compared to CFSR. However, the difference between daily maximum and minimum temperature proves to be more realistic for CFSR. Both datasets compare well to the baseline, deeming them suitable for modeling purposes. Annual average precipitation is similar for all datasets, however CFSR tends to overestimate rainfall at the lower-middle part of the study area.

Islam and Cartwright (2020) evaluated the performance of the European Centre for Medium-Range Weather Forecasts (ECMWF) Reanalysis V5 (ERA5) and CFSR precipitation products in Bangladesh over a 5-year time period, with the resolution aggregated at the daily scale. CFSR tends to overestimate rainfall patterns across 90% of the domain. ERA5 tends to overestimate rainfall for over 50% of the area while still performing reasonably well. However, above the

50^{th} or the 75^{th} percentile of rainfall records, it shows a 49% and 85% underestimation, respectively, in contrast with CFSR. The study evaluated also the ability of the products to detect rainfall. Using the Probability of Detection (POD) and Volumetric Hit Index (VHI) metrics, both datasets display superior performance in detecting the occurrence of rainfall, with CFSR outperforming ERA5 for higher rainfall values. The number of false alarms was also evaluated using the False Alarm Ratio (FAR), where CFSR displays the poorest performance, especially for higher rainfall thresholds. Jiang *et al.* (2021) evaluated the performance of ERA5 precipitation for a 12-year period over Chinese mainland. The results confirm its optimal rainfall detection capacity and its tendency to overestimate overall precipitation while underestimating heavy rainfall events, which is consistent with other recent findings (Hénin *et al.*, 2018; Beck *et al.*, 2019; Mahto and Mishra, 2019; Sharifi, Eitzinger and Dorigo, 2019; Xu *et al.*, 2019; Amjad *et al.*, 2020; Nogueira, 2020). At a smaller scale, Khan *et al.* (2020) assessed the application of the Japanese Reanalysis (JRA-55) and ERA-Interim precipitation for the Pindiali, Dande and Sarobi dams, located in the Khyber-Pakhtunkhwa province of Pakistan. When monthly averaged, both products show great rainfall overestimation for the period 1979-2010, during both wet and dry seasons.

The potential of reanalysis precipitation has also been investigated in rainfall-runoff applications. Wang *et al.* (2020) tested the efficiency of the China Meteorological Assimilation Driving Datasets (CMADS) and CFSR in the Xihe river basin in China. Regarding precipitation performance at the watershed scale, CMADS tends to underestimate mean precipitation compared to observations, especially during wet season. CFSR shows great overestimation, with annual rainfall approximations off by roughly 80%. In rainfall detection, CMADS displays adequate ablity to capture rainfall events in addition to acceptable FAR scores. According to the POD metric, CFSR performs rather poorly when capturing rainfall, contradicting Islam and Cartwright (2020). The aforementioned products were used as an input in the Soil & Water Assessment Tool (SWAT). Simulations were performed at the monthly scale from 01/2009 till 12/2015. The use of the CFSR dataset proved to be inadequate and was discarded as an option, while CMADS led to severe runoff underestimation. Hafizi and Sorman (2021) evaluated the performance of ERA5 precipitation in the Karasu basin in eastern Turkey, over the period 2014-2019 at a daily timestep. Overall, the product shows high detectability for low and moderate precipitation, regardless of seasonality. In terms of streamflow reproducibility, performance was measured using the Kling-Gupta (KGE) and Nash-Sutcliffe (NSE) efficiency metrics. The simulation performs weakly when the model parameters are calibrated using observed data. When calibrated individually, flow reproducibility is high for both calibration and validation periods. Not much has been investigated for snowmelt-driven runoff, however Bhattacharya, Khare and Arora (2019) suggest that reanalysis datasets can outperform observations at the monthly scale.

As of December 2021, for reanalysis datasets, research has been mostly focused on intercomparisons between variables derived from different products at coarse spatial and temporal scales. Fewer publications have focused on the validity of these variables when used as an input in rainfall-runoff applications. In publications that do, most reanalyses undergo some bias-correction adjustment before any further use. At the time of writing, according to the author's best knowledge, no rainfall-runoff validation has been made on European watersheds for datasets that have not been post-processed. In addition, a multi-catchment analysis has yet to be conducted, where correlations can be made between reanalysis performance on streamflow simulation and different watershed characteristics.

The aforementioned facts lead to the following research questions:

- How close are reanalyses to weather station observations in a country within Europe?
- How do unprocessed reanalyses perform in hydrological applications?
- Are reanalyses a valuable product for rainfall-runoff applications in a country within Europe?
- Is reanalysis performance varying depending on discharge regimes and watershed characteristics?
- Is reanalysis performance varying across the country's spatial domain?

Therefore, the objective of this study is evaluate the potential of the ERA5 (Hersbach *et al.*, 2020) and COSMO-REA6 (Bollmeyer and Keller, 2015) reanalyses across multiple water basins in Slovenia at the hourly time-step. Initially, a comparison of reanalysis precipitation and temperature will be conducted against station observations using various performance metrics. The rainfall detection skill of these products will also be investigated. Furthermore, an evaluation of discharge simulations will be performed and possible deductions will be made according to watershed characteristics. An additional effort will be made to inspect how the performance of the modeled atmospheric variables can provide insight on their streamflow simulation results before used as an input in the rainfall-runoff model.

2 MATERIALS AND METHODS

2.1 Study area and gauged data

Twenty Slovenian catchments were initially selected for the present case study, representing the five different discharge regimes defined by Frantar, Dolinar and Kurnik (2008). **Table 1** illustrates watershed selection and characteristics.

Table 1: Catchment characteristics

Catchment-Station	Catchment area (km^2)	Catchment median elevation (m)	Water regime
Mislinja-Otiški vrh	230.9	950.4	Alpine pluvial-nival
Dravinja-Zreče	41.4	972.5	Pannonian pluvial-nival
Pesnica-Zamušani	477.8	474.7	Pannonian pluvial-nival
Radovna-Podhom	166.8	1556.7	Alpine nival-pluvial
Kokra-Kokra	112.2	1561.5	Alpine pluvial-nival
Poljanska Sora -Zminec	305.5	945.9	Alpine pluvial-nival
Selška Sora-Železniki	104.1	1065.1	Alpine pluvial-nival
Mirna-Jelovec	270.0	530.2	Pannonian pluvial-nival
Kolpa-Petrina	460.0	863.8	Alpine pluvial-nival
Lahinja-Gradac	221.3	593.5	Dinaric pluvial-nival
Cerkniščica-Cerknica	47.3	819.5	Dinaric pluvial-nival
Savinja-Nazarje	457.3	1344.9	Alpine pluvial-nival
Bolska-Dvas	175.1	876.5	Dinaric pluvial-nival
Voglanja-Crnolica	53.7	470.1	Pannonian pluvial-nival
Hudinja-SVas	156.5	875.5	Alpine pluvial-nival
Soča-Kobarid	437.0	1526.9	Alpine nivial-pluvial
Idrijca-Hotešk	442.8	831.6	Dinaric pluvial-nival
Bača-Bača pri Modreju	142.3	1069.8	Alpine pluvial-nival
Reka-CMlin	377.9	801.4	Mediterranean pluvial
Rižana-Kubed	204.5	554.8	Mediterranean pluvial

Alpine nival-pluvial regimes occur in catchments whose greater part reach into high mountains, where snow melt effects are especially pronounced in May/June, while Alpine pluvial-nivial regimes describe water behavior for catchments located in the medium height of Alpine mountains. Lahinja, Cerkniščica, Bolska and Idrijca rivers comprise the Dinaric area and follow a Dinaric pluvial-nival regime, where discharge peaks occur during spring and autumn. The rivers flowing through the hills of the Pannonian area are described by early summer and late autumn peaks which are strongly equalised, exhibiting low rates mainly during the summer. Cathments located in the south-western part of Slovenia show a Mediterranean pluvial regime with main peaks occurring during the months of November and December, with the lowest water movement observed in August. For each watershed, hourly discharge measurements were obtained for the period 2000-2020, along with observations derived from two networks, in total consisting of 196 rainfall and 201 temperature stations, provided by the Slovenian Environment Agency (ARSO). Both rainfall and temperature networks are presented in **Table 2**.

Table 2: Available precipitation stations (network 1) and their respective missing measurements

Precipitation station network 1		
Station No.	Total NA values	Total NA values - percentage %
3	37221	20
8	809	0
20	133664	72
21	134792	73
22	123704	67
29	184104	100
30	143312	77
38	123032	66
40	138032	74
48	81390	44
51	34615	18
52	146072	79
53	184104	100
61	139040	75
65	138032	74
68	131624	71
75	132128	71
92	136352	74
96	62387	33
97	34614	18
107	141344	76
121	147416	80
133	143360	77
136	34632	18
142	143360	77
147	123704	67
152	141344	76
158	139880	75
164	140504	76
174	137648	74
176	142016	77
185	131624	71
189	139880	75
192	1372	0
197	139880	75
205	132128	71
206	60104	32
210	144224	78
221	184104	100
241	51179	27
249	34614	18
251	141344	76
257	34643	18
268	70856	38
272	127640	69

275	132128	71
276	138032	74
278	132128	71
280	142616	77
285	144224	78
287	81224	44
289	144776	78
296	129248	70
301	144224	78
310	43054	23
311	34640	18
321	835	0
336	37222	20
339	125744	68
343	184104	100
348	141344	76
355	801	0
357	144776	78
360	63576	34
399	3028	1
403	37097	20
408	35023	19
432	140504	76
436	146432	79
437	145928	79
452	34614	18
461	37206	20
464	1343	0
473	34958	18
474	34889	18
482	132512	71
495	35280	19
498	34832	18
510	139040	75
551	19014	10
552	55160	29
553	34658	18
554	46695	25
555	3532	1
559	146648	79
571	144800	78
580	144248	78
581	40923	22
606	34715	18
622	78170	42
623	44240	24
641	34847	18
653	125744	68

654	136352	74
655	143288	77
656	123704	67
657	184104	100
660	184104	100
661	65768	35
688	184104	100
706	184104	100
708	184104	100
710	142856	77
719	53888	29
721	34877	18
722	140448	76
725	76897	41
726	82760	44
730	78151	42
731	141164	76
733	91544	49
734	34912	18
735	34965	18
736	35239	19
737	37061	20
742	184104	100
749	40895	22
750	41512	22
753	184104	100
755	184104	100
756	184104	100
757	63305	34
758	184104	100
759	184104	100
770	184104	100
771	56312	30
772	95864	52
776	60608	32
789	77865	42
790	64352	34
812	139880	75
813	139040	75
814	144776	78
815	144536	78
816	136352	74
817	146432	79
818	136352	74
819	144752	78
820	140504	76
821	133664	72
822	144512	78

823	143360	77
824	143360	77
825	144728	78
826	144224	78
827	144728	78
828	137576	74
829	140504	76
830	144536	78
831	134144	72
832	123704	67
834	124136	67
835	158336	86
836	148424	80
861	148256	80

Table 3: Available precipitation stations (network 2) and their respective missing measurements

Precipitation station network 2		
Station No.	Total NA values	Total NA values - percentage %
2	160215	87
8	183193	99
18	184103	99
21	168721	91
22	184098	99
27	161237	87
35	160548	87
45	181002	98
47	182433	99
51	164549	89
52	165732	90
53	163113	88
55	184103	99
57	184101	99
58	180522	98
61	165024	89
68	156292	84
76	161120	87
81	158709	86
83	161210	87
84	173161	94
86	160423	87
88	183703	99
96	182928	99
97	164332	89
107	168592	91
129	180040	97
136	162567	88

144	163076	88
161	166279	90
162	162929	88
174	161455	87
186	172548	93
192	163144	88
205	170908	92
249	166054	90
257	164163	89
264	181657	98
268	166841	90
279	162158	88
301	169825	92
310	174193	94
311	168158	91
321	165672	89
331	167760	91
336	182814	99
339	168358	91
348	178328	96
355	169507	92
358	172293	93
403	166443	90
437	162814	88
452	171674	93
461	182989	99
464	168637	91
482	163022	88
498	182885	99
554	183219	99
571	169694	92
576	184063	99
580	182390	99
606	183204	99
607	184092	99
622	183268	99
623	183406	99
624	181378	98
721	183402	99
747	168350	91
781	172630	93
785	176382	95
786	176755	96
833	181770	98
853	182278	99

Table 4: Available temperature stations (network 1) and their respective missing measurements

Temperature station network 1		
Station No.	Total NA values	Total NA values - percentage %
3	13773	7
8	75	0
21	135254	73
22	123250	66
29	184104	100
38	123188	66
40	138092	75
48	3072	1
51	2620	1
52	146283	79
61	139514	75
65	141878	77
75	136912	74
92	136689	74
96	114902	62
97	1164	0
107	141366	76
121	147427	80
133	184104	100
136	1577	0
142	143803	78
147	123144	66
158	140475	76
164	140705	76
174	137732	74
176	142209	77
185	131840	71
189	139892	75
192	889	0
197	139896	75
205	132187	71
206	130266	70
210	144880	78
241	55134	29
249	1693	0
257	21097	11
268	71051	38
272	127547	69
275	132720	72
276	138465	75
280	142741	77
285	144332	78
287	81514	44
289	144793	78
296	137338	74

301	144353	78
310	10243	5
311	15063	8
321	506	0
336	11934	6
348	141414	76
355	519	0
360	49183	26
403	37696	20
408	143326	77
432	144923	78
436	146680	79
437	146137	79
441	178657	97
452	5793	3
461	6235	3
464	19	0
482	132597	72
498	4943	2
510	139084	75
551	13071	7
552	6217	3
553	6566	3
554	20984	11
555	15798	8
559	146664	79
580	144262	78
581	45296	24
606	3063	1
622	54692	29
623	44872	24
641	8287	4
653	125816	68
654	136371	74
655	143560	77
656	123198	66
657	114372	62
659	14024	7
661	18540	10
719	184104	100
721	184104	100
722	184104	100
723	184104	100
724	184104	100
729	184104	100
731	184104	100
732	184104	100
733	184104	100

734	114474	62
735	114702	62
736	114180	62
737	114449	62
742	114171	62
743	12531	6
745	183721	99
749	42106	22
750	43133	23
770	55137	29
771	57219	31
772	61828	33
776	64742	35
812	139897	75
813	139335	75
814	149949	81
815	145900	79
816	136496	74
817	148147	80
818	136574	74
819	145280	78
820	140516	76
823	143540	77
824	143528	77
825	145058	78
826	146872	79
827	144945	78
828	137637	74
829	140603	76
830	145125	78
831	135208	73
832	123329	66
836	148592	80
861	148259	80

Table 5: Available temperature stations (network 2) and their respective missing measurements

Temperature station network 2		
Station No.	Total NA values	Total NA values - percentage %
6	68420	37
8	175322	95
45	172412	93
48	173975	94
51	175326	95
65	48038	26
92	57288	31
96	181779	98

97	175321	95
102	75594	41
107	120187	65
120	36219	19
129	170855	92
136	175322	95
143	24478	13
147	68346	37
162	22423	12
189	74409	40
192	161833	87
199	36676	19
219	24278	13
245	24236	13
249	175321	95
253	84334	45
257	181034	98
268	170203	92
280	55361	30
285	48229	26
296	182141	98
310	175321	95
317	25231	13
321	175321	95
331	142413	77
346	23335	12
349	182429	99
355	175321	95
432	167639	91
437	22593	12
452	175321	95
464	175321	95
482	147005	79
498	175625	95
524	180745	98
553	183289	99
554	175783	95
559	140278	76
581	153821	83
606	175472	95
622	175408	95
623	137326	74
625	181563	98
626	181588	98
653	69975	38
654	59530	32
655	46747	25
656	66385	36

668	170054	92
669	176741	96
748	175734	95
779	174725	94
786	156855	85
811	173964	94
836	151987	82

A spatial proximity analysis was conducted to identify the weather stations from each network, within a 15-km radius of each catchment. The results of the analysis are depicted in **Table 6**. A spatial representation of the rainfall, temperature and discharge network is illustrated in **Figure 1.**

Table 6: Precipitation stations (network 1) located within a 15-km radius of each watershed's centroid

Catchment-Station	Precipitation network 1 Available Stations at 15 km proximity
Mislinja-Otiški vrh	733, 287, 321, 461, 275, 285, 289, 296, 710, 825
Dravinja-Zreče	757, 461, 301, 825
Pesnica-Zamušani	726, 555, 310, 311, 336, 554, 339, 653, 836, 861
Radovna-Podhom	48, 403, 553, 21, 22, 38, 40, 437, 482, 817, 830
Kokra-Kokra	3, 8, 30, 280, 510, 656, 815, 820
Poljanska Sora - Zminec	719, 721, 722, 789, 750, 20, 21, 22, 75, 147, 185, 189, 197, 559, 656, 812, 817, 819, 832, 835
Selška Sora-Železniki	789, 553, 750, 20, 21, 22, 75, 185, 482, 812, 817, 819
Mirna-Jelovec	661, 241, 249, 452, 205, 206, 210, 654
Kolpa-Petrina	498, 164, 174, 176, 821, 827
Lahinja-Gradac	257, 251, 432
Cerkniščica-Cerknica	725, 152, 158, 813, 831
Savinja-Nazarje	730, 3, 272, 275, 276, 278, 280, 285, 289, 510, 710, 815, 820, 829
Bolska-Dvas	730, 735, 736, 661, 268, 206, 210, 272, 275, 276, 278, 296, 710, 829
Voglanja-Crnolica	757, 452, 622, 641, 301, 822
Hudinja-SVas	735, 736, 757, 268, 321, 461, 296, 301, 825
Soča-Kobarid	48, 51, 553, 606, 40, 52, 61, 65, 68, 436, 437, 823, 828, 830
Idrijca-Hotešk	552, 722, 789, 772, 750, 20, 21, 22, 68, 75, 142, 147, 437, 482, 559, 812, 816, 817, 819, 828, 832, 835
Bača-Bača pri Modreju	789, 553, 21, 22, 65, 68, 75, 437, 482, 812, 817, 819, 828
Reka-CMlin	581, 136, 623, 133, 142, 655, 824, 827, 831
Rižana-Kubed	551, 581, 623, 121, 655, 824

Table 7: Precipitation stations (network 2) located within a 15-km radius of each watershed's centroid

Catchment-Station	Precipitation network 2 Available Stations at 15 km proximity
Mislinja-Otiški vrh	321, 747

Dravinja-Zreče	301, 747
Pesnica-Zamušani	310, 311, 331, 336, 339, 786
Radovna-Podhom	21, 22, 35, 45, 55, 403, 437, 482, 46, 47, 576
Kokra-Kokra	2, 27, 279
Poljanska Sora -Zminec	18, 21, 22, 76, 144, 186, 81
Selška Sora-Železniki	18, 21, 22, 45, 186, 482
Mirna-Jelovec	205, 249, 452, 206
Kolpa-Petrina	162, 174
Lahinja-Gradac	257
Cerkniščica-Cerknica	162, 161
Savinja-Nazarje	2, 27, 279
Bolska-Dvas	206
Voglanja-Crnolica	301, 452
Hudinja-SVas	268, 301, 321, 747
Soča-Kobarid	45, 51, 53, 55, 65, 68, 437, 46, 47, 52, 57, 61, 576, 607, 624
Idrijca-Hotešk	18, 21, 22, 45, 68, 76, 84, 144, 437, 482, 81, 83
Bača-Bača pri Modreju	18, 21, 22, 45, 65, 68, 76, 84, 437, 482, 46, 47
Reka-CMlin	129, 136, 161
Rižana-Kubed	129

Table 8: Temperature stations (network 1) located within a 15-km radius of each watershed's centroid

Catchment-Station	Temperature network 1 Available Stations at 15 km proximity
Mislinja-Otiški vrh	801, 805, 807, 287, 321, 461, 275, 285, 289, 296, 825
Dravinja-Zreče	757, 805, 461, 301, 825
Pesnica-Zamušani	343, 688, 726, 804, 805, 555, 742, 310, 311, 336, 554, 653, 836, 861
Radovna-Podhom	756, 791, 803, 48, 403, 553, 21, 22, 38, 40, 437, 482, 817, 830
Kokra-Kokra	3, 8, 280, 510, 656, 815, 820
Poljanska Sora -Zminec	789, 750, 21, 22, 75, 147, 185, 189, 197, 559, 656, 812, 817, 819, 832
Selška Sora-Železniki	756, 789, 803, 553, 750, 21, 22, 75, 185, 482, 812, 817, 819
Mirna-Jelovec	221, 660, 659, 661, 743, 241, 249, 452, 205, 206, 210, 654
Kolpa-Petrina	498, 164, 174, 176, 827
Lahinja-Gradac	257, 432
Cerkniščica-Cerknica	725, 158, 813, 831
Savinja-Nazarje	801, 3, 272, 275, 276, 280, 285, 289, 510, 815, 820, 829
Bolska-Dvas	660, 735, 736, 801, 659, 661, 743, 268, 206, 210, 272, 275, 276, 296, 829
Voglanja-Crnolica	757, 758, 797, 452, 641, 301, 622
Hudinja-SVas	221, 735, 736, 757, 797, 657, 268, 321, 461, 296, 301, 825
Soča-Kobarid	53, 759, 796, 803, 48, 51, 553, 606, 40, 52, 61, 65, 436, 437, 823, 828, 830
Idrijca-Hotešk	552, 789, 803, 772, 750, 21, 22, 75142, 147, 437, 482, 559, 812, 816, 817, 819, 828, 832
Bača-Bača pri Modreju	789, 803, 553, 21, 22, 65, 75, 437, 482, 812, 817, 819, 828
Reka-CMlin	755, 581, 136, 623, 142, 655, 824, 827, 831
Rižana-Kubed	551, 755, 581, 623, 121, 655, 824

Table 9: Temperature stations (network 2) located within a 15-km radius of each watershed's centroid

Catchment-Station	Temperature network 2 Available Stations at 15 km proximity
Mislinja-Otiški vrh	321, 285, 317
Dravinja-Zreče	301
Pesnica-Zamušani	309, 310, 311, 331, 334, 786, 346, 653
Radovna-Podhom	38, 48, 403, 437, 482
Kokra-Kokra	3, 8, 26, 6, 280, 656
Poljanska Sora -Zminec	76, 189, 147, 559, 656
Selška Sora-Železniki	482
Mirna-Jelovec	205, 241, 249, 452, 206, 654
Kolpa-Petrina	174, 162, 164
Lahinja-Gradac	257, 432, 253
Cerkniščica-Cerknica	158, 162
Savinja-Nazarje	3, 6, 219, 280, 285
Bolska-Dvas	268, 206, 219
Voglanja-Crnolica	301, 452
Hudinja-SVas	268, 301, 321
Soča-Kobarid	48, 51, 437, 65
Idrijca-Hotešk	76, 102, 437, 143, 147, 482, 559
Bača-Bača pri Modreju	76, 437, 65, 482
Reka-CMlin	136, 143, 655
Rižana-Kubed	120, 655

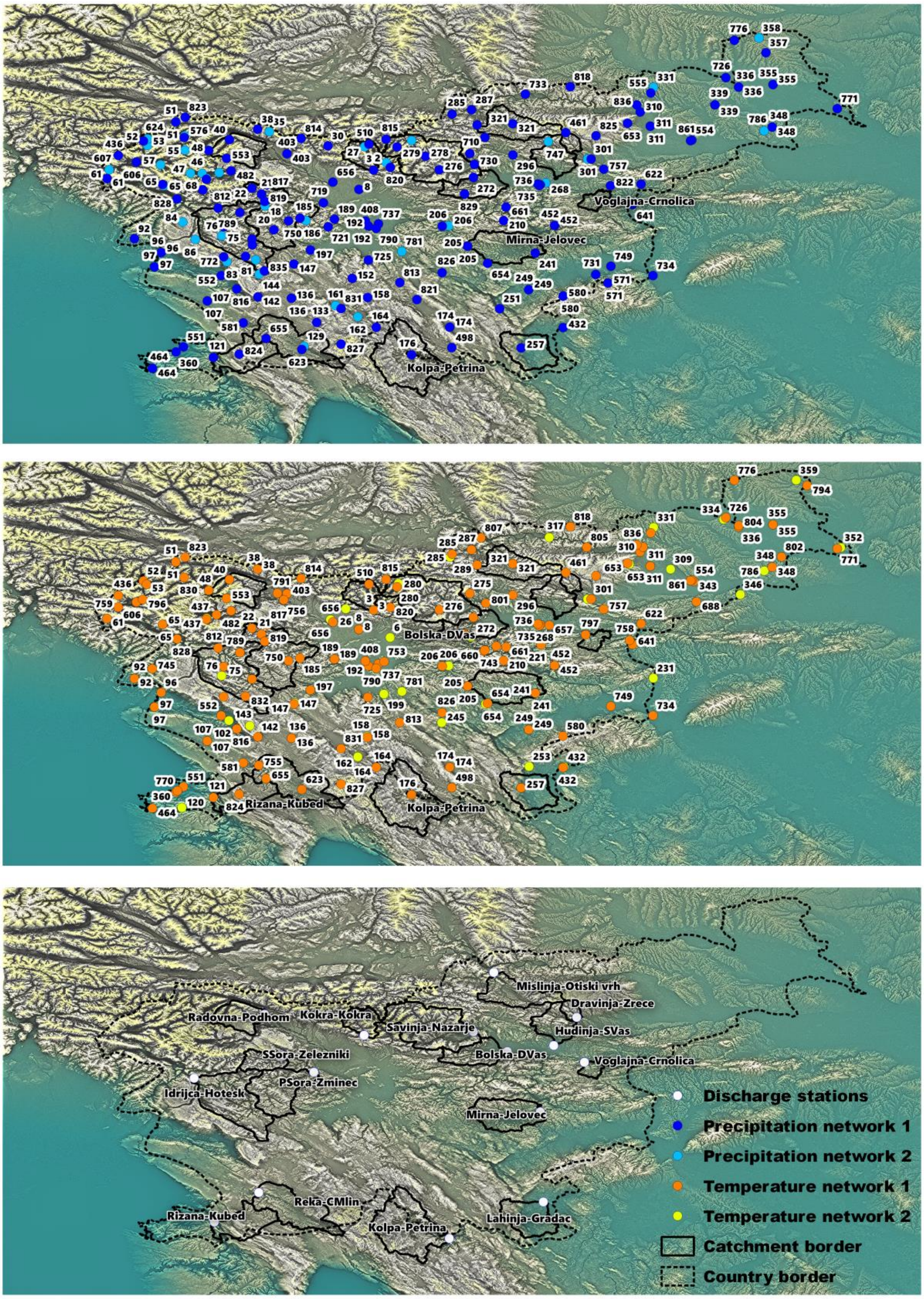

Data: Slovenian Environment Agency, Ministry of the Environment and Spatial Planning, 2020
NASA Shuttle Radar Topography Mission, Distributed by OpenTopography, 2013

Figure 1: Selected watersheds and total precipitation, temperature and discharge station network, based on the spatial proximity analysis

To set up observational time-series for precipitation and temperature, one representative station was selected per catchment. The selection of each representative station was derived based on its proximity to the respective catchments's centroid and its percentage of missing values. Once selected, a correlation analysis between representative stations, and stations within the 15-km radius was conducted. Stations with a correlation coefficient below 0.6 were screened out. Remaining stations were classified in a descending order based on the previously-calculated correlation coefficient. To account for missing values in each representative station, values were borrowed by the station with the highest correlation, and if missing, by the station with the second-best correlation etc. An example for the Selška Sora watershed is displayed in **Table 10**.

Table 10: Selška Sora precipitation and temperature stations, along with their Pearson correlation coefficient

Selška Sora precipitation and temperature stations			
Precipitation station	Correlation coefficient	Temperature station	Correlation coefficient
750	-	750	-
21	0.77	656	0.97
789	0.73	147	0.96

The borrowed values were transformed following a linear regression scheme between the two stations. Due to limited data availability in various areas, missing values remained after this process for both variables, which narrowed the period of available data for each watershed. In addition, the time periods for which discharge data was not available were also ruled out. A schematic illustration is displayed in **Figure 2**.

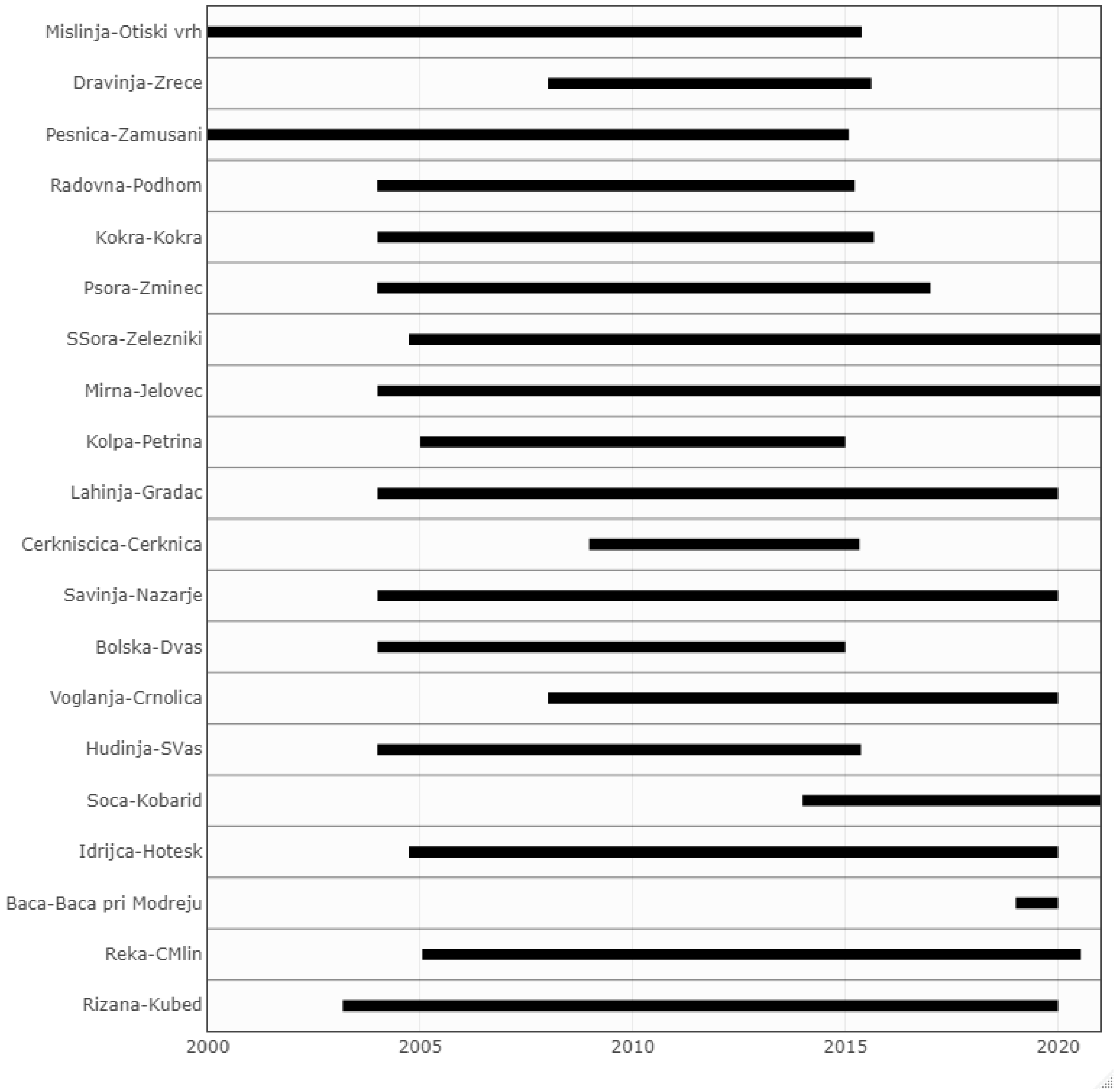

Figure 2: Precipitation, temperature and discharge data availability, by catchment

For consistent results, the simulation period was narrowed down to seven years (2008-01-01 00:00:00 – 2014-12-31 23:00:00). The Bača and Soča rivers were exluded because of data scarcity. The Cerkniščica and Pesnica rivers were also ruled out because of inconsistencies between precipitation and discharge measurements. The selected stations misrepresented rainfall intensity, challenging the hydrological modeling process. The respective precipitation and temperature stations used for each catchment is displayed in **Figure 3**.

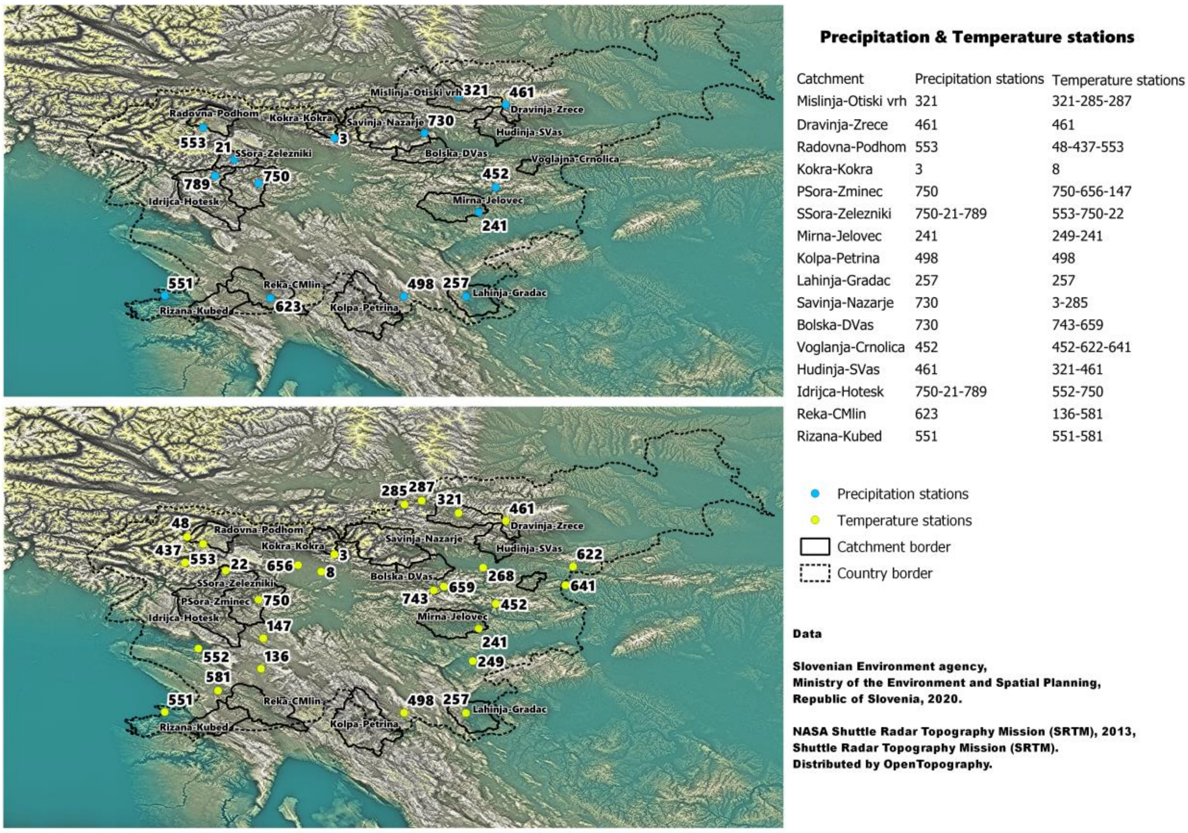

Figure 3: Corresponding precipitation and temperature stations used for each watershed

2.2 Reanalysis data

This study evaluates the performance of two precipitation and temperature reanalyses. ERA5 is the 5th generation climate reanalysis dataset produced by ECMWF. Considered the ERA-Interim successor, it holds substantial upgrades with a finer spatial scale and a higher time resolution. The dataset implements a 12-hourly 4DVar data assimilation system. COSMO-REA6 is a regional reanalysis product developed for Europe, with a higher spatial resolution version covering Germany. The assimilation system follows a continuous nudging scheme to allow the continuous assimilation of observations. Summary information of the reanalyses is shown in **Table 11**. Points from the reanalysis grid cells were acquired based on their spatial overlap with the respective catchment's centroid.

Table 11: Main features of the precipitation and temperature products

Product	Spatial coverage	Period	Spatial resolution	Temporal resolution	Vertical levels
ERA5	Global	1950-Present	0.28° × 0.28°	1 h	137
COSMO-REA6	Europe	1995-2019	0.055° × 0.055°	1 h	40

2.3 Hydrological model

In the current study, the hydrological utility of precipitation and temperature products is evaluated with the use of the lumped conceptual GR4H and GR4H CemaNeige models. The GR4H model is based on the three-parameter version of the Genie Rural Journalier (GRJ) model, developed by Perrin (2002), scaled to an hourly timestep, with the aim of simulating rainfall-runoff by introducing the least amount of parameters. The variables used in the conceptual model are precipitation (*P*) and potential evapotranspiration (*E*). *E* is a function of surface temperature (*T*) and can be calculated at an hourly timestep using the Oudin formula (Oudin *et al.*, 2005). Four variables are ingrained in the model: *X1* represents the maximum capacity of the production store (mm), i.e., the storage at the surface of the soil that holds rainfall; *X2* is the groundwater exchange coefficient (mm), i.e., a function representing groundwater exchange: when positive, water exits the aquifer and adds to the routing store, and when negative, water infiltrates to the aquifer. *X3* accounts for the one day ahead maximum capacity of the routing store (mm); and *X4* is the unit hydrograph time base. A schematic representation is illustrated in **Figure 4**. *P* and *E* data is used to calculate net rainfall (*Pn*), which is then used to fill the production store (*Ps*) and to perform run-off routing (*Pn−Ps*). The production store is emptied by percolation (*Perc=f(S, X1)*, where *S* the production store level) or by the rate of evaporation (*Es=f(S, X1, En),* where *En* the net evapotranspiration). The difference between net rainfall and rainfall that is used to fill the production store (*Pn−Ps*) is then used together with percolation from the production store (*Perc*) to calculate flow (*Pr*). Multiple routing steps are then applied to simulate flow values. *Pr* is divided into two parts, 90% is being routed by the unit hydrograph HU1 (*X4*) and a routing store (*X3*) while 10% is routed by the unit hydrograph HU2 (*X4*). In the case of the HU2 and the routing store, a groundwater exchange term (gain or loss) is also introduced (*X2* parameter). Further details about the lumped conceptual rainfall-runoff model can be found in Perrin, Michel and Andréassian (2003).

The CemaNeige model is a semi-distributed Snow Accounting Routine (SAR) implementing a snowmelt factor and a cold-content factor. The inputs required are P and T. For modeling purposes at the catchment scale, the catchment is divided into five elevation zones of equal area. In each elevation band and for each time step, the five functions described in Valery, 2010; Valéry, Andréassian and Perrin, 2014a, 2014b are executed in order to compute rain and snowmelt. The outputs from each elevation zone are averaged with an equal weight and used as an input in the GR4H module. Solid precipitation was calculated by multiplying average yearly rainfall on each catchment, with the catchment's percentage of snowmelt. The percentage of snowmelt was calculated by using the following equation:

$$snowmelt = 0.0168 \cdot ME + 3.5128$$

The equation was empirically derived from data gathered at the daily scale in the two precipitation networks (ARSO), over the period 2010-2016.

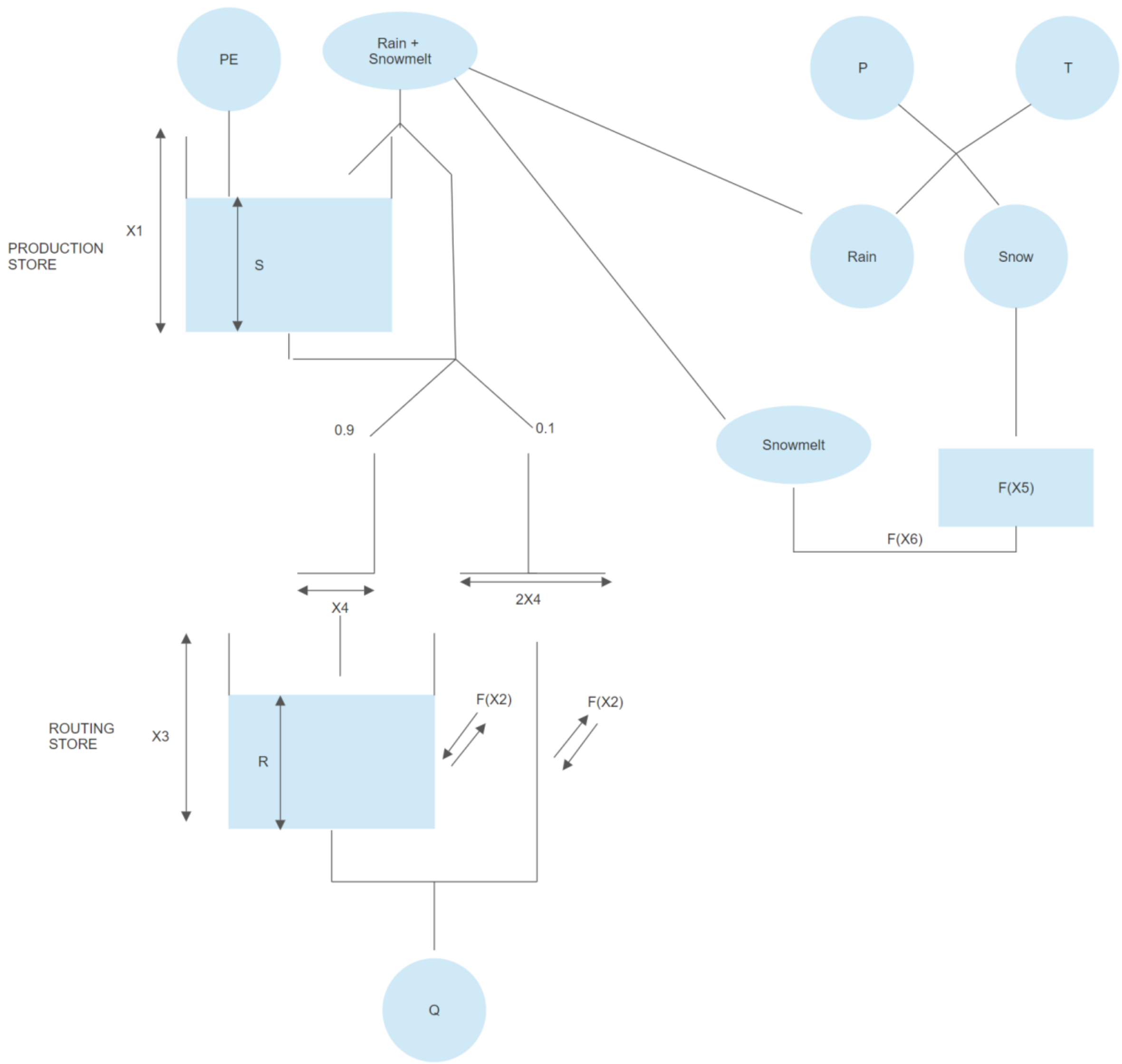

Figure 4: Schematic representation of the CemaNeige semi-distributed model

2.4 Dataset performance assessment

For the study period described in sub-section **2.1**, precipitation products (PP), temperature products (TP) and simulated discharges (Qs) are compared with the representative precipitation, temperature and observed discharge of each watershed, respectively. For effective comparison between the modelled and observed data, the Percent Bias (PBIAS) metric is used (Sorooshian, Duan and Gupta, 1993; Yapo, Gupta and Sorooshian, 1996), which estimates the average tendency of the simulated data to be larger or smaller than its observed counterpart (Gupta, Sorooshian and Yapo, 1999). The optimal value is 0.0, with values of low magnitude suggesting adequate simulation performance. Positive values indicate model overestimation bias, and negative values underestimation bias. In addition, the Pearson correlation coefficient and modified Index of Agreement (IOA) (Willmott, 1981) are calculated to measure PP and TP performance. For discharge, the KGE efficiency is used (Gupta *et al.*, 2009; Kling, Fuchs and Paulin, 2012), which is a combination of bias, variability ratio and correlation. Just like other performance metrics (Nash and Sutcliffe, 1970), KGE = 1 suggests perfect agreement between observations and simulations. According to some authors (Koskinen *et al.*, 2017; Castaneda-Gonzalez *et al.*, 2018), KGE < 0 indicates that the mean of observation provides better estimates than the simulated mean, while others consider negative KGE values simply undesirable (Andersson *et al.*, 2017; Fowler *et al.*, 2018; Siqueira *et al.*, 2018). PPs are examined for their ability to detect rainfall events using: the bias ratio (BR) metric, referring to the ratio of total reanalysis measurements to the reference observations, the POD metric, which represents the ratio of the number of correctly detected rainfall events to the total number of observed rainfall events, and the FAR metric, which denotes the ratio of the number of falsely detected precipitation events to the total number of reanalysis precipitation events.

The simulation period was split-sampled into: a calibration period (2009-01-01 01:00:00 – 2012-01-01 12:00:00) using a warm-up period of one year (2008-01-01 00:00:00 – 2009-01-01 00:00:00), and a validation period (2012-01-01 13:00:00 – 2014-12-31 23:00:00), with a warm-up period of four years (2008-01-01 00:00:00 – 2012-01-01 12:00:00). For an overall evaluation of ERA5 and REA6 performance, model runs are performed using the following data configurations as an input for both simulation periods:

1. Observed precipitation and temperature (Pobs & Tobs)
2. ERA5 precipitation and observed temperature (Pera5 & Tobs)
3. REA6 precipitation and observed temperature (Prea6 & Tobs)
4. Observed precipitation and ERA5 temperature (Pobs & Tera5)
5. Observed precipitation and REA6 temperature (Pobs & Trea6)
6. ERA5 precipitation and ERA5 temperature (Pera5 & Tera5)
7. REA6 precipitation and REA6 temperature (Prea6 & Trea6)

Four model runs are performed for each simulation period. The GR4H and GR4H CemaNeige modules are used twice. Initially, the variables ingrained within the model (*X1, X2, X3, X4)* are calibrated using configuration 1, and used for the remaining six data configurations. Then, simulations are repeated for a second time, implementing the Michel calibration algorithm (Michel, 1991) for each data configuration, in order to further evaluate the applicability of the ERA5 and REA6 datasets within the rainfall-runoff model used in the current study.

3 RESULTS AND DISCUSSION

3.1 Precipitation and temperature performance

Mean annual precipitation was computed over the course of the study period 2008-2014 for both datasets, depicted in **Figure 5**.

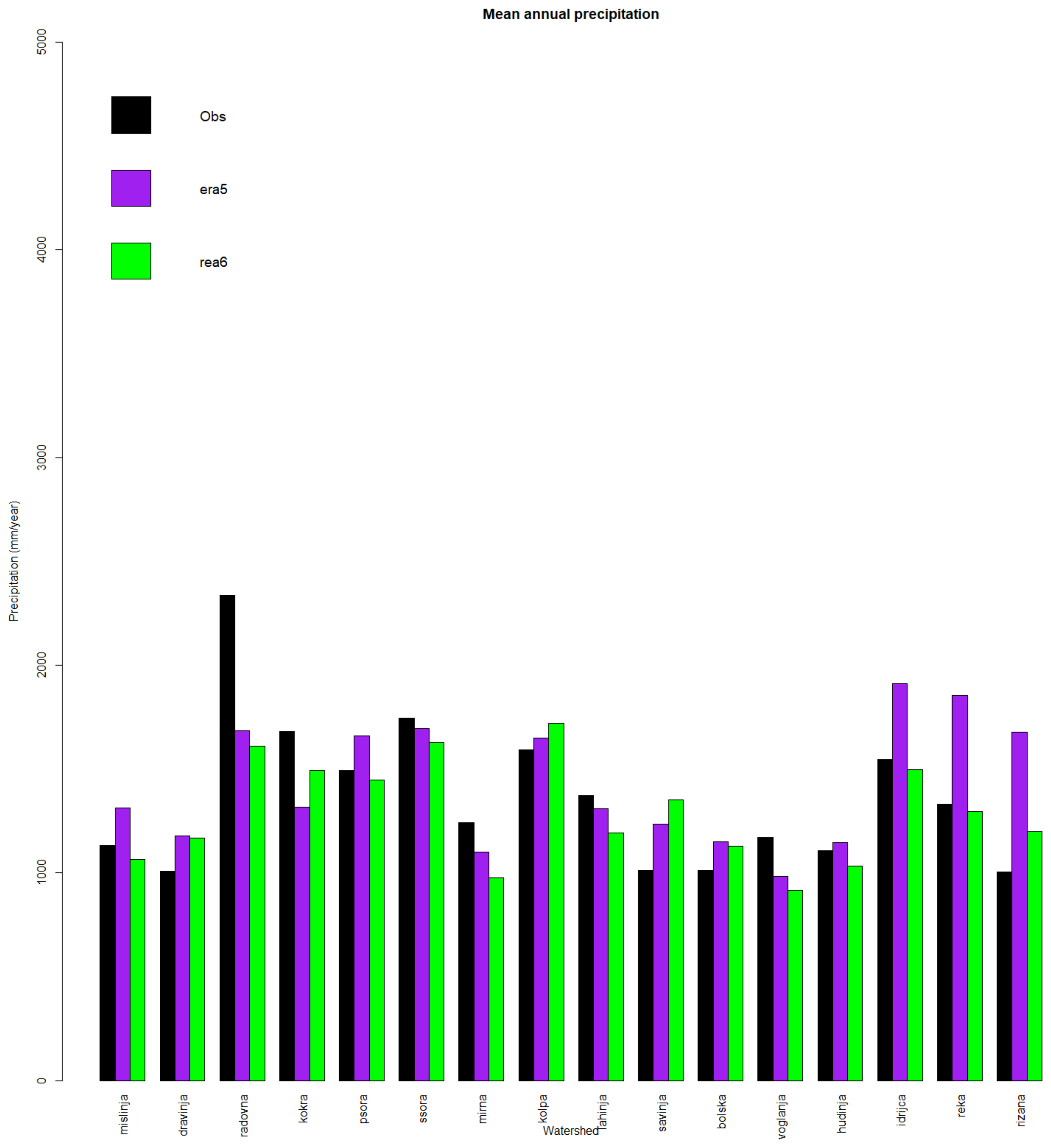

Figure 5: Mean annual observed, ERA5 and REA6 precipitation (2008-2014)

ERA5 is overestimating the amount of measured rainfall in 60% of the cases (Rižana, Reka, Idrijca, Hudinja, Bolska, Savinja, Kolpa, Poljanska Sora , Dravinja, Mislinja), and the phenomenon is more profound for the catchments that follow mediterranean-pluvial regimes in the south-western part of the country. This overestimation is additionally evident by using the

BR metric, depicted in **Figure 6**. The BR metrics represents the ratio between the sum of the total amount of model rainfall to the total amount of reference rainfall. REA6 is consistently underestimating measured rainfall, with the exception of the watersheds located in the north-central part of the country. In this area, ERA5 and REA6 estimates tend to be quantitatively similar with each other.

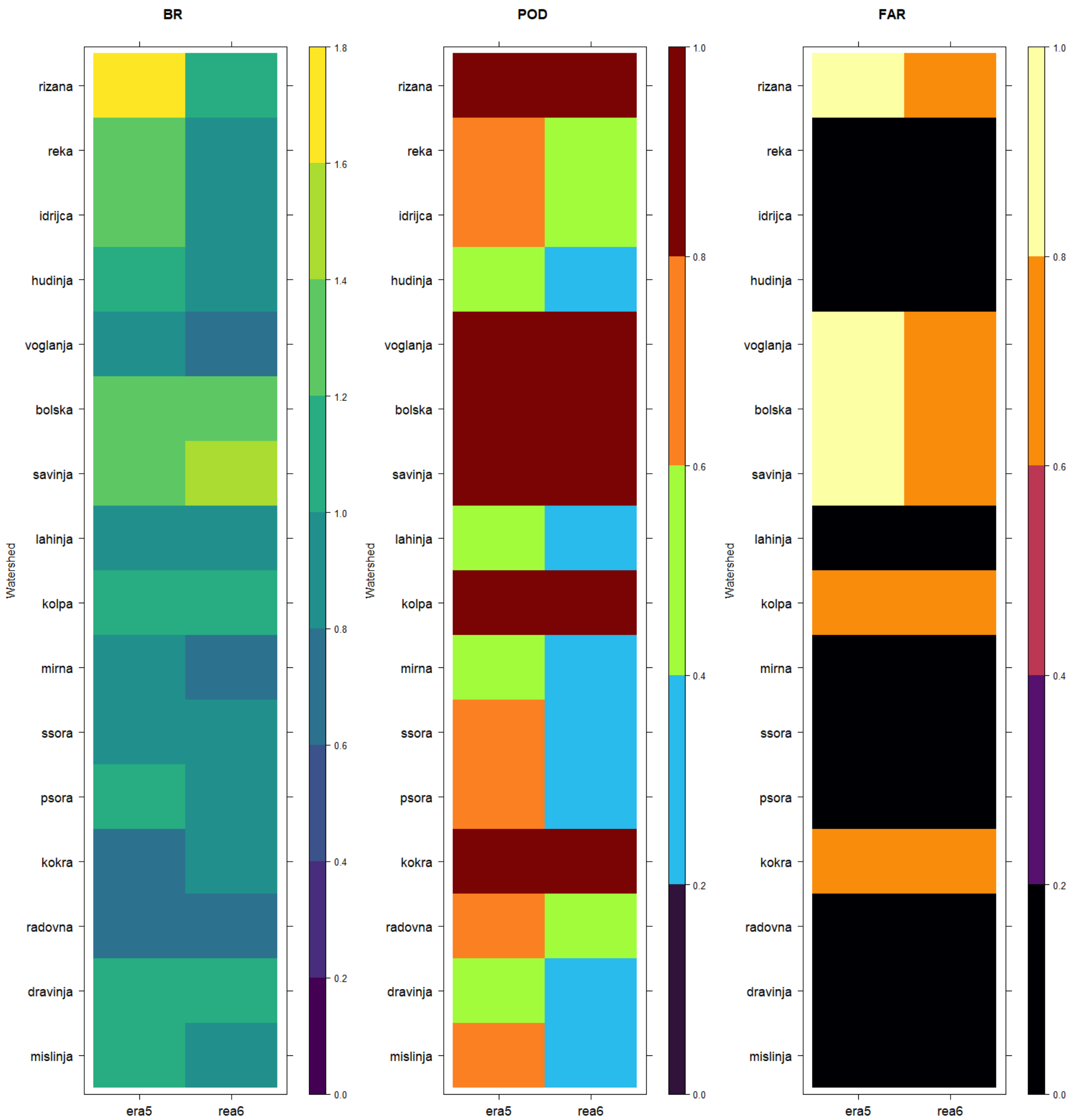

Figure 6: ERA5 and REA6 precipitation metrics

As illustrated in **Figure 6**, ERA5 exhibits strong rainfall occurrence detectability (POD) for approximately 70% of the selected watersheds (except for Mislinja, Radovna, Poljanska Sora , Selška Sora, Idrijca and Reka), demonstrating superior performance for catchments that follow mostly alpine pluvial-nival regimes. REA6 is performing very well in the Kokra, Kolpa, Savinja, Bolska, Voglanja and Rižana stations. Extremely poor results are present in Mislinja, and Dravinja. The FAR (measure to calculate tendency to detect rainfall events when observed precipitation equals zero) is pretty low in most cases, however many false alarms occur in the drainage areas located in the northern and southern part of the country, for both datasets.

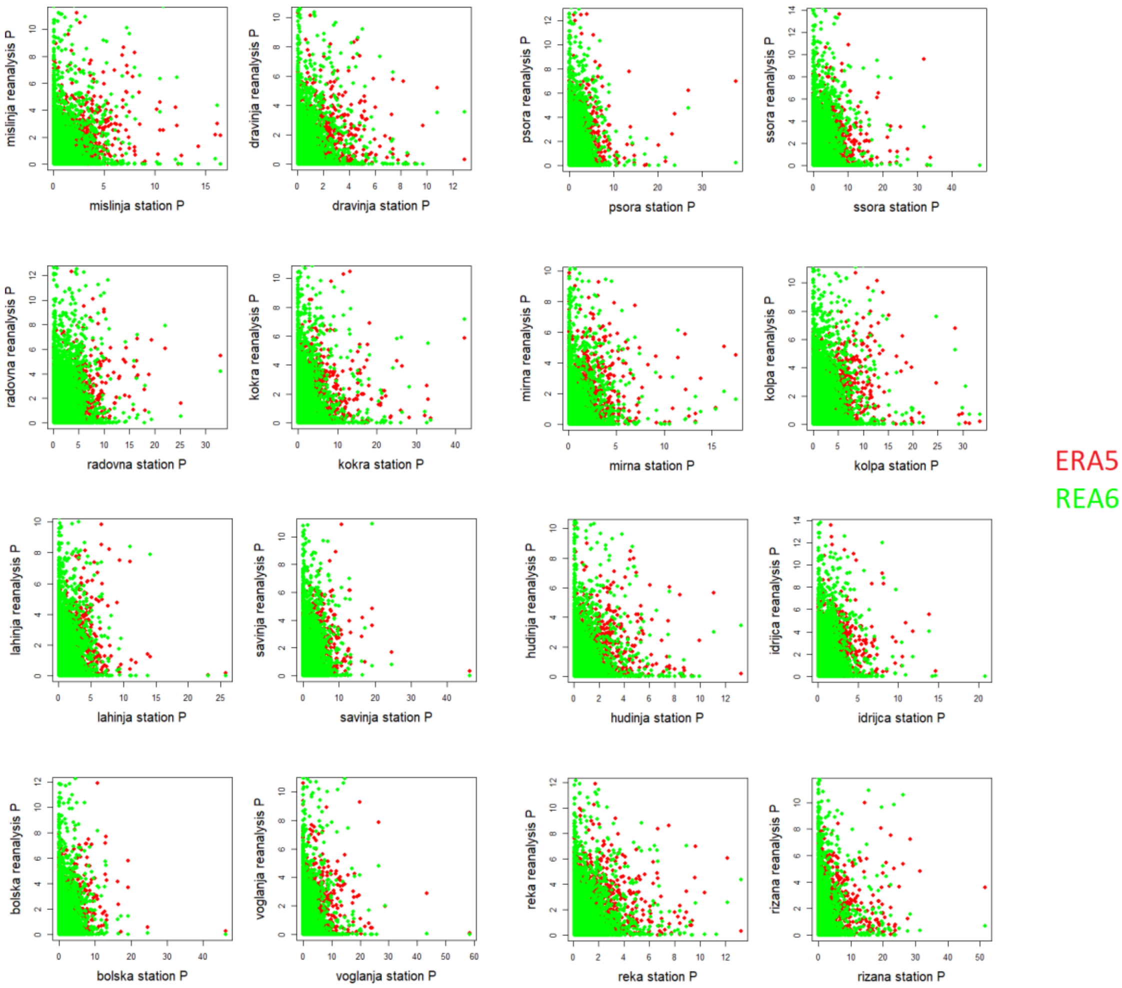

Figure 7: Scatterplots comparing ERA5 and REA6 rainfall to observations, per catchment

Figure 7 illustrates scatter plots between observed and reanalysis rainfall. Both datasets display poor fit to observations, across all selected watersheds. Conversely, ERA5 and REA6 temperature is in agreement with station temperature, with both datasets performing similarly, as expected (**Figure 8**).

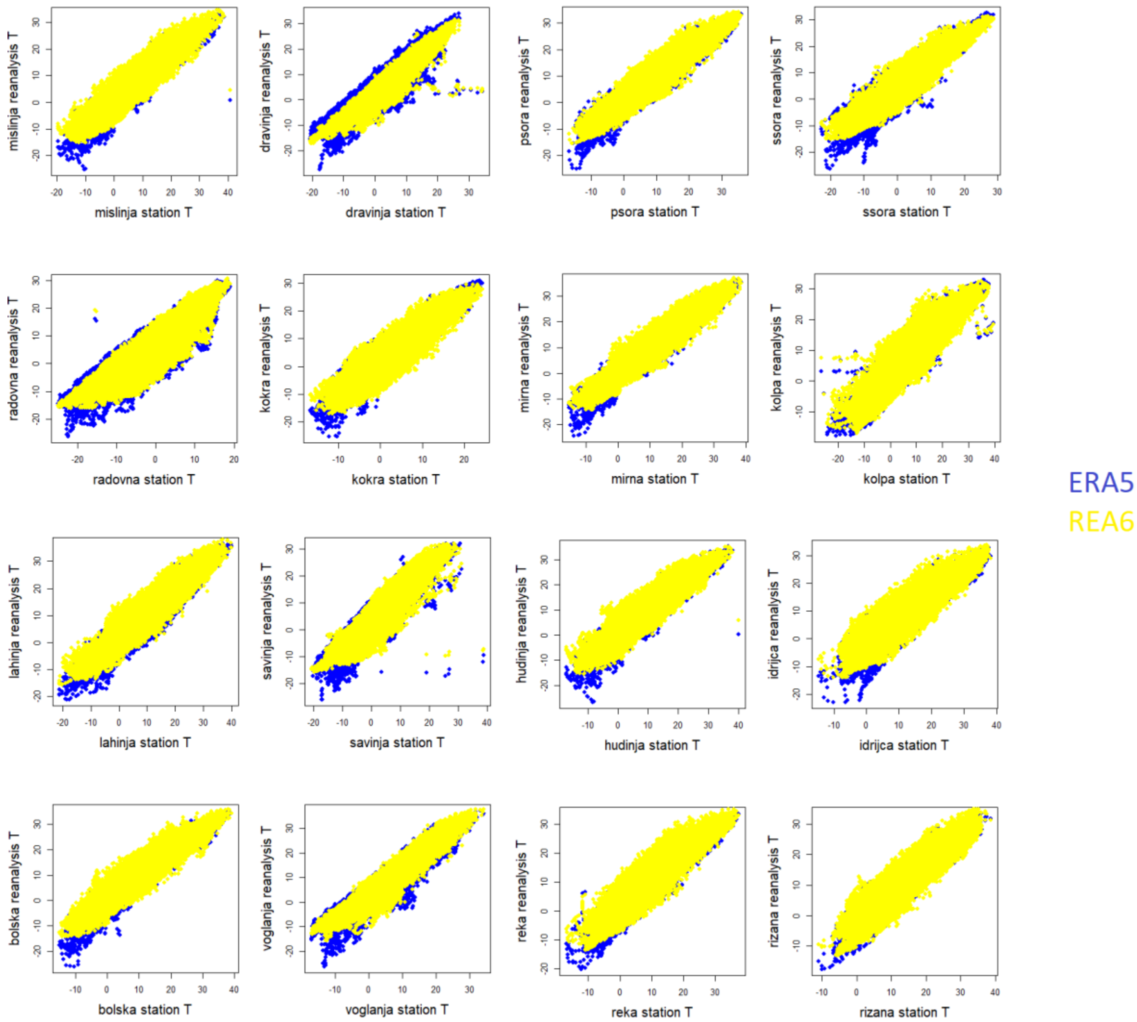

Figure 8: Scatterplots comparing ERA5 and REA6 temperature to observations, per catchment

The modified Index of Agreement is a standardized measure of the degree of model prediction error, varying between 0 and 1. The IOA scores show good agreement between ERA5 and observed precipitation for almost half of the selected watersheds (**Figure 9**). REA6 is underperforming in comparison to ERA5, however, both datasets prove to be adequate when matching temperature observations.

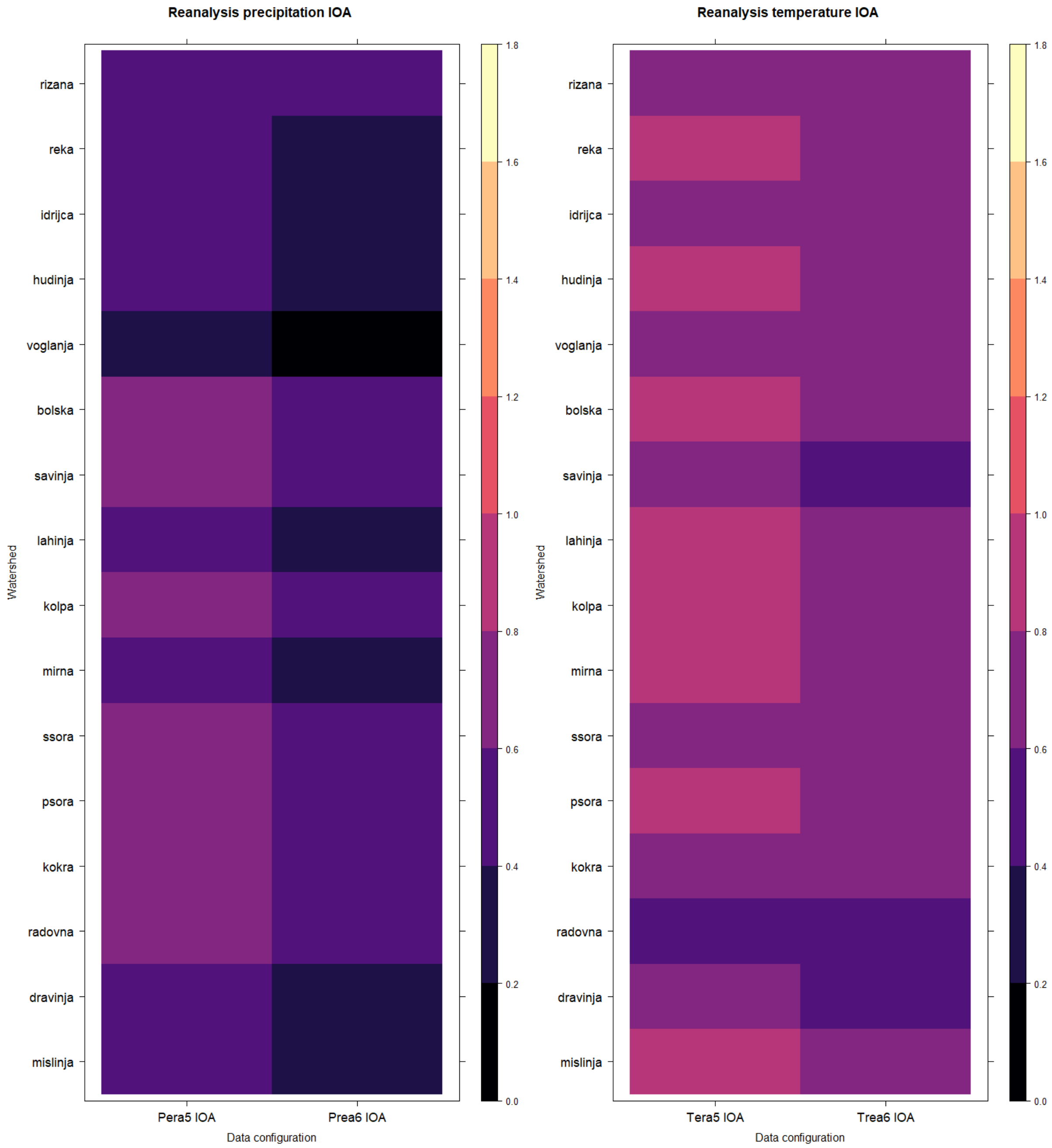

Figure 9: IOA scores for reanalysis precipitation and temperature

It should be noted that IOA scores are expected to perform better for variables that do not tend to flunctuate alot, given their sensitivity to extreme values due to the squared differences (Legates and McCabe, 1999).

ERA5 displays strong correlation with measurements {Pearson{0.8-1}), outperforming REA6 in all 16 catchments (**Table 12**). In the Kolpa, Bolska, Reka and Rižana catchments, REA6 precipitation is negatively correlated with observations, and performs poorly (0-0.2) on the rest of the modeling domain. In addition, ERA5 also shows poor correlation results. This may be partially explained due to the significant variation in rainfall, which can be present even at hourly intervals.

Table 12: ERA5 and REA6 precipitation and temperature Pearson correlation coefficient, per catchment

Precipitation and temperature correlation per catchment				
Catchment-Station	Pera5 Pearson cc	Prea6 Pearson cc	Tera5 Pearson cc	Trea6 Pearson cc
Mislinja-Otiški vrh	0.43	0.33	0.95	0.93
Dravinja-Zreče	0.42	0.27	0.93	0.97
Radovna-Podhom	0.56	0.42	0.89	0.91
Kokra-Kokra	0.42	0.27	0.95	0.91
Poljanska Sora - Zminec	0.47	0.33	0.96	0.95
Selška Sora-Železniki	0.44	0.34	0.95	0.94
Mirna-Jelovec	0.45	0.29	0.96	0.95
Kolpa-Petrina	0.49	0.33	0.94	0.90
Lahinja-Gradac	0.47	0.30	0.95	0.94
Savinja-Nazarje	0.46	0.32	0.93	0.94
Bolska-Dvas	0.45	0.30	0.96	0.94
Voglanja-Crnolica	0.42	0.27	0.94	0.96
Hudinja-SVas	0.44	0.28	0.95	0.92
Idrijca-Hotešk	0.46	0.35	0.94	0.91
Reka-CMlin	0.42	0.31	0.96	0.93
Rižana-Kubed	0.32	0.22	0.96	0.93

Figure 10 illustrates the PP and TP PBIAS scores. PBIAS is a metric used to discretize the tendency of model predictions to overestimate/underestimate reference observations. ERA5 rainfall shows great overestimation bias for most watersheds, which is consistent with the findings presented in **Figure 6** and **Figure 6**. Moreover, REA6 underestimates rainfall across 80% of the modeling terrain, of which 60% is considered alpine. The extreme underestimation in the Voglanja catchment is expected, since it was greatly overestimated. The magnitude of PBIAS is similar for both datasets in most watersheds. Temperature is extremely underestimated for the Radovna watershed, with its value out of bounds. Significant underestimation is present in most alpine areas, and in watersheds that follow mediterranean or dinaric regimes.

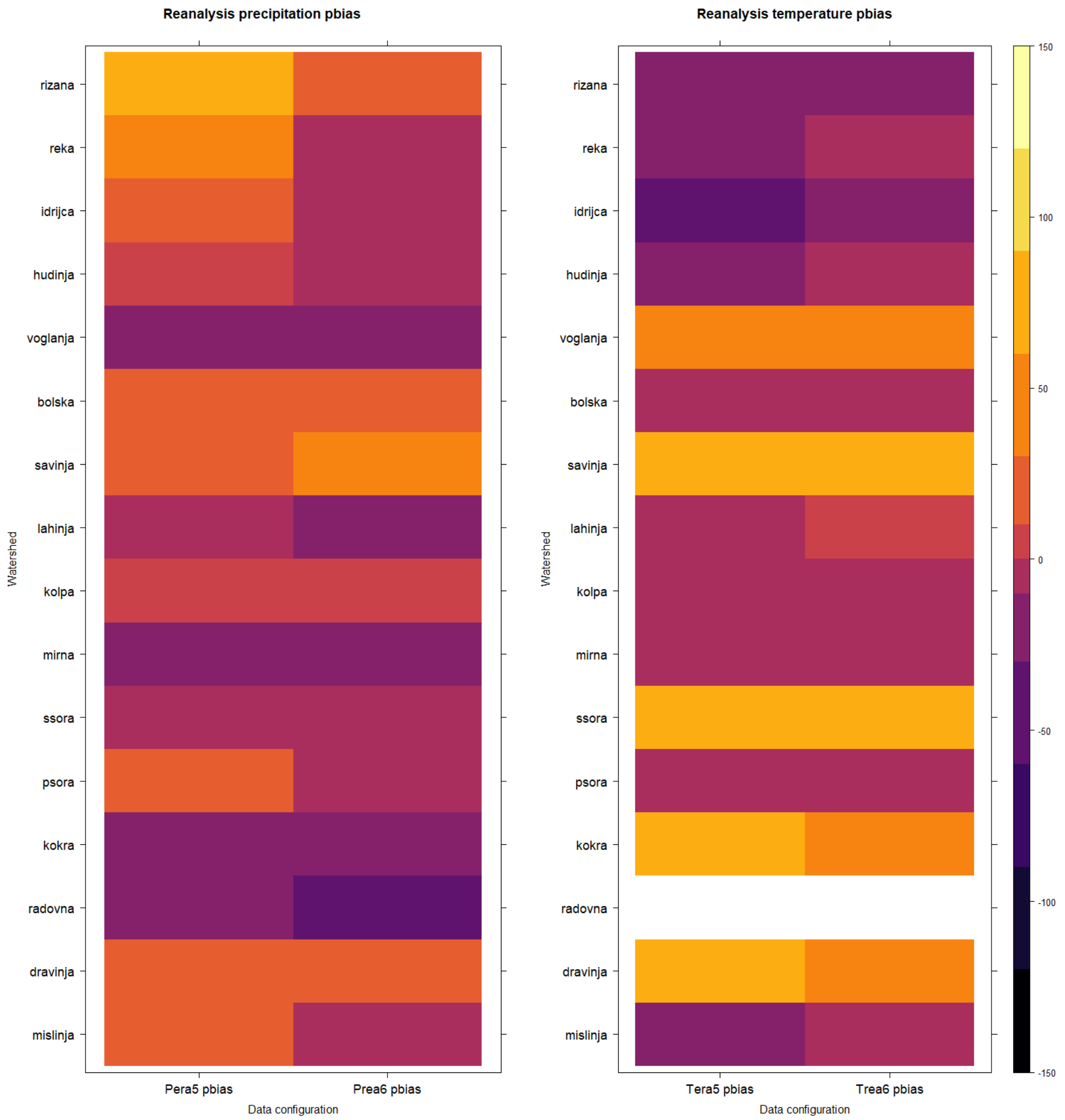

Figure 10: PBIAS scores for reanalysis precipitation and temperature

3.2 Discharge performance

Overall, alpine pluvial-nival catchments that cover areas greater than 200 km^2, such as Poljanska Sora , Kolpa, Savinja and Idrijca, tend to demonstrate higher discharge regimes. Additionally, catchments whose spatial domain does not exceed 150 km^2 (e.g., Dravinja, Kokra, Selška Sora), are characterized by low flow rates (**Figure 11**). Measurements tend to be fairly consistent over all years of the study period.

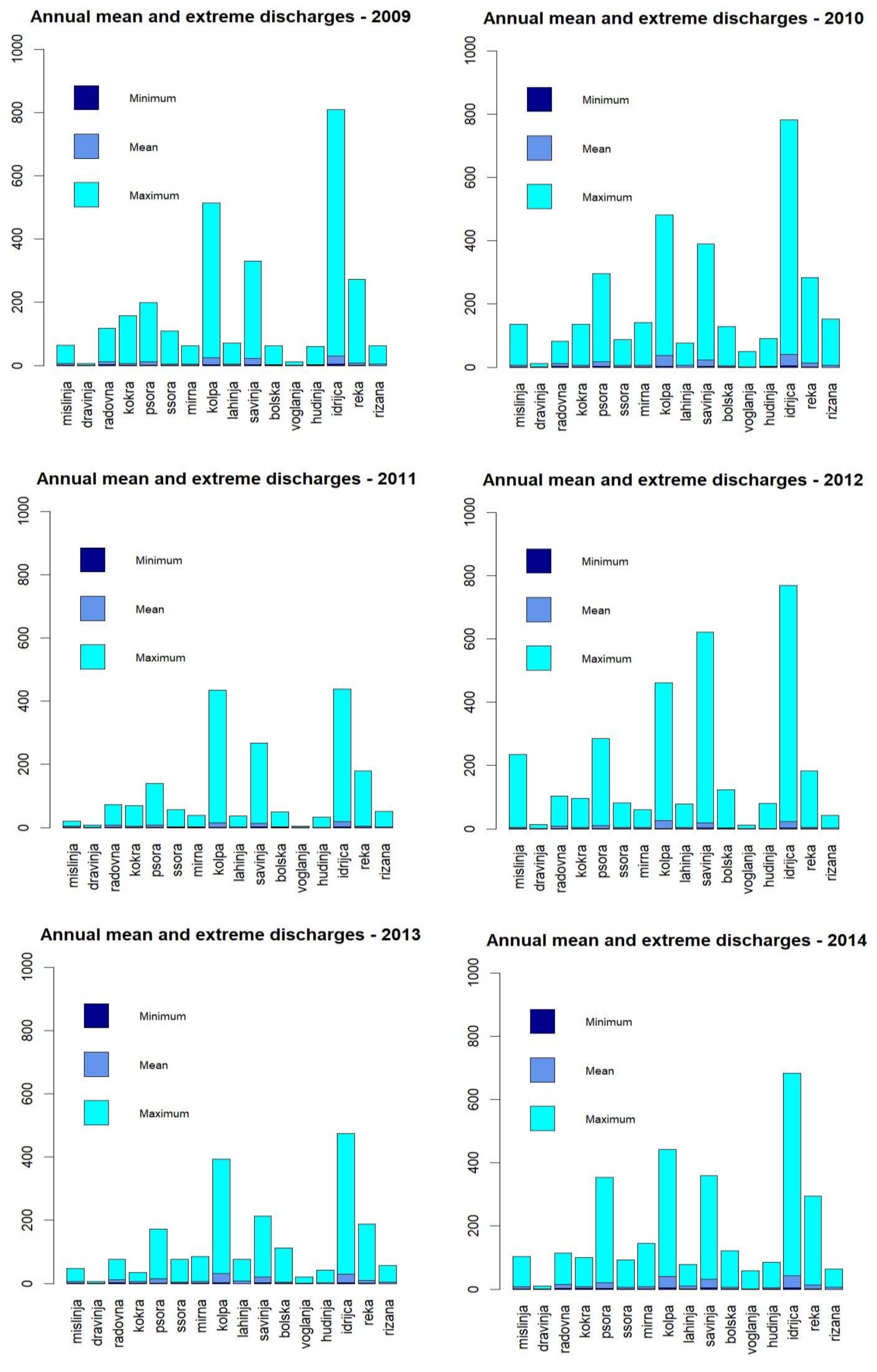

Figure 11: Mean annual observed discharge (2009-2014)

The GR4H and GR4H CemaNeige models were initially set up for all 16 catchments using configuration 1. Results directly exported from the models (calibration and validation period, GR4H-GR4H Cema Neige) for the Kolpa catchment are depicted in **Figure 12**. Displayed are precipitation (mm/h), simulated and observed streamflows (mm/h), 30-day rolling mean (simulated/observed), probability of exceedance (simulated/observed), and a scatter plot matching model prediction to observations.

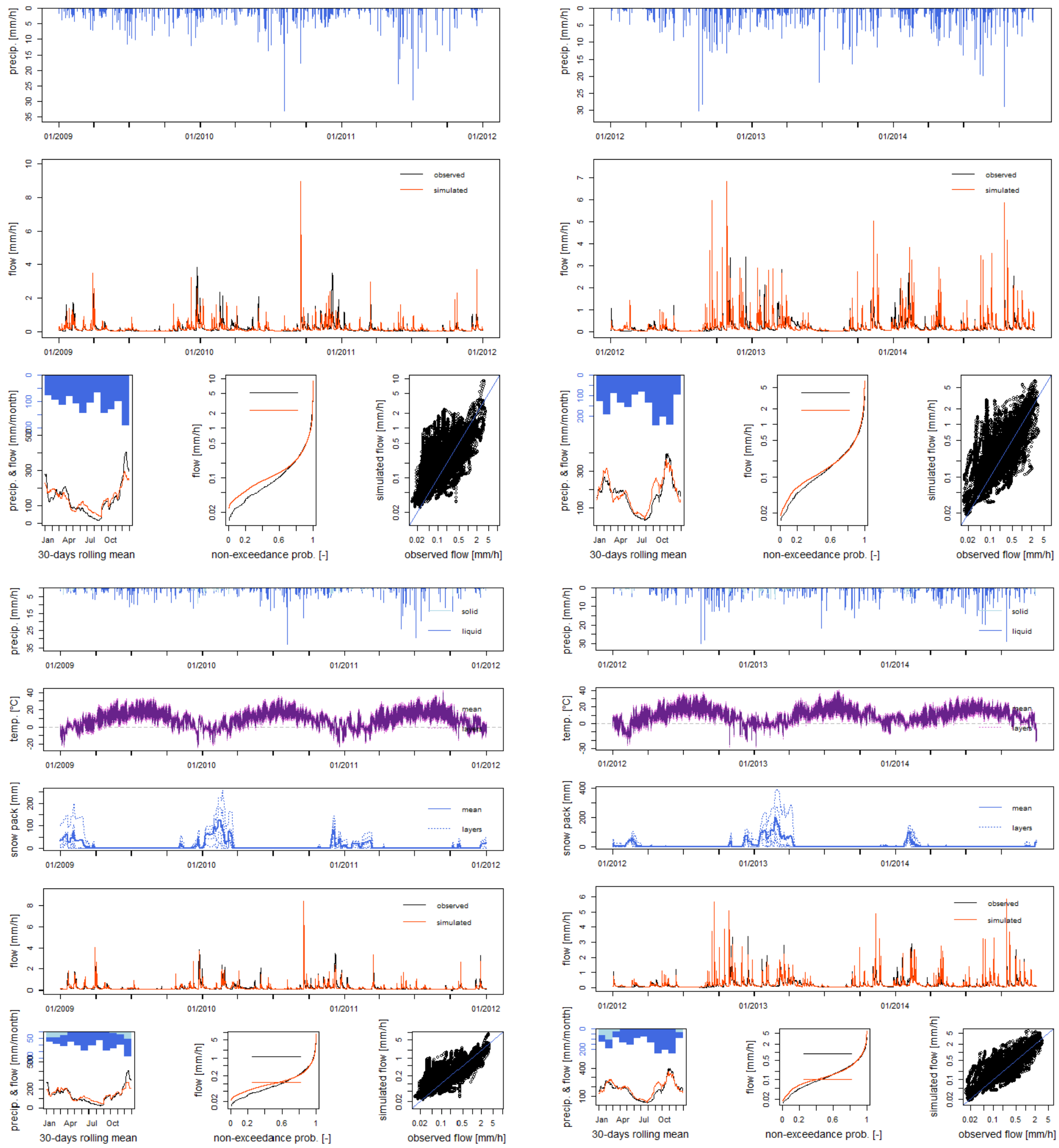

Figure 12: Exported results (conf. 1, GR4H (top)-GR4H CemaNeige (bottom), calibration (left) and validation (right) period) for the Kolpa watershed

The observed and simulated discharge time-series for the entire study period (all watersheds) are presented in **Figure 13**.

Figure 13: Observed and simulated discharge per catchment

For each watershed, all seven configurations were tested and evaluated for the four different model runs. A representation of the computed discharges for the Kolpa catchment is shown in **Figure 14**.

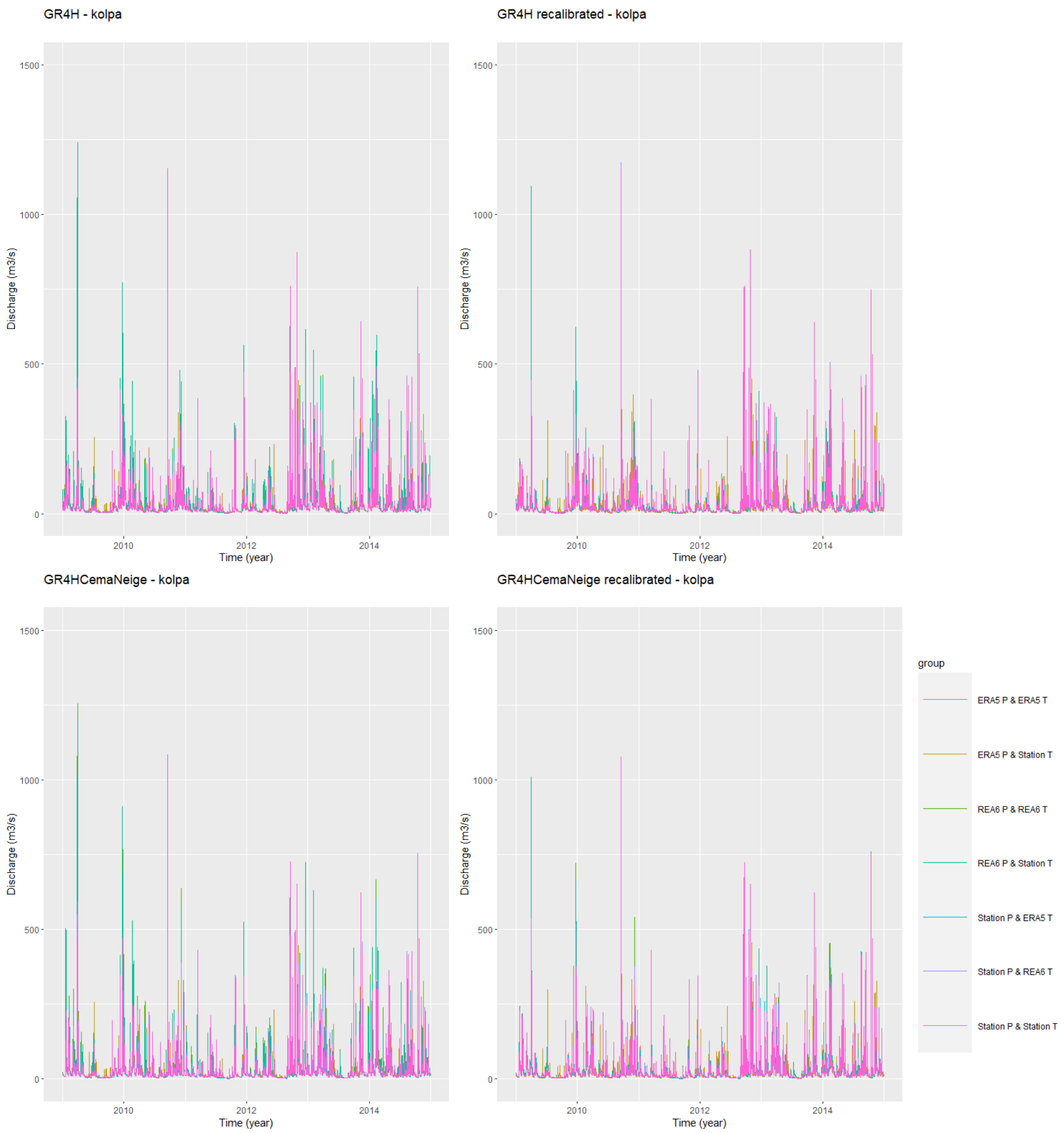

Figure 14: Discharge time series derived from the 7 data configurations - Kolpa catchment

Figure 15 illustrates intercomparisons between all seven configurations for each drainage basin for minimum, mean and maximum streamflows (GR4H). Minimal differences are observed between observations and reanalysis flows, albeit ERA5 and REA6 tend to estimate minima of lower magnitude in 11 watersheds (Mislinja, Dravinja, Radovna, Kokra, Poljanska Sora, Selška Sora, Mirna, Lahinja, Voglanja, Hudinja, Reka). In larger basins (Kolpa, Savinja), ERA5 rainfall (conf. 2) overestimates observations and simulations under conf. 1, however, the effect is reduced under configurations that use both reanalysis variables. When reanalysis T is used, discharge minima tend to be more consistent with conf. 1, except for the Radovna, Lahinja and Idrijca stations.

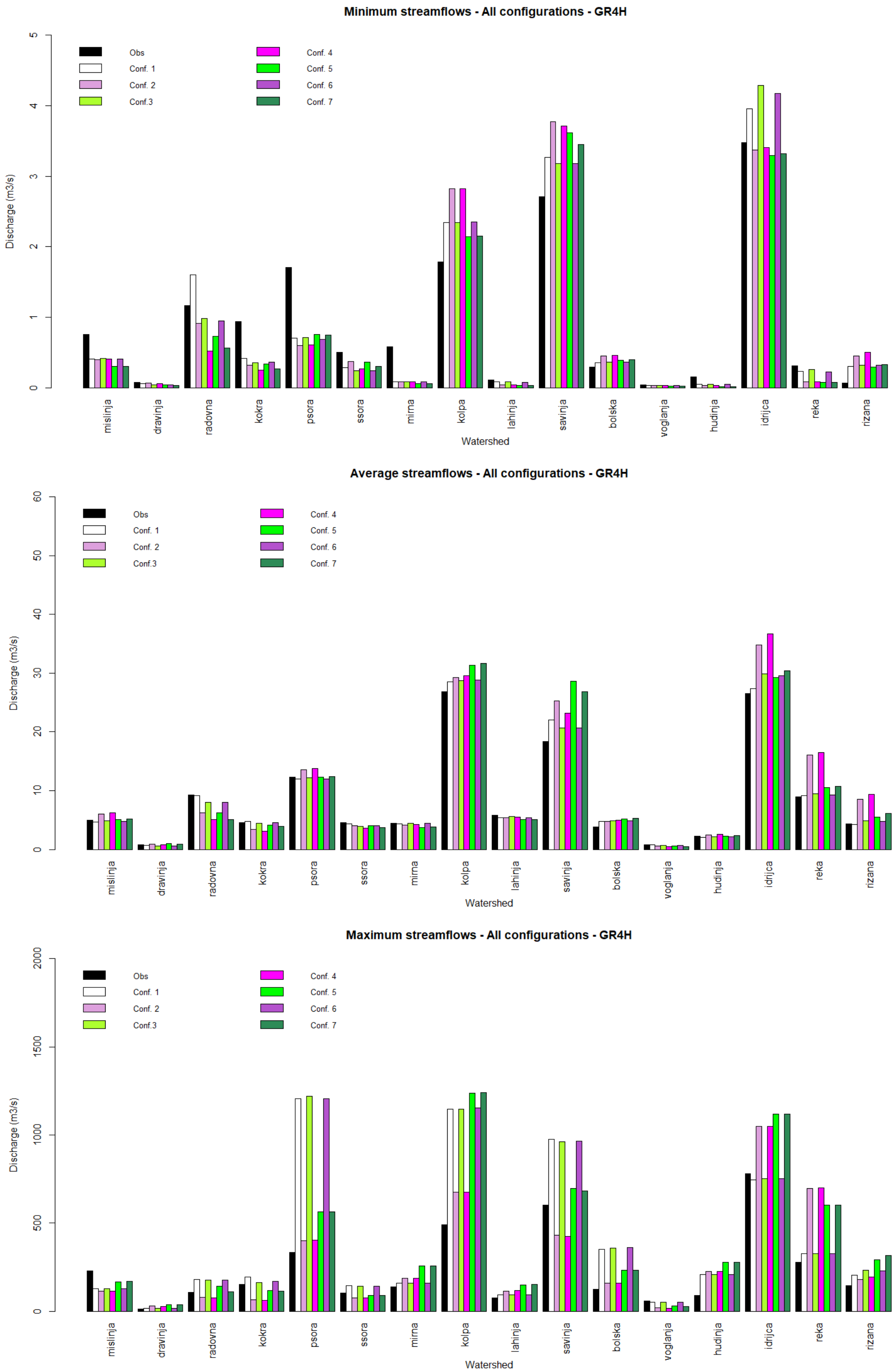

Figure 15: Intercomparison under all conf. - Minimum, average and maximum streamflows (2009-2014)

Average flows are more or less consistent under conf. 2-7, with no great variations between reanalyses, observations and conf. 1. Notable exceptions are present for catchments located in the western part of the country (Idrijca, Reka, Rižana), when ERA5 products are used individually, but not under conf. 4 or 6. Regarding maximum flows, in drainage areas characterized by high discharge peaks (Poljanska Sora, Kolpa, Savinja, Idrijca), ERA5 and REA6 overestimate maxima in at least one configuration, but no further conlcusion can be made, since the individual use of reanalysis temperature (Kolpa) or rainfall (Idrijca) can lead to the aforementioned overstimation.

The calibrated parameters for all four runs under all 7 configurations are illustrated in **Table 13**.

Table 13: Calibrated parameters under all configurations, per catchment - GR4H

Catchment-Data configuration	X1	X2	X3	X4
Mislinja Pobs & Tobs	17.01	0.10	138.30	12.64
Mislinja Pera5 & Tobs	35.13	-0.48	153.52	17.28
Mislinja Prea6 & Tobs	36.53	0.24	203.44	16.46
Mislinja Pobs & Tera5	17.75	-0.01	137.93	13.21
Mislinja Pobs & Trea6	17.16	-0.00	139.12	12.97
Mislinja Pera5 & Tera5	37.60	-0.71	152.05	17.63
Mislinja Prea6 & Trea6	39.14	0.13	201.72	16.67
Dravinja Pobs & Tobs	70.80	-0.28	112.16	2.41
Dravinja Pera5 & Tobs	120.61	-2.39	275.29	4.32
Dravinja Prea6 & Tobs	98.98	-5.24	720.95	5.75
Dravinja Pobs & Tera5	45.01	0.19	127.32	2.26
Dravinja Pobs & Trea6	56.80	0.07	114.51	2.14
Dravinja Pera5 & Tera5	45.31	-1.43	468.62	4.07
Dravinja Prea6 & Trea6	51.92	-5.01	944.71	5.63
Radovna Pobs & Tobs	155.18	-1.38	310.74	10.49
Radovna Pera5 & Tobs	72.97	1.23	217.39	10.34
Radovna Prea6 & Tobs	120.97	1.69	360.43	12.48
Radovna Pobs & Tera5	214.85	-0.09	293.24	10.29
Radovna Pobs & Trea6	205.82	-0.07	300.30	10.25
Radovna Pera5 & Tera5	92.62	2.05	192.90	9.40
Radovna Prea6 & Trea6	241.84	2.33	237.56	12.29
Kokra Pobs & Tobs	113.50	0.26	138.31	3.72
Kokra Pera5 & Tobs	48.87	0.96	65.42	4.23
Kokra Prea6 & Tobs	88.54	0.70	120.72	4.53
Kokra Pobs & Tera5	121.51	0.55	125.21	3.61
Kokra Pobs & Trea6	118.82	0.48	128.01	3.75
Kokra Pera5 & Tera5	50.71	1.07	58.32	4.32
Kokra Prea6 & Trea6	89.55	0.88	111.58	4.48
Poljanska Sora Pobs & Tobs	47.57	0.76	78.54	6.44
Poljanska Sora Pera5 & Tobs	78.92	0.68	87.17	7.69
Poljanska Sora Prea6 & Tobs	87.29	1.15	124.56	8.27
Poljanska Sora Pobs & Tera5	46.77	0.72	79.67	6.37
Poljanska Sora Pobs & Trea6	47.26	0.76	80.48	6.35

Poljanska Sora Pera5 & Tera5	75.94	0.63	90.01	7.69
Poljanska Sora Prea6 & Trea6	82.21	1.14	130.92	8.27
Selška Sora Pobs & Tobs	199.97	0.03	204.15	3.87
Selška Sora Pera5 & Tobs	72.91	0.59	127.53	4.76
Selška Sora Prea6 & Tobs	86.64	0.70	231.53	5.78
Selška Sora Pobs & Tera5	221.40	0.52	184.93	3.85
Selška Sora Pobs & Trea6	219.69	0.46	189.29	3.78
Selška Sora Pera5 & Tera5	83.74	0.93	117.56	4.62
Selška Sora Prea6 & Trea6	88.01	1.14	229.92	5.70
Mirna Pobs & Tobs	37.66	-0.35	36.89	14.45
Mirna Pera5 & Tobs	55.70	-0.12	76.70	10.33
Mirna Prea6 & Tobs	98.49	0.29	92.75	12.49
Mirna Pobs & Tera5	37.71	-0.40	36.23	14.41
Mirna Pobs & Trea6	38.32	-0.38	35.59	14.57
Mirna Pera5 & Tera5	54.59	-0.20	76.70	10.33
Mirna Prea6 & Trea6	96.54	0.24	95.58	12.49
Kolpa Pobs & Tobs	113.29	1.34	54.09	8.29
Kolpa Pera5 & Tobs	66.02	1.02	42.52	11.29
Kolpa Prea6 & Tobs	72.35	1.86	157.52	7.42
Kolpa Pobs & Tera5	106.92	1.40	58.15	8.21
Kolpa Pobs & Trea6	105.81	1.45	62.50	7.40
Kolpa Pera5 & Tera5	64.71	1.02	43.38	11.29
Kolpa Prea6 & Trea6	69.58	1.82	158.52	7.64
Lahinja Pobs & Tobs	47.82	0.00	11.74	29.60
Lahinja Pera5 & Tobs	133.57	0.14	25.69	26.74
Lahinja Prea6 & Tobs	113.29	0.45	77.47	18.49
Lahinja Pobs & Tera5	48.47	-0.00	12.01	29.50
Lahinja Pobs & Trea6	47.87	0.01	11.55	29.67
Lahinja Pera5 & Tera5	125.71	0.11	27.41	26.38
Lahinja Prea6 & Trea6	113.29	0.45	78.25	18.25
Savinja Pobs & Tobs	19.91	2.31	116.47	5.32
Savinja Pera5 & Tobs	43.92	0.90	58.78	8.30
Savinja Prea6 & Tobs	73.70	0.94	126.05	7.72
Savinja Pobs & Tera5	18.01	2.45	112.79	4.46
Savinja Pobs & Trea6	17.90	2.43	112.79	4.54
Savinja Pera5 & Tera5	46.10	1.05	51.30	7.70
Savinja Prea6 & Trea6	76.01	1.23	114.29	7.28
Bolska Pobs & Tobs	22.41	0.81	101.63	4.24
Bolska Pera5 & Tobs	39.25	0.17	43.38	4.57
Bolska Prea6 & Tobs	57.97	0.10	78.25	7.45
Bolska Pobs & Tera5	24.18	0.78	100.55	4.29
Bolska Pobs & Trea6	24.42	0.78	100.55	4.29
Bolska Pera5 & Tera5	38.86	0.12	44.70	4.81
Bolska Prea6 & Trea6	56.26	0.04	82.26	7.45
Voglanja Pobs & Tobs	122.62	-2.44	161.07	5.54
Voglanja Pera5 & Tobs	33.98	-0.40	67.76	3.18
Voglanja Prea6 & Tobs	50.91	-0.27	90.02	5.78
Voglanja Pobs & Tera5	132.19	-1.60	150.22	5.39

Voglanja Pobs & Trea6	136.42	-1.42	145.88	5.32
Voglanja Pera5 & Tera5	30.56	-0.18	67.35	2.90
Voglanja Prea6 & Trea6	47.94	0.00	87.35	5.53
Hudinja Pobs & Tobs	46.06	-0.17	16.28	4.57
Hudinja Pera5 & Tobs	97.04	-0.41	41.37	3.42
Hudinja Prea6 & Tobs	183.09	-0.08	42.52	5.29
Hudinja Pobs & Tera5	44.90	-0.23	16.55	4.71
Hudinja Pobs & Trea6	45.44	-0.22	16.16	4.70
Hudinja Pera5 & Tera5	83.93	-0.62	44.70	3.61
Hudinja Prea6 & Trea6	170.71	-0.20	45.60	5.29
Idrijca Pobs & Tobs	7.10	0.67	14.62	9.37
Idrijca Pera5 & Tobs	51.41	0.99	36.23	10.33
Idrijca Prea6 & Tobs	51.93	1.39	40.44	12.49
Idrijca Pobs & Tera5	6.74	0.65	16.80	8.97
Idrijca Pobs & Trea6	7.086	0.66	16.40	9.05
Idrijca Pera5 & Tera5	51.93	0.86	38.09	10.57
Idrijca Prea6 & Trea6	56.82	1.28	40.44	12.73
Reka Pobs & Tobs	21.41	0.03	15.40	15.94
Reka Pera5 & Tobs	154.76	-1.75	96.50	11.61
Reka Prea6 & Tobs	66.41	0.04	118.17	10.29
Reka Pobs & Tera5	21.09	0.00	15.46	15.81
Reka Pobs & Trea6	21.65	0.02	15.63	15.73
Reka Pera5 & Tera5	152.36	-1.99	98.56	11.65
Reka Prea6 & Trea6	61.43	-0.02	125.47	10.26
Rižana Pobs & Tobs	232.75	0.76	62.17	11.77
Rižana Pera5 & Tobs	162.67	-1.33	169.11	11.59
Rižana Prea6 & Tobs	27.91	0.16	199.18	9.86
Rižana Pobs & Tera5	228.14	0.59	76.70	11.53
Rižana Pobs & Trea6	223.63	0.60	75.94	11.53
Rižana Pera5 & Tera5	158.67	-2.09	169.23	12.55
Rižana Prea6 & Trea6	28.75	-0.24	207.29	10.40

Table 14: Calibrated parameters under all configurations, per catchment - GR4H Cema Neige

Catchment-Data configuration	X1	X2	X3	X4	X5	X6
Mislinja Pobs & Tobs	13.27	0.03	164.90	13.25	0.00	0.53
Mislinja Pera5 & Tobs	46.44	-0.33	135.29	18.24	0.00	0.49
Mislinja Prea6 & Tobs	55.69	0.39	154.12	17.20	0.57	0.46
Mislinja Pobs & Tera5	12.50	-0.16	165.08	13.87	0.40	1.23
Mislinja Pobs & Trea6	8.63	-0.34	180.80	14.41	0.00	1.73
Mislinja Pera5 & Tera5	43.65	-0.65	141.36	19.38	0.45	0.88
Mislinja Prea6 & Trea6	45.29	0.13	187.35	18.45	0.00	0.95
Dravinja Pobs & Tobs	6.80	-1.85	378.18	2.87	0.00	3.86
Dravinja Pera5 & Tobs	55.28	-4.35	473.36	5.24	0.00	4.30
Dravinja Prea6 & Tobs	167.29	-4.83	543.28	7.46	0.32	48.80
Dravinja Pobs & Tera5	8.22	-0.21	263.16	2.83	0.00	2.40
Dravinja Pobs & Trea6	8.68	-0.47	279.26	2.81	0.00	4.96

Dravinja Pera5 & Tera5	95.77	-0.92	279.71	4.74	0.00	2.10
Dravinja Prea6 & Trea6	132.76	-2.72	461.71	5.90	0.00	5.57
Radovna Pobs & Tobs	3751.83	-0.17	14.29	30.49	0.00	2.77
Radovna Pera5 & Tobs	1370.52	0.06	3.89	37.65	0.00	2.42
Radovna Prea6 & Tobs	1324.46	0.02	0.91	46.51	0.00	2.46
Radovna Pobs & Tera5	518.01	-0.24	96.54	17.29	0.01	0.27
Radovna Pobs & Trea6	757.48	-0.21	95.58	17.53	0.00	0.22
Radovna Pera5 & Tera5	357.80	0.98	76.70	15.61	0.00	3.86
Radovna Prea6 & Trea6	1702.75	0.79	56.26	26.65	0.01	12.20
Kokra Pobs & Tobs	104.58	0.06	135.63	4.33	0.70	9.79
Kokra Pera5 & Tobs	47.04	0.87	68.37	6.28	0.70	9.05
Kokra Prea6 & Tobs	85.71	0.57	131.13	4.67	0.70	10.28
Kokra Pobs & Tera5	116.67	0.45	124.29	3.26	0.00	16.13
Kokra Pobs & Trea6	127.50	0.26	103.91	4.43	0.00	0.56
Kokra Pera5 & Tera5	50.05	0.98	55.82	4.57	0.69	6.91
Kokra Prea6 & Trea6	98.22	0.67	105.71	5.17	0.01	1.19
Poljanska Sora Pobs & Tobs	52.28	0.89	100.87	5.90	0.70	1.02
Poljanska Sora Pera5 & Tobs	84.62	0.70	96.37	7.39	0.75	0.99
Poljanska Sora Prea6 & Tobs	89.85	1.22	144.60	7.43	0.00	0.78
Poljanska Sora Pobs & Tera5	48.62	0.78	95.76	6.26	0.00	1.99
Poljanska Sora Pobs & Trea6	40.867	0.85	106.37	6.15	0.00	2.41
Poljanska Sora Pera5 & Tera5	77.92	0.63	99.51	7.67	0.47	1.79
Poljanska Sora Prea6 & Trea6	78.44	1.22	163.66	7.67	0.27	1.83
Selška Sora Pobs & Tobs	210.04	0.00	212.44	4.54	0.00	3.53
Selška Sora Pera5 & Tobs	71.52	0.43	137.00	6.49	0.56	2.77
Selška Sora Prea6 & Tobs	76.35	0.47	274.26	6.17	0.15	2.74
Selška Sora Pobs & Tera5	267.73	0.49	172.43	4.09	0.69	4.27
Selška Sora Pobs & Trea6	254.20	0.48	192.88	4.13	0.00	10.26
Selška Sora Pera5 & Tera5	87.41	0.91	124.75	5.12	0.29	3.27
Selška Sora Prea6 & Trea6	72.59	1.27	305.81	5.71	0.00	12.61
Mirna Pobs & Tobs	34.57	-0.58	61.13	12.49	0.90	0.24
Mirna Pera5 & Tobs	62.17	-0.13	76.70	10.57	0.98	0.49
Mirna Prea6 & Tobs	116.74	0.31	87.35	12.73	0.98	0.52
Mirna Pobs & Tera5	30.84	-0.65	58.82	13.73	0.05	0.36
Mirna Pobs & Trea6	22.65	-0.92	83.88	12.47	0.00	0.54
Mirna Pera5 & Tera5	56.82	-0.26	84.77	11.53	0.94	0.60
Mirna Prea6 & Trea6	121.62	0.28	90.24	14.59	0.76	0.69
Kolpa Pobs & Tobs	126.00	1.20	46.90	10.18	0.95	0.58
Kolpa Pera5 & Tobs	75.18	1.03	44.70	11.29	0.96	0.54
Kolpa Prea6 & Tobs	47.15	2.19	228.38	6.09	0.69	0.44
Kolpa Pobs & Tera5	126.72	1.10	41.95	11.23	0.93	0.88
Kolpa Pobs & Trea6	132.64	1.10	42.40	11.34	0.89	0.98
Kolpa Pera5 & Tera5	75.94	0.96	41.26	12.25	0.93	0.81
Kolpa Prea6 & Trea6	38.33	2.31	265.73	5.37	0.00	1.23
Lahinja Pobs & Tobs	49.64	-0.00	39.84	22.39	0.95	0.65
Lahinja Pera5 & Tobs	109.72	0.15	40.85	22.68	0.94	0.60
Lahinja Prea6 & Tobs	114.43	0.42	77.47	19.45	0.95	0.72
Lahinja Pobs & Tera5	54.03	-0.04	34.07	25.60	0.97	0.57

Lahinja Pobs & Trea6	53.51	-0.00	40.44	24.49	0.95	0.41
Lahinja Pera5 & Tera5	103.54	0.10	42.52	25.21	0.97	0.61
Lahinja Prea6 & Trea6	114.21	0.45	86.79	21.25	0.95	0.59
Savinja Pobs & Tobs	33.59	0.19	2.51	24.56	0.00	0.42
Savinja Pera5 & Tobs	54.82	0.61	38.94	14.58	0.00	1.49
Savinja Prea6 & Tobs	80.54	0.63	94.01	10.17	0.00	1.66
Savinja Pobs & Tera5	27.59	2.04	80.77	6.47	0.68	6.20
Savinja Pobs & Trea6	26.97	1.97	72.96	6.49	0.00	0.10
Savinja Pera5 & Tera5	49.40	0.90	42.52	11.29	0.68	4.35
Savinja Prea6 & Trea6	82.55	1.05	106.35	8.34	0.00	0.59
Bolska Pobs & Tobs	27.15	0.87	96.13	4.34	0.80	0.72
Bolska Pera5 & Tobs	42.45	0.18	43.26	4.50	0.94	1.56
Bolska Prea6 & Tobs	63.24	0.11	78.25	7.45	0.91	0.77
Bolska Pobs & Tera5	27.12	0.81	96.29	4.51	0.89	2.20
Bolska Pobs & Trea6	27.70	0.84	100.03	4.29	0.96	8.73
Bolska Pera5 & Tera5	41.68	0.12	47.76	5.44	0.93	2.23
Bolska Prea6 & Trea6	61.19	0.04	93.24	7.69	0.90	1.43
Voglanja Pobs & Tobs	138.53	-2.39	167.04	5.50	0.34	0.48
Voglanja Pera5 & Tobs	36.59	-0.33	47.94	27.13	0.42	0.35
Voglanja Prea6 & Tobs	51.41	-0.34	101.49	6.01	0.00	0.30
Voglanja Pobs & Tera5	161.12	-1.39	137.97	3.54	0.95	0.79
Voglanja Pobs & Trea6	159.23	-1.27	140.69	5.57	0.04	0.84
Voglanja Pera5 & Tera5	34.81	-0.16	66.69	3.62	0.96	0.50
Voglanja Prea6 & Trea6	51.94	0.01	89.12	5.78	0.00	0.30
Hudinja Pobs & Tobs	46.70	-0.21	20.42	4.27	0.68	0.45
Hudinja Pera5 & Tobs	84.77	-0.43	43.38	3.85	0.94	1.40
Hudinja Prea6 & Tobs	156.02	-0.10	49.17	5.13	0.96	1.39
Hudinja Pobs & Tera5	43.38	-0.35	24.53	4.33	0.66	0.87
Hudinja Pobs & Trea6	42.25	-0.39	30.57	3.94	0.00	1.85
Hudinja Pera5 & Tera5	76.70	-0.62	45.15	4.57	0.77	1.40
Hudinja Prea6 & Trea6	143.93	-0.25	54.94	5.39	0.54	2.48
Idrijca Pobs & Tobs	7.09	0.74	16.94	8.89	0.96	0.28
Idrijca Pera5 & Tobs	53.34	0.99	36.44	10.05	0.94	0.38
Idrijca Prea6 & Tobs	45.44	1.76	59.07	9.75	0.95	0.32
Idrijca Pobs & Tera5	12.11	0.68	17.08	11.62	0.97	91.41
Idrijca Pobs & Trea6	10.50	0.69	16.97	10.47	0.98	6.33
Idrijca Pera5 & Tera5	57.39	0.86	40.44	10.57	0.93	3.78
Idrijca Prea6 & Trea6	60.62	1.24	39.90	13.80	0.94	1.75
Reka Pobs & Tobs	23.42	0.03	24.93	13.13	0.70	109.03
Reka Pera5 & Tobs	151.08	-1.86	103.11	10.88	0.00	109.03
Reka Prea6 & Tobs	63.79	0.03	124.87	9.44	0.55	109.03
Reka Pobs & Tera5	23.19	-0.00	24.39	14.48	0.42	62.59
Reka Pobs & Trea6	25.27	0.02	21.75	15.13	0.58	0.39
Reka Pera5 & Tera5	146.88	-2.16	108.99	10.80	0.00	100.19
Reka Prea6 & Trea6	58.13	-0.03	137.39	9.70	0.37	4.44
Rižana Pobs & Tobs	230.59	0.77	63.11	11.56	0.72	0.03
Rižana Pera5 & Tobs	162.92	-1.37	174.04	11.45	0.73	0.30
Rižana Prea6 & Tobs	27.93	0.16	201.20	9.78	0.73	0.14

Rižana Pobs & Tera5	230.44	0.58	76.70	12.25	0.99	64.17
Rižana Pobs & Trea6	228.14	0.61	76.70	12.49	0.60	2.80
Rižana Pera5 & Tera5	164.76	-2.14	173.92	12.23	0.02	0.88
Rižana Prea6 & Trea6	28.19	-0.26	213.12	10.42	0.02	12.45

As a general trend, it can be observed that the X1 (capacity of production store), X3 (capacity of routing store) and X6 (degree-day melt coefficient) parameters derived from the reanalysis products show the most deviation from their initial value, especially under configurations 2, 3, 6, 7, where reanalysis P is inserted in the model. Strong deviations in the X2 (intercatchment exchange coefficient) and X4 (unit hydrograph time constant) parameters occur mostly in drainage areas where reanalysis precipitation is in strong disagreement with observations (e.g., $IOA_{VOGLANJA}$). The X6 variable is especially sensitive to strong variations between reanalysis and station temperature (conf. 4-7, GR4H CemaNeige) (e.g., $IOA_{RADOVNA}$, $IOA_{DRAVINJA\text{-}REA6}$, $IOA_{SAVINJA\text{-}REA6}$).

Figure 16 and **Figure 18** show the performance of each data configuration for the GR4H and GR4H CemaNeige modules, respectively. In the GR4H module, simulations based on observed atmospheric variables perform adequately for twelve and nine watersheds in each study period. Exceptional performance (KGE{0.8-1}) is exhibited in the Selška Sora, Poljanska Sora, Radovna and Mislinja watersheds for the first half of the simulation, while good performance (KGE{0.6-0.8}) is exhibited in the Rižana, Idrijca, Kolpa, Mirna, Selška Sora, Poljanska Sora, Radovna and Mislinja watersheds during the validation period. For the calibration period, good performance is observed for configuration (conf.) 2 in Poljanska Sora and Kolpa, and Rižana for conf. 3. The recalibration of the model parameters leads to improvement in all cases, with the exception of Mislinja, Poljanska Sora , Rižana and Lahinja for conf. 3, and Poljanska Sora and Kolpa for conf. 2.

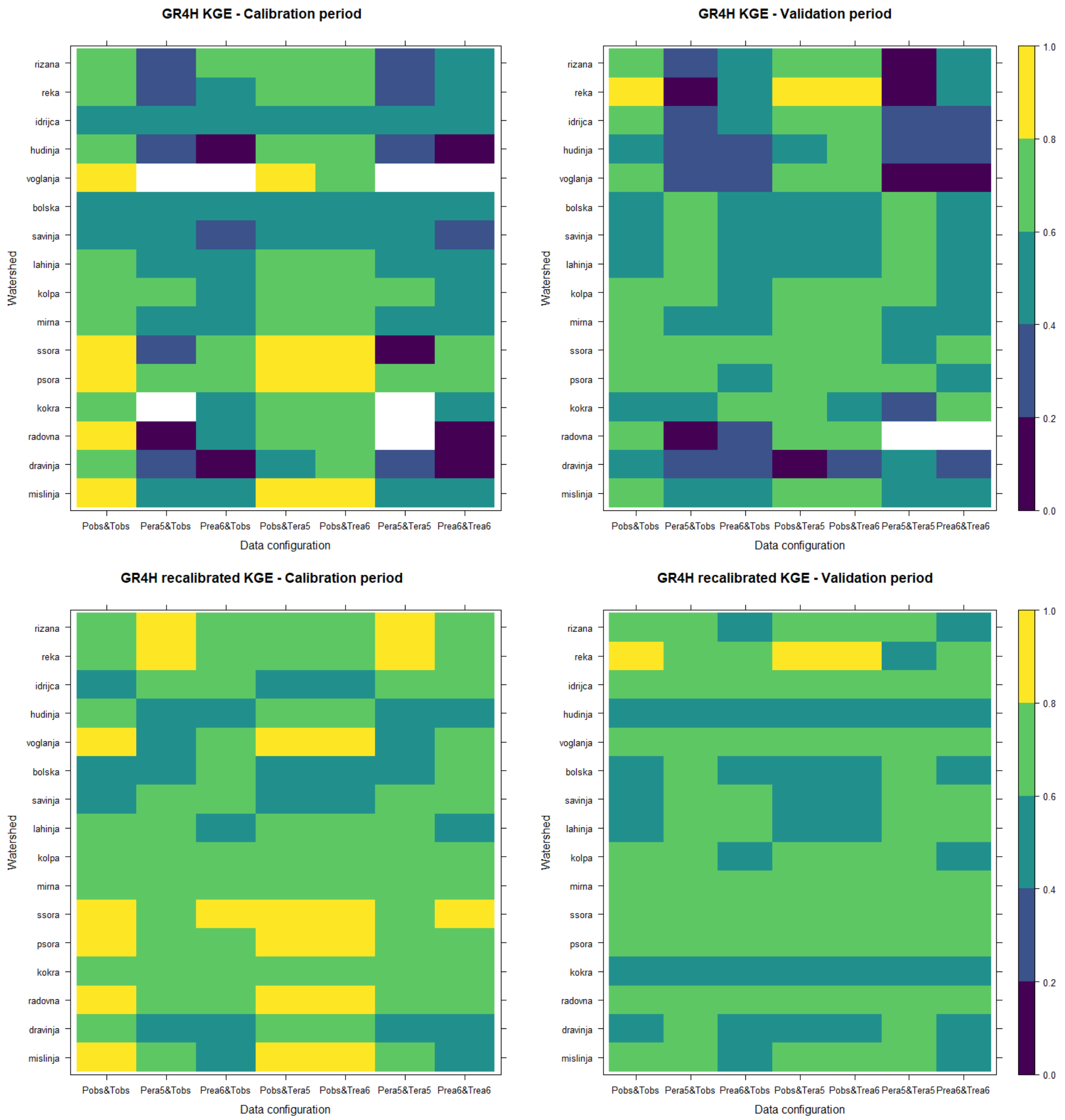

Figure 16: KGE discharge scores - GR4H

For conf. 4 and 5, reanalyses perform similarly to observations, with the exception of the Dravinja and Radovna stations. Recalibrating the model seems to be effective only in the aforementioned stations. Conf. 6 and 7 lead to poor results, with values out of bounds for the Voglanja, Kokra and Radovna catchments. Adequate results are present in Poljanska Sora and Kolpa for conf. 6, and Poljanska Sora and Selška Sora for conf. 7. Recalibration of the model parameters improves significantly performance, introducing good results for catchments with initial KGE values out of bounds. ERA5 and REA6 reanalyses outperform observations in the Rižana, Reka, Idrijca, Voglanja, Savinja and Voglanja, Bolska, Savinja watersheds, respectively. During the validation period, conf. 2 performs poorly in most cases, except for Selška Sora, Poljanska Sora , Kolpa, Lahinja, Savinja and Bolska, and conf. 3 performs well in the Selška Sora, Kokra and Kolpa watersheds. Recalibration of the parameters leads to significant improvement for configuration 2, while performance actually worsens for conf. 3 in the Kokra station. Compared to observations, REA6 and ERA5 temperatures lead to improved simulations in the Hudinja and Kokra catchments, respectively. REA6 precipitation and temperature is consistent with observations in Selška Sora, Lahinja, Savinja and Bolska, while ERA5 is in agreement with observations in the Poljanska Sora , Kolpa and Dravinja catchments. Conf. 7 outperforms conf. 6 in the Reka, Rižana, Selška Sora and Kokra stations. Recalibration leads to 10 good ERA5 performances, compared to the previous five, proving its effectiveness.

Simulations tend to be adequate for observations closer to the median value. This is illustrated in **Figure 17**, where KGE efficiency was applied for values in the {1-25} and {75-99} percentiles throughout both study periods for all catchments in the GR4H model. Performance is poor for all catchments, with the exception of Selška Sora under conf. 3 and 6. Especially in low streamflow rates, KGE is out of bounds for most catchments in at least one conf.

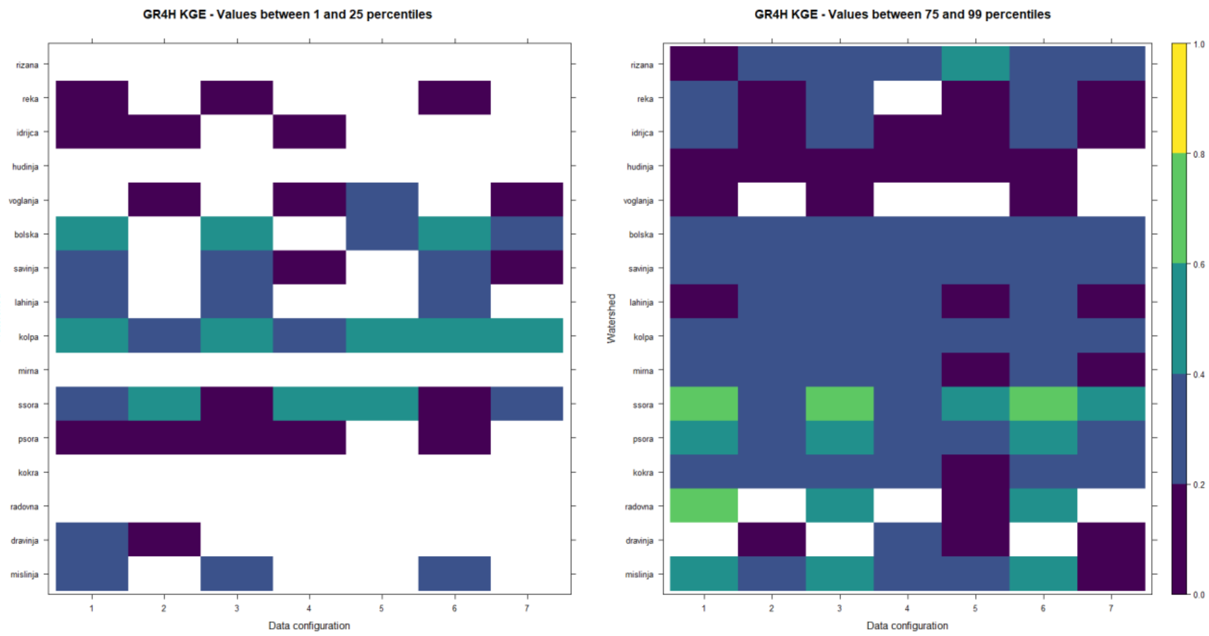

Figure 17: KGE efficiency (GR4H, calibration and validation period) for the {1-25} and {75-99} percentiles

Nine and seven catchments are simulated effectively using observed P and T for the calibration and validation period, respectively. Altough a smaller percentage of the selected catchments is accurately modeled in comparison with the GR4H module, KGE efficiency lies between 0.8-1 for five catchments in the calibration period, and three in the validation period. Conf. 2 and 3 perform well in the Poljanska Sora , Mirna, Kolpa and Lahinja stations. All cases perform well during the recalibration process, with the exception of conf. 2 in the Kokra and Savinja catchments. Similar performance to observations is present for conf. 4 and 5 vs conf. 1, except for the Voglanja, Kolpa, Mirna, and Mislinja stations. Reanalysis T outperforms observations in the Lahinja, Kokra and Radovna stations. Model parameter calibration improves performance in seven catchments. In both GR4H and GR4H CemaNeige modules, conf. 6 and 7 are in agreement with observations for the Rižana, Reka and Bolska catchments, although performance is considered poor (KGE{0.4-0.6}). However, in the CemaNeige module, ERA5 P and T performs similarly to observations also in Savinja, Kolpa, Poljanska Sora and Dravinja.

Furthermore, REA6 agrees with observations in the Savinja, Lahinja and Kokra catchments. By recalibrating the model parameters, conf. 6 and 7 outperform observations in 10 and 6 catchments, respectively. Additionally, all stations acquire acceptable KGE values, especially Hudinja and Radovna for conf. 4, 5, 6, 7. Seven catchments (conf. 6) show good results (KGE{0.6-0.8}) in the validation period for GR4H CemaNeige, compared to four for GR4H, four of which outperform observations. REA6 performs well only in the Kolpa, Selška Sora and Poljanska Sora stations. Recalibration improves significantly six catchments for conf. 6 and three catchments for conf. 7. For the purpose of this study, KGE values ≥ 0.6 are considered acceptable. For both study periods, ERA5 and REA6 are mostly in agreement under conf. 4 and 5. Both perform adequately for most catchments in the GR4H and recalibrated GR4H and GR4H CemaNeige modules, which is to be expected since T is not as impactful as P in rainfall-runoff simulations.

Table 15: ERA5 and REA6 intercomparison

	GR4H	GR4H RC	GR4H CemaNeige	GR4H CemaNeige RC	Intercomparison
Conf. 2 and 3	3	16	3	13	ERA5~REA6
Conf. 4 and 5	20	21	14	19	
Conf. 6 and 7	1	14	2	18	
Conf. 2 and 3	6	8	8	6	ERA5>REA6
Conf. 4 and 5	-	-	14	5	
Conf. 6 and 7	6	9	8	7	
Conf. 2 and 3	5	2	3	6	ERA5<REA6
Conf. 4 and 5	2	-	-	2	
Conf. 6 and 7	3	4	2	4	

Table 15 shows the No. of catchments for which acceptable modeling results are present, when ERA5 and REA6 perform similarly, ERA5 outperforms REA6, and REA6 is superior to ERA5. ERA5 provides more acceptable performance than REA6 for most cases in the GR4H CemaNeige and GR4H modules under conf. 2 and 3, GR4H CemaNeige module under conf. 4 and 5, and all four model setups under conf. 6 and 7.

The performance improvement by means of recalibration is more profound under conf. 2, 3, 6 and 7. Recalibration of model parameters is deemed unnecessary under conf. 4 and 5, since a total of 22 and 28 adequate simulations (out of a total of 32 simulations) are achieved in the GR4H and GR4H CemaNeige modules, which are then reduced to 21 and 26, respectively, post-recalibration. Almost double the amount of watersheds are simulated well after the recalibration process under conf. 2 and 3 (26 vs 14 and 25 vs 14 in GR4H and GR4H CemaNeige, respectively). When using reanalysis P and T, recalibration proves to be even more effective, with a total of 27 vs 10 succesful simulations in GR4H, and 29 vs 12 succesful simulations in GR4H CemaNeige. Moreover, GR4H CemaNeige shows better skill in exploiting reanalysis information, since a greater number of watersheds display good performance in comparison to GR4H. This is expected, since snowmelt is taken into account during the simulation process. Improvements are notable especially for REA6 in the Mirna, Kolpa and Selška Sora alpine catchments during the calibration period.

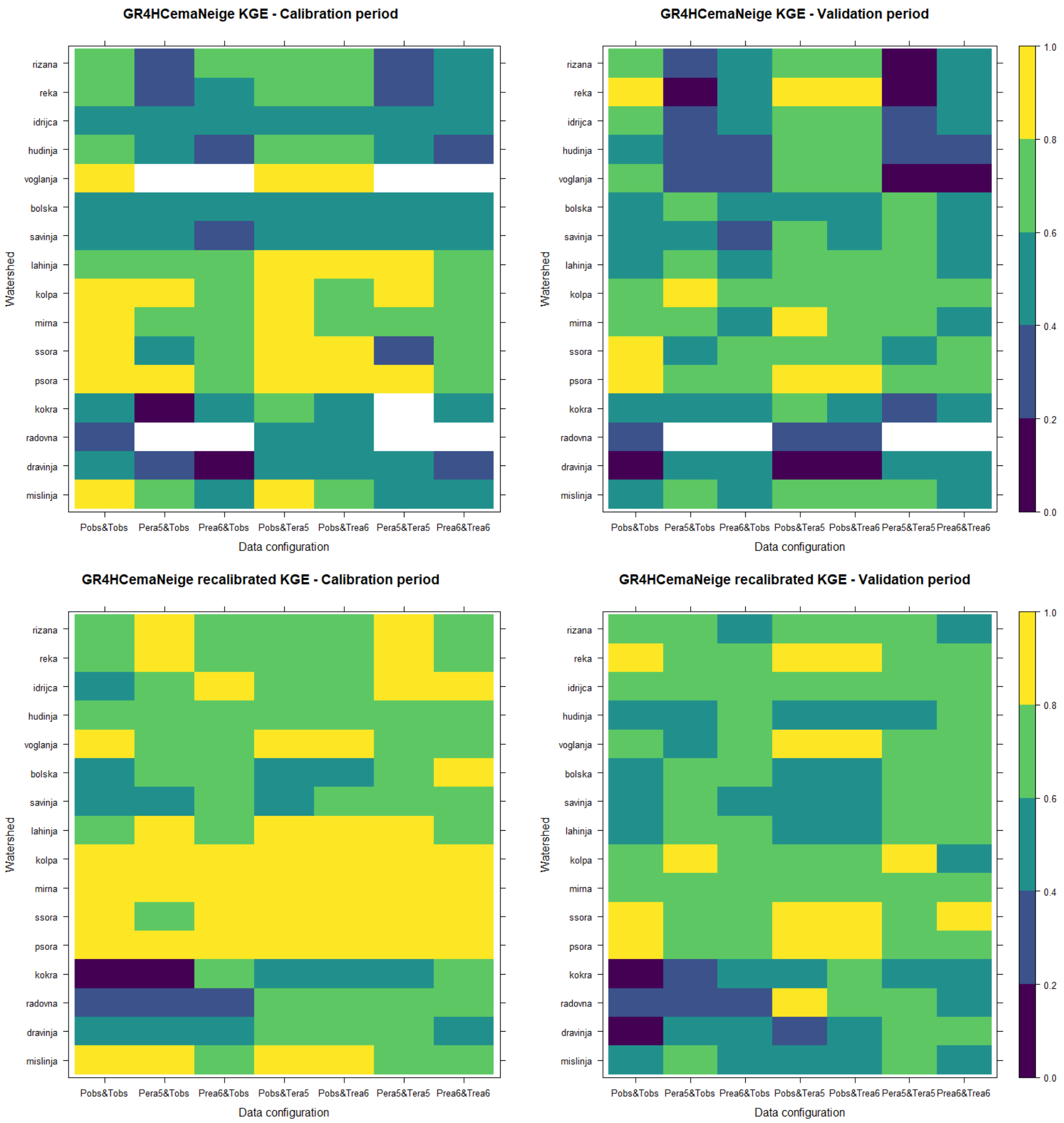

Figure 18: KGE discharge scores - GR4H CemaNeige

Regarding P reanalysis: the mediterranean-pluvial nival catchments perform poorly under conf. 2, 3, 6, 7, with the exception of REA6 for the Rižana catchment. However, recalibration of the models improves dramatically the performance of ERA5 in both stations. The Bolska dinaric-pluvial nival catchment was not modeled adequately using observed data, however ERA5 provides reliable results during the validation period under conf. 2 and 6 (GR4H-GR4H CemaNeige). Recalibration of the model parameters proves to be effective for improved performance in the GR4H module for both reanalyses. Proper set-up for Lahinja was feasible exclusively during the calibration period, with reanalyses performing similar to observations only in the GR4H module. In the validation period, ERA5 proves to be a good substitute under conf. 2 and 6. Dravinja performance is poor under almost all configurations. Reanalyses perform very good for both study periods in the Mirna basin exclusively in the GR4H module, which is expected since the watershed is comprised mostly from low-land areas. In the Poljanska Sora alpine catchment, reanalyses perform well except for REA6 in the GR4H CemaNeige validation period, however results improve with further refinement of the model parameters. REA6 outperforms ERA5 in the alpine Selška Sora station in most cases, but not significantly. Hudinja reanalysis is poor, and parameter calibration is effective in the GR4H module during the calibration period. For the Savinja alpine basin, recalibration of the parameters aids in adequate model performance under conf. 6 and 7 for both study periods. Kolpa simulations perform well and are consistent with observations, and in this case the recalibration process does not prove to be beneficial.

Temperature data quality does not impact significantly simulation results. ERA5 T data quality is superior to REA6, however REA6 Qs is superior to ERA5 in the Reka, Hudinja, Bolska, Lahinja and Poljanska Sora watersheds in both GR4H and GR4H CemaNeige modules, emphasizing how P quality holds more importance in rainfall-runoff applications. Furthermore, when assessing P quality, this study shows how various efficiency metrics may not be good predictors of its rainfall-runoff performance. The ERA5 IOA index is superior to REA6 in the Rižana, Reka, Selška Sora, Kokra, Radovna and Idrijca catchments. Nonetheless, REA6 Qs is superior to ERA5 in the Selška Sora and Kokra stations in the GR4H and GR4H CemaNeige modules during the calibration period, in the Idrijca station during the validation period, and Reka, Rižana during both study periods. According to **Figure 5** and **Figure 6**, datasets that compute approximately the same amount of annual rainfall to observations do not guarantee good rainfall-runoff results, which is the case for Kolpa (conf. 3-both study periods-GR4H), Rižana (conf. 2-calibration period-GR4H-GR4H CemaNeige, conf. 2 and 3-validation period-GR4H-GR4H CemaNeige) and Hudinja (conf. 2 and 3-both study periods-GR4H-GR4H CemaNeige). The ERA5 POD index is superior to REA6 in all 16 watersheds (**Figure 6**). Still, REA6 Qs outperforms REA5 Qs for the calibration period in Hudinja, Selška Sora (GR4H) and Kokra (GR4H CemaNeige), for the validation period in Idrijca (GR4H-GR4H CemaNeige) and Selška Sora (GR4H CemaNeige), and for both study periods in Rižana, Reka (GR4H-GR4H CemaNeige), Radovna and Kokra (GR4H). FAR scores are good for the Reka, Idrijca, Hudinja, Radovna, Dravinja and Mislinja stations (**Figure 6**). During both study periods, their discharge performance is sub-optimal under conf. 2 and 3 (GR4H-GR4H CemaNeige). Poor results directly exported for the Dravinja watershed (conf. 2-3, GR4H, calibration and validation period) are illustrated in **Figure 19**. Discharge is consistently overestimated by model predictions, especially during periods of low streamflow rates. The phenomenon is more profound during the calibration period.

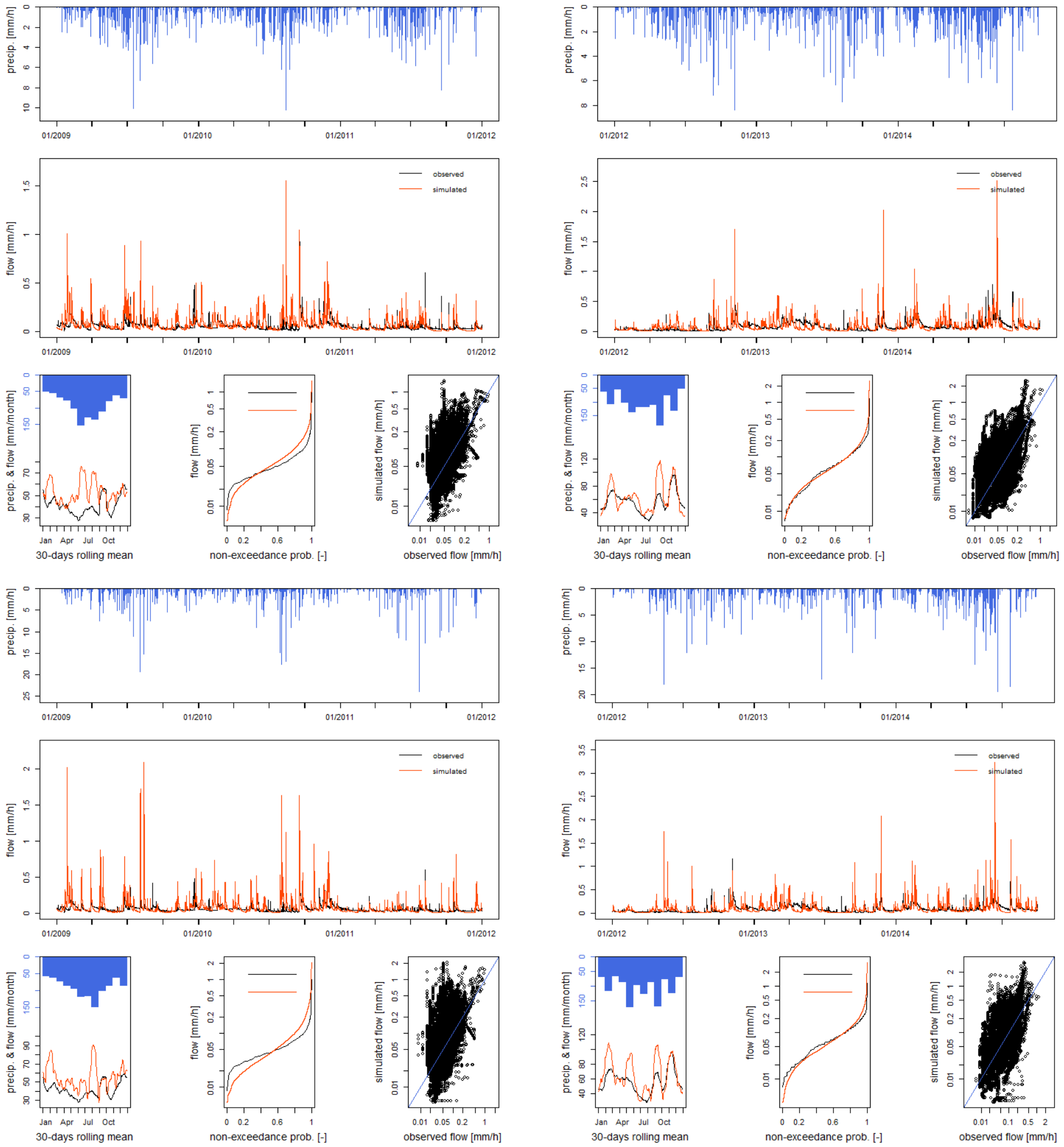

Figure 19: Dravinja GR4H results for configurations 2 (top) and 3 (bottom)

Correlation measurements may be providing some information for hydrological results. Good performance is present for 12 (calibration period) and 9 watersheds (validation period) for GR4H, and 9 (calibration period) and 7 watersheds (validation period) for GR4H CemaNeige, using observed P and T (**Table 12**). In GR4H, only two and three catchments perform good under conf. 2 and 3, respectively, during the calibration period. Results tend to be better during the validation period for conf. 2. A more thorough investigation is required on the matter, by applying the same metrics on the reanalyses when split-sampled, in addition to the inspection of the P stations used on each study period during the construction of the representative time-series. PBIAS displays more potential on forecasting hydrological performance for PPs. It can be observed that: for Voglanja, PBIAS {-60, -90} with all KGE values out of bounds in conf. 2, 3, 6, 7 (**Figure 10**). REA6 PBIAS{-30, -60} leads to KGE{0.2, 0.6} or out of bounds values for Reka, Idrijca and Radovna stations. REA6 PBIAS{30,60} results in KGE{0.0, 0.6} for

Dravinja and Savinja. REA6 PBIAS{-10, -30} leads to KGE{0, 0.6} in the Mislinja, Kolpa, Hudinja and Rižana catchments, except for Rižana during the calibration period (GR4H-GR4H CemaNeige) under conf. 3, and Kolpa during both study periods (GR4H CemaNeige). For Rižana, ERA5 PBIAS{90, 120} results in KGE values in the {0, 0.4} range under conf. 2, 4, 6, 7. ERA5 PBIAS{-30, -60} leads to KGE{0.0, 0.6} in the Radovna, Kokra and Mirna basins, except for Mirna during both study periods (GR4H CemaNeige). Nevertheless, a deeper investigation on the matter is deemed necessary in order to make further conclusions.

In general, conf. 2, 3, 6, 7 are better able to capture stream flow dynamics for larger drainage areas, namely catchments whose area exceeds 200 km^2. With the exception of Selška Sora, a minimal amount of adequate simulations are observed under any configuration for the Dravinja, Radovna, Kokra, Bolska, Voglanja and Hudinja catchments. This is to be expected, since it was not feasible to set-up a rainfall-runoff model that matches observed discharge using their respective weather stations. The drainage area of these catchments covers a small percentage of the available gauge network spatial domain. Regarding the present study, the poor simulation performance of the Radovna, Voglanja and Hudinja watersheds can be attributed to the location of the precipitation stations used in order to construct the representative time-series. Interestingly, for Kolpa, P station No. 498 was used, which was located approximately 16 km away from the catchment's centroid. This is the catchment with the second-best number of acceptable simulation results amongst all selected basins (conf. 2, 3, 6, 7), with KGE{0.6-1} under conf. 1 (GR4H-GR4H CemaNeige) for both study periods. This may suggest that P station location may not hold as much significance as previously assumed. The results show that rainfall intensity may not vary significantly across some of the country's regions. Generally, reanalysis P was better able to substitute observed P in watersheds that follow either alpine or dinaric pluvial-nival regimes. Under conf. 2, 3, 6, 7, Poljanska Sora , Kolpa, Selška Sora and Lahinja had the greatest number of acceptable model results. REA6 outperformed ERA5 exclusively in the Selška Sora watershed. Furthermore, no remarkable deductions can be made between simulation results and watershed location within the country.

4 CONCLUSIONS

A thorough assessment of two reanalysis datasets has been made in this study. Its significance lies in the comparison of these reanalyses at the hourly temporal scale, which to the author's best knowledge at the time of writing, has not been performed in regions within the European border. For the period 2009-2014, an evaluation of the ERA5 and REA6 PPs and TPs has been made against observations for 16 watersheds located within the borders of Slovenia. This evaluation was performed using the BR, Pearson correlation coefficient, PBIAS and IOA metrics. Findings indicate that ERA5 P is superior to REA6 P when compared against observations, based on the selected performance metrics. ERA5 tends to overestimate the amount of rainfall in most basins, while REA6 is mostly underestimating it. Both T reanalyses rank similary, albeit ERA5 shows stronger resemblance to observations. ERA5 displays superiority in rainfall detection skills, while its FAR is consistent with ERA6 in 80% of the cases, with good results in 70% of the study domain.

The potential of these two reanalyses in hydrological applications was investigated using the lumped conceptual rainfall-runoff GR4H and GR4H CemaNeige models, using a split-sampling scheme. Six different configurations were tested (three per each individual product), in order to fully capture the modeling capacity of reanalysis P and T. Additionally, each model was executed twice. An initial run was performed by calibrating the model parameters using observed P and T. Then, a second run was carried out, where model parameters were recalibrated for each individual reanalysis configuration, in order to identify the potential of this specific lumped conceptual rainfall-runoff model to predict streamflow dynamics. That way, it is examined whether the four parameters ingrained within the model can make up for poor P data quality. Moreover, it was tested whether the goodness-of-fit measures applied in the atmospheric variables could give an insight on their hydrological performance. As expected, the quality of temperature data does not impact significantly modeling performance, and both reanalyses can be used as a proxy when observations are absent. When using reanalysis P, GR4H CemaNeige performs comparatively better to GR4H, especially during the calibration period, which is expected since two additional parameters are recalibrated within the model to describe the rainfall-runoff process. This phenomenon is more profound in alpine catchments, where a greater amount of precipitation is induced by snowmelt. Depending on basin selection, inserting both reanalysis variables in the model, instead of using exclusively reanalysis P, can either improve or impair simulation results. Constant recalibration of model parameters proved to be beneficial in most watersheds under all configurations, removing out of bounds KGE values and further improving performance for basins that were already exhibiting acceptable results, validating the initial hypothesis. From all the efficiency metrics applied to the atmospheric variables, PBIAS is possibly the only indicator that can forecast their hydrological performance, although a more thorough investigation is required.

All in all, the present study shows that the non-bias corrected ERA5 and REA6 reanalyses produce mixed results when applied in hydrological applications, although they tend to be more adequate for large basins that follow alpine pluvial-nival regimes with high streamflow rates. Findings showed that no definitive conclusions can be made between reanalysis performance and watershed location across the country. ERA5 outperforms REA6 in most cases, however this effect is subsided if the calibration of the model parameters is based on newly-introduced input data. Indeed, constant parameter calibration proved beneficial in both GR4H and GR4H CemaNeige models, especially in the dinaric and mediterranean pluvial watersheds. These results suggest that the non-bias corrected reanalysis products used in this study may be used as a proxy for continuous rainfall-runoff simulations scaled down to the hourly timestep. Nonetheless, more research is required before their application in ungauged basins.

5 REFERENCES

Amitai, E. *et al.* (2012) 'Multiplatform comparisons of rain intensity for extreme precipitation events', *IEEE Transactions on Geoscience and Remote Sensing*, 50(3), pp. 675–686. doi: 10.1109/TGRS.2011.2162737.

Amjad, M. *et al.* (2020) 'Performance evaluation of satellite- and model-based precipitation products over varying climate and complex topography', *Journal of Hydrology*, 584, p. 124707. doi: 10.1016/J.JHYDROL.2020.124707.

Andersson, J. C. M. *et al.* (2017) 'Process refinements improve a hydrological model concept applied to the Niger River basin', *Hydrological Processes*, 31(25), pp. 4540–4554. doi: 10.1002/HYP.11376.

Arsenault, R. *et al.* (2019) 'Streamflow prediction in ungauged basins: analysis of regionalization methods in a hydrologically heterogeneous region of Mexico', *Hydrological Sciences Journal*, 64(11), pp. 1297–1311. doi: 10.1080/02626667.2019.1639716.

Ashouri, H. *et al.* (2015) 'PERSIANN-CDR: Daily precipitation climate data record from multisatellite observations for hydrological and climate studies', *Bulletin of the American Meteorological Society*, 96(1), pp. 69–83. doi: 10.1175/BAMS-D-13-00068.1.

Bao, Z. *et al.* (2012) 'Comparison of regionalization approaches based on regression and similarity for predictions in ungauged catchments under multiple hydro-climatic conditions', *Journal of Hydrology*, 466–467, pp. 37–46. doi: 10.1016/J.JHYDROL.2012.07.048.

Barszcz, M. P. (2019) 'Quantitative rainfall analysis and flow simulation for an urban catchment using input from a weather radar',*Journal of Hydrological Sciences, http://www.tandfonline.com/action/journalInformation?show=aimsScope&journalCode=tgnh20#.VsXodSCLRhE*, 10(1), pp. 2129–2144. doi: 10.1080/19475705.2019.1682065.

Beck, H. E. *et al.* (2017) 'Global-scale evaluation of 22 precipitation datasets using gauge observations and hydrological modeling', *Hydrology and Earth System Sciences*, 21(12), pp. 6201–6217. doi: 10.5194/HESS-21-6201-2017.

Beck, H. E. *et al.* (2019) 'Daily evaluation of 26 precipitation datasets using Stage-IV gauge-radar data for the CONUS', *Hydrology and Earth System Sciences*, 23(1), pp. 207–224. doi: 10.5194/hess-23-207-2019.

Becker, A. *et al.* (2013) 'A description of the global land-surface precipitation data products of the Global Precipitation Climatology Centre with sample applications including centennial (trend) analysis from 1901-present', *Earth System Science Data*, 5(1), pp. 71–99. doi: 10.5194/ESSD-5-71-2013.

Berenguer, M. *et al.* (2005) 'Hydrological Validation of a Radar-Based Nowcasting Technique', *Journal of Hydrometeorology*, 6(4), pp. 532–549. doi: 10.1175/JHM433.1.

Berg, P., Feldmann, H. and Panitz, H. J. (2012) 'Bias correction of high resolution regional climate model data', *Journal of Hydrology*, 448–449, pp. 80–92. doi: 10.1016/j.jhydrol.2012.04.026.

Bhattacharya, T., Khare, D. and Arora, M. (2019) 'A case study for the assessment of the suitability of gridded reanalysis weather data for hydrological simulation in Beas river basin of North Western Himalaya', *Applied Water Science*, 9(4), pp. 1–15. doi: 10.1007/s13201-019-0993-x.

Bollmeyer, C. and Keller, J. (2015) 'A high-resolution regional reanalysis for the European CORDEX domain A high resolution regional reanalysis for the European CORDEX domain HErZ - Climate Monitoring Branch', (April), pp. 0–11.

Burn, D. H. and Boorman, D. B. (1993) 'Estimation of hydrological parameters at ungauged catchments', *Journal of Hydrology*, 143(3–4), pp. 429–454. doi: 10.1016/0022-1694(93)90203-L.

Castaneda-Gonzalez, M. *et al.* (2018) 'Impacts of Regional Climate Model Spatial Resolution on Summer Flood Simulation', *EPiC Series in Engineering*, 3, pp. 372–380. doi: 10.29007/HD8L.

Cecinati, F. *et al.* (2017) 'Optimal Temporal Resolution of Rainfall for Urban Applications and Uncertainty Propagation', *Water 2017, Vol. 9, Page 762*, 9(10), p. 762. doi: 10.3390/W9100762.

Chen, J., Brissette, F. P. and Chen, H. (2018) *Using reanalysis-driven regional climate model outputs for hydrology modelling*, *Hydrological Processes*. doi: 10.1002/hyp.13251.

Chen, S. *et al.* (2013) 'Performance evaluation of radar and satellite rainfalls for Typhoon Morakot over Taiwan: Are remote-sensing products ready for gauge denial scenario of extreme events?', *Journal of Hydrology*, 506, pp. 4–13. doi: 10.1016/J.JHYDROL.2012.12.026.

Ciabatta, L. *et al.* (2018) 'SM2RAIN-CCI: A new global long-term rainfall data set derived from ESA CCI soil moisture', *Earth System Science Data*, 10(1), pp. 267–280. doi: 10.5194/ESSD-10-267-2018.

Dee, D. P. *et al.* (2011) 'The ERA-Interim reanalysis: configuration and performance of the data assimilation system', *Quarterly Journal of the Royal Meteorological Society*, 137(656), pp. 553–597. doi: 10.1002/QJ.828.

Dinku, T. *et al.* (2007) 'Validation of satellite rainfall products over East Africa's complex topography', *International journal of remote sensing, http://dx.doi.org/10.1080/01431160600954688*, 28(7), pp. 1503–1526. doi: 10.1080/01431160600954688.

Egbuniwe, N. and Todd, D. K. (1976) 'Application of the Stanford Watershed Model To Nigerian Watersheds', *JAWRA Journal of the American Water Resources Association*, 12(3), pp. 449–460. doi: 10.1111/j.1752-1688.1976.tb02710.x.

Emerton, R. *et al.* (2017) 'Complex picture for likelihood of ENSO-driven flood hazard', *Nature Communications 2017 8:1*, 8(1), pp. 1–9. doi: 10.1038/ncomms14796.

Essou, G. R. C. *et al.* (2016) 'Can precipitation and temperature from meteorological reanalyses be used for hydrological modeling?', *Journal of Hydrometeorology*, 17(7), pp. 1929–1950. doi: 10.1175/JHM-D-15-0138.1.

Essou, G. R. C., Brissette, F. and Lucas-Picher, P. (2017) 'The Use of Reanalyses and Gridded Observations as Weather Input Data for a Hydrological Model: Comparison of Performances of Simulated River Flows Based on the Density of Weather Stations', *Journal of Hydrometeorology*, 18(2), pp. 497–513. doi: 10.1175/JHM-D-16-0088.1.

Fang, G. H. *et al.* (2015) 'Comparing bias correction methods in downscaling meteorological variables for a hydrologic impact study in an arid area in China', *Hydrology and Earth System Sciences*, 19(6), pp. 2547–2559. doi: 10.5194/HESS-19-2547-2015.

Fowler, K. *et al.* (2018) 'Simulating Runoff Under Changing Climatic Conditions: A Framework for Model Improvement', *Water Resources Research*, 54(12), pp. 9812–9832. doi: 10.1029/2018WR023989.

Frantar, P., Dolinar, M. and Kurnik, B. (2008) 'Water balance of Slovenia 1971 – 2000', *IOP Conference Series: Earth and Environmental Science*, 4(1), p. 012020. doi: 10.1088/1755-1307/4/1/012020.

Gao, Y. *et al.* (2016) 'Radar-rainfall estimation from S-band Radar and its impact on the runoff simulation of a heavy rainfall event in the Huaihe River basin', *Journal of the Meteorological Society of Japan*, 94(1), pp. 75–89. doi: 10.2151/jmsj.2016-005.

Gelaro, R. *et al.* (2017) 'The Modern-Era Retrospective Analysis for Research and Applications, Version 2 (MERRA-2)', *Journal of Climate*, 30(14), pp. 5419–5454. doi: 10.1175/JCLI-D-16-0758.1.

Germann, U. *et al.* (2006) 'Radar precipitation measurement in a mountainous region', *Quarterly Journal of the Royal Meteorological Society*, 132(618), pp. 1669–1692. doi:

10.1256/QJ.05.190.
Ghaju, S. and Alfredsen, K. (2016) 'Evaluation of Satellite Based Precipitations and Their Applicability for Rainfall Runoff Modelling in Narayani Basin of Nepal', *Journal of Hydrology and Meteorology*, 8(1), pp. 22–31. doi: 10.3126/jhm.v8i1.15569.
Gilewski, P. and Nawalany, M. (2018) 'Inter-comparison of Rain-Gauge, Radar, and Satellite (IMERG GPM) precipitation estimates performance for rainfall-runoff modeling in a mountainous catchment in Poland', *Water (Switzerland)*, 10(11), pp. 1–23. doi: 10.3390/w10111665.
Giuseppe, F. Di *et al.* (2016) 'The Potential Predictability of Fire Danger Provided by Numerical Weather Prediction', *Journal of Applied Meteorology and Climatology*, 55(11), pp. 2469–2491. doi: 10.1175/JAMC-D-15-0297.1.
Gottschalk, L. *et al.* (1979) 'Hydrologic regions in the Nordic countries.', *Nordic Hydrology*, 10(5), pp. 273–286. doi: 10.2166/nh.1979.0010.
Goudenhoofdt, E., Delobbe, L. and Willems, P. (2017) 'Regional frequency analysis of extreme rainfall in Belgium based on radar estimates', *Hydrology and Earth System Sciences*, 21(10), pp. 5385–5399. doi: 10.5194/hess-21-5385-2017.
Grimley, L. E., Quintero, F. and Krajewski, W. F. (2020) 'Streamflow predictions in a small urban-rural watershed: The effects of radar rainfall resolution and urban rainfall-runoff dynamics', *Atmosphere*, 11(8). doi: 10.3390/ATMOS11080774.
Gupta, H. V. *et al.* (2009) 'Decomposition of the mean squared error and NSE performance criteria: Implications for improving hydrological modelling', *Journal of Hydrology*, 377(1–2), pp. 80–91. doi: 10.1016/J.JHYDROL.2009.08.003.
Gupta, H. V., Sorooshian, S. and Yapo, P. O. (1999) 'Status of Automatic Calibration for Hydrologic Models: Comparison with Multilevel Expert Calibration', *Journal of Hydrologic Engineering*, 4(2), pp. 135–143. doi: 10.1061/(ASCE)1084-0699(1999)4:2(135).
Hafizi, H. and Sorman, A. A. (2021) 'Assessment of Satellite and Reanalysis Precipitation Products for Rainfall–Runoff Modelling in a Mountainous Basin', *Environmental Sciences Proceedings*, 8(1), p. 25. doi: 10.3390/ecas2021-10345.
Haylock, M. R. *et al.* (2008) 'A European daily high-resolution gridded data set of surface temperature and precipitation for 1950–2006', *Journal of Geophysical Research: Atmospheres*, 113(D20), p. 20119. doi: 10.1029/2008JD010201.
He, Y., Bárdossy, A. and Zehe, E. (2011) 'A review of regionalisation for continuous streamflow simulation', *Hydrology and Earth System Sciences*, 15(11), pp. 3539–3553. doi: 10.5194/hess-15-3539-2011.
Hénin, R. *et al.* (2018) 'Assessing the Use of Satellite-Based Estimates and High-Resolution Precipitation Datasets for the Study of Extreme Precipitation Events over the Iberian Peninsula', *Water 2018, Vol. 10, Page 1688*, 10(11), p. 1688. doi: 10.3390/W10111688.
Hersbach, H. *et al.* (2020) 'The ERA5 global reanalysis', *Quarterly Journal of the Royal Meteorological Society*, 146(730), pp. 1999–2049. doi: 10.1002/QJ.3803.
Heuvelink, D. *et al.* (2020) 'Hydrological application of radar rainfall nowcasting in the Netherlands', *Environment International*, 136, p. 105431. doi: 10.1016/J.ENVINT.2019.105431.
Hou, A. Y. *et al.* (2008) 'Global precipitation measurement', *Precipitation: Advances in Measurement, Estimation and Prediction*, pp. 131–169. doi: 10.1007/978-3-540-77655-0_6.
Hrachowitz, M. *et al.* (2013) 'A decade of Predictions in Ungauged Basins (PUB)-a review', *Hydrological Sciences Journal*, 58(6), pp. 1198–1255. doi: 10.1080/02626667.2013.803183.
Huffman, G. J. *et al.* (2007) 'The TRMM Multisatellite Precipitation Analysis (TMPA): Quasi-global, multiyear, combined-sensor precipitation estimates at fine scales', *Journal of Hydrometeorology*, 8(1), pp. 38–55. doi: 10.1175/JHM560.1.
Huffman, G. J. *et al.* (2010) 'The TRMM Multi-Satellite Precipitation Analysis (TMPA)',

Satellite Rainfall Applications for Surface Hydrology, pp. 3–22. doi: 10.1007/978-90-481-2915-7_1.

Islam, M. A. and Cartwright, N. (2020) ‘Evaluation of climate reanalysis and space-borne precipitation products over Bangladesh’, *Hydrological Sciences Journal*, 65(7), pp. 1112–1128. doi: 10.1080/02626667.2020.1730845.

Isotta, F. A. *et al.* (2014) ‘The climate of daily precipitation in the Alps: development and analysis of a high-resolution grid dataset from pan-Alpine rain-gauge data’, *International Journal of Climatology*, 34(5), pp. 1657–1675. doi: 10.1002/JOC.3794.

James, L. D. (1972) ‘Hydrologic modeling, parameter estimation, and watershed characteristics’, *Journal of Hydrology*, 17(4), pp. 283–307. doi: 10.1016/0022-1694(72)90089-3.

Jeffrey, S. J. *et al.* (2001) ‘Using spatial interpolation to construct a comprehensive archive of Australian climate data’, *Environmental Modelling & Software*, 16(4), pp. 309–330. doi: 10.1016/S1364-8152(01)00008-1.

Jiang, Q. *et al.* (2021) *Evaluation of the ERA5 reanalysis precipitation dataset over Chinese Mainland*, *Journal of Hydrology*. Elsevier B.V. doi: 10.1016/j.jhydrol.2020.125660.

Josephine, V. S., Mudgal, B. V. and Thampi, S. B. (2014) ‘Applicability of Doppler weather radar based rainfall data for runoff estimation in Indian watersheds - A case study of Chennai basin’, *Sadhana - Academy Proceedings in Engineering Sciences*, 39(4), pp. 989–997. doi: 10.1007/s12046-014-0258-1.

Khan, W. *et al.* (2020) ‘Evaluation of hydrological modeling using climatic station and gridded precipitation dataset’, *Mausam*, 71(4), pp. 717–728.

Kling, H., Fuchs, M. and Paulin, M. (2012) ‘Runoff conditions in the upper Danube basin under an ensemble of climate change scenarios’, *Journal of Hydrology*, 424–425, pp. 264–277. doi: 10.1016/J.JHYDROL.2012.01.011.

KOBAYASHI, S. *et al.* (2015) ‘The JRA-55 Reanalysis: General Specifications and Basic Characteristics’, *Journal of the Meteorological Society of Japan. Ser. II*, 93(1), pp. 5–48. doi: 10.2151/JMSJ.2015-001.

Kokkonen, T. S. *et al.* (2003) ‘Predicting daily flows in ungauged catchments: Model regionalization from catchment descriptors at the Coweeta Hydrologic Laboratory, North Carolina’, *Hydrological Processes*, 17(11), pp. 2219–2238. doi: 10.1002/hyp.1329.

Koskinen, M. *et al.* (2017) ‘Restoration of nutrient-rich forestry-drained peatlands poses a risk for high exports of dissolved organic carbon, nitrogen, and phosphorus’, *The Science of the total environment*, 586, pp. 858–869. doi: 10.1016/J.SCITOTENV.2017.02.065.

Kubota, T. *et al.* (2020) ‘Global Satellite Mapping of Precipitation (GSMaP) Products in the GPM Era’, *Advances in Global Change Research*, 67, pp. 355–373. doi: 10.1007/978-3-030-24568-9_20.

Lafon, T. *et al.* (2013) ‘Bias correction of daily precipitation simulated by a regional climate model: a comparison of methods’, *International Journal of Climatology*, 33(6), pp. 1367–1381. doi: 10.1002/JOC.3518.

Lauri, H., Räsänen, T. A. and Kummu, M. (2014) ‘Using Reanalysis and Remotely Sensed Temperature and Precipitation Data for Hydrological Modeling in Monsoon Climate: Mekong River Case Study’, *Journal of Hydrometeorology*, 15(4), pp. 1532–1545. doi: 10.1175/jhm-d-13-084.1.

Ledesma, J. L. J. and Futter, M. N. (2017) ‘Gridded climate data products are an alternative to instrumental measurements as inputs to rainfall–runoff models’, *Hydrological Processes*, 31(18), pp. 3283–3293. doi: 10.1002/hyp.11269.

Legates, D. R. and McCabe, G. J. (1999) ‘Evaluating the use of “goodness-of-fit” Measures in hydrologic and hydroclimatic model validation’, *Water Resources Research*, 35(1), pp. 233–241. doi: 10.1029/1998WR900018.

Magette, W. L., Shanholtz, V. O. and Carr, J. C. (1976) 'Estimating selected parameters for the Kentucky Watershed Model from watershed characteristics', *Water Resources Research*, 12(3), pp. 472–476. doi: 10.1029/WR012i003p00472.
Mahto, S. S. and Mishra, V. (2019) 'Does ERA-5 Outperform Other Reanalysis Products for Hydrologic Applications in India?', *Journal of Geophysical Research: Atmospheres*, 124(16), pp. 9423–9441. doi: 10.1029/2019JD031155.
Maidment, R. I. *et al.* (2017) 'A new, long-term daily satellite-based rainfall dataset for operational monitoring in Africa', *Scientific Data 2017 4:1*, 4(1), pp. 1–19. doi: 10.1038/sdata.2017.63.
Maraun, D. *et al.* (2010) 'Precipitation downscaling under climate change: Recent developments to bridge the gap between dynamical models and the end user', *Reviews of Geophysics*, 48(3). doi: 10.1029/2009RG000314.
Maraun, D. and Widmann, M. (2018) 'Statistical Downscaling and Bias Correction for Climate Research', *Statistical Downscaling and Bias Correction for Climate Research*. doi: 10.1017/9781107588783.
Marques, C. A. F. *et al.* (2009) 'Global atmospheric energetics from NCEP - Reanalysis 2 and ECMWF-ERA40 reanalysis', *International Journal of Climatology*, 29(2), pp. 159–174. doi: 10.1002/JOC.1704.
Marra, F. *et al.* (2017) 'Intensity-duration-frequency curves from remote sensing rainfall estimates: Comparing satellite and weather radar over the eastern Mediterranean', *Hydrology and Earth System Sciences*, 21(5), pp. 2389–2404. doi: 10.5194/hess-21-2389-2017.
Marra, F. and Morin, E. (2015) 'Use of radar QPE for the derivation of Intensity-Duration-Frequency curves in a range of climatic regimes', *Journal of Hydrology*, 531, pp. 427–440. doi: 10.1016/j.jhydrol.2015.08.064.
McIntyre, N. *et al.* (2005) 'Ensemble predictions of runoff in ungauged catchments', *Water Resources Research*, 41(12), pp. 1–14. doi: 10.1029/2005WR004289.
Merz, R. and Blöschl, G. (2003) 'A process typology of regional floods', *Water Resources Research*, 39(12), pp. 1–20. doi: 10.1029/2002WR001952.
Merz, R., Blöschl, G. and Parajka, J. (2006) 'Regionalization methods in rainfall-runoff modelling using large catchment samples', *IAHS-AISH Publication*, (307), pp. 117–125.
Michel C (1991) 'Hydrologie appliquée aux petits bassins ruraux.', *Hydrology handbook (in French)*. Available at: https://rdrr.io/cran/airGR/man/Calibration_Michel.html (Accessed: 23 November 2021).
Muñoz-Sabater, J. *et al.* (2021) 'ERA5-Land: A state-of-the-art global reanalysis dataset for land applications', *Earth System Science Data*, 13(9), pp. 4349–4383. doi: 10.5194/essd-13-4349-2021.
Nash, J. E. and Sutcliffe, J. V. (1970) 'River flow forecasting through conceptual models part I — A discussion of principles', *Journal of Hydrology*, 10(3), pp. 282–290. doi: 10.1016/0022-1694(70)90255-6.
Nathan, R. J. and McMahon, T. A. (1990) 'Identification of homogeneous regions for the purposes of regionalisation', *Journal of Hydrology*, 121(1–4), pp. 217–238. doi: 10.1016/0022-1694(90)90233-N.
Nogueira, M. (2020) 'Inter-comparison of ERA-5, ERA-interim and GPCP rainfall over the last 40 years: Process-based analysis of systematic and random differences', *Journal of Hydrology*, 583. doi: 10.1016/*Journal of Hydrology*, .2020.124632.
Novella, N. S. and Thiaw, W. M. (2013) 'African rainfall climatology version 2 for famine early warning systems', *Journal of Applied Meteorology and Climatology*, 52(3), pp. 588–606. doi: 10.1175/JAMC-D-11-0238.1.
Novella, N. and Thiaw, W. (2009) 'Validation of Satellite-Derived Rainfall Products over the Sahel'.

Onogi, K. *et al.* (2007) 'The JRA-25 Reanalysis', *Journal of the Meteorological Society of Japan. Ser. II*, 85(3), pp. 369–432. doi: 10.2151/JMSJ.85.369.
Oudin, L. *et al.* (2005) 'Which potential evapotranspiration input for a lumped rainfall–runoff model?: Part 2—Towards a simple and efficient potential evapotranspiration model for rainfall–runoff modelling', *Journal of Hydrology*, 303(1–4), pp. 290–306. doi: 10.1016/J.JHYDROL.2004.08.026.
Oudin, L. *et al.* (2008) 'Spatial proximity, physical similarity, regression and ungaged catchments: A comparison of regionalization approaches based on 913 French catchments', *Water Resources Research*, 44(3), pp. 1–15. doi: 10.1029/2007WR006240.
Oudin, L. *et al.* (2010) 'Are seemingly physically similar catchments truly hydrologically similar?', *Water Resources Research*, 46(11), pp. 1–15. doi: 10.1029/2009WR008887.
Oyerinde, G. T., Fademi, I. O. and Denton, O. A. (2017) 'Modeling runoff with satellite-based rainfall estimates in the Niger basin', *Cogent Food & Agriculture*, 3(1), p. 1363340. doi: 10.1080/23311932.2017.1363340.
Pakoksung, K. and Takagi, M. (2016) 'Effect of satellite based rainfall products on river basin responses of runoff simulation on flood event', *Modeling Earth Systems and Environment*, 2(3), pp. 1–14. doi: 10.1007/s40808-016-0200-0.
Parajka, J., Merz, R. and Blöschl, G. (2005) 'A comparison of regionalisation methods for catchment model parameters', *Hydrology and Earth System Sciences*, 9(3), pp. 157–171. doi: 10.5194/hess-9-157-2005.
Perrin, C. (2002) 'Vers une amélioration d'un modèle global pluie-débit au travers d'une approche comparative', *La Houille Blanche*, 88(6–7), pp. 84–91. doi: 10.1051/lhb/2002089.
Perrin, C., Michel, C. and Andréassian, V. (2003) 'Improvement of a parsimonious model for streamflow simulation', *Journal of Hydrology*, 279(1–4), pp. 275–289. doi: 10.1016/S0022-1694(03)00225-7.
Razavi, T. and Coulibaly, P. (2013) 'Streamflow Prediction in Ungauged Basins: Review of Regionalization Methods', *Journal of Hydrologic Engineering*, 18(8), pp. 958–975. doi: 10.1061/(asce)he.1943-5584.0000690.
Reichl, J. P. C. *et al.* (2009) 'Optimization of a similarity measure for estimating ungauged streamflow', *Water Resources Research*, 45(10), pp. 1–15. doi: 10.1029/2008WR007248.
Rienecker, M. M. *et al.* (2011) 'MERRA: NASA's Modern-Era Retrospective Analysis for Research and Applications', *Journal of Climate*, 24(14), pp. 3624–3648. doi: 10.1175/JCLI-D-11-00015.1.
Ruane, A. C., Goldberg, R. and Chryssanthacopoulos, J. (2015) 'Climate forcing datasets for agricultural modeling: Merged products for gap-filling and historical climate series estimation', *Agricultural and Forest Meteorology*, 200, pp. 233–248. doi: 10.1016/J.AGRFORMET.2014.09.016.
Ruffault, J. *et al.* (2017) 'Daily synoptic conditions associated with large fire occurrence in Mediterranean France: evidence for a wind-driven fire regime', *International Journal of Climatology*, 37(1), pp. 524–533. doi: 10.1002/joc.4680.
Ruiz-Villanueva, V. *et al.* (2012) 'Extreme flood response to short-duration convective rainfall in South-West Germany', *Hydrology and Earth System Sciences*, 16(5), pp. 1543–1559. doi: 10.5194/hess-16-1543-2012.
Runo, L. *et al.* (2020) 'Accuracy Analysis of IMERG Satellite Rainfall Data', *Water*, 12(2177), pp. 1–22.
Saha, S. *et al.* (2010) 'The NCEP Climate Forecast System Reanalysis', *Bulletin of the American Meteorological Society*, 91(8), pp. 1015–1058. doi: 10.1175/2010BAMS3001.1.
Saha, S. *et al.* (2014) 'The NCEP Climate Forecast System Version 2', *Journal of Climate*, 27(6), pp. 2185–2208. doi: 10.1175/JCLI-D-12-00823.1.
Salinas, J. L. *et al.* (2013) 'Comparative assessment of predictions in ungauged basins-Part 2:

Flood and low flow studies', *Hydrology and Earth System Sciences*, 17(7), pp. 2637–2652. doi: 10.5194/hess-17-2637-2013.
Samuel, J., Coulibaly, P. and Metcalfe, R. A. (2011) 'Estimation of Continuous Streamflow in Ontario Ungauged Basins: Comparison of Regionalization Methods', *Journal of Hydrologic Engineering*, 16(5), pp. 447–459. doi: 10.1061/(asce)he.1943-5584.0000338.
Satgé, F. *et al.* (2020) 'Evaluation of 23 gridded precipitation datasets across West Africa', *Journal of Hydrology*, 581. doi: 10.1016/j.jhydrol.2019.124412.
Sefton, C. E. M. and Howarth, S. M. (1998) 'Relationships between dynamic response characteristics and physical descriptors of catchments in England and Wales', *Journal of Hydrology*, 211(1–4), pp. 1–16. doi: 10.1016/S0022-1694(98)00163-2.
Seguinot, J. *et al.* (2014) 'The effect of climate forcing on numerical simulations of the cordilleran ice sheet at the last glacial maximum', *Cryosphere*, 8(3), pp. 1087–1103. doi: 10.5194/TC-8-1087-2014.
Sharifi, E., Eitzinger, J. and Dorigo, W. (2019) 'Performance of the State-Of-The-Art Gridded Precipitation Products over Mountainous Terrain: A Regional Study over Austria', *Remote Sensing 2019, Vol. 11, Page 2018*, 11(17), p. 2018. doi: 10.3390/RS11172018.
Shrestha, M., Acharya, S. C. and Shrestha, P. K. (2017) 'Bias correction of climate models for hydrological modelling – are simple methods still useful?', *Meteorological Applications*, 24(3), pp. 531–539. doi: 10.1002/MET.1655.
Siqueira, V. A. *et al.* (2018) 'Toward continental hydrologic-hydrodynamic modeling in South America', *Hydrology and Earth System Sciences*, 22(9), pp. 4815–4842. doi: 10.5194/HESS-22-4815-2018.
Sivapalan, M. *et al.* (2003) 'IAHS Decade on Predictions in Ungauged Basins (PUB), 2003-2012: Shaping an exciting future for the hydrological sciences', *Hydrological Sciences Journal*, 48(6), pp. 857–880. doi: 10.1623/hysj.48.6.857.51421.
Skop, E. (1996) 'Scale Issues in Hydrological Modeling', *Eos, Transactions American Geophysical Union*, 77(20), p. 190. doi: 10.1029/96eo00131.
Smith, J. A. *et al.* (2007) 'Radar rainfall estimation for flash flood forecasting in small urban watersheds', *Advances in Water Resources*, 10(30), pp. 2087–2097. doi: 10.1016/J.ADVWATRES.2006.09.007.
Sorooshian, S., Duan, Q. and Gupta, V. K. (1993) 'Calibration of rainfall-runoff models: Application of global optimization to the Sacramento Soil Moisture Accounting Model', *Water Resources Research*, 29(4), pp. 1185–1194. doi: 10.1029/92WR02617.
Tapiador, F. J. *et al.* (2012) 'Global precipitation measurement: Methods, datasets and applications', *Atmospheric Research*, 104–105, pp. 70–97. doi: 10.1016/J.ATMOSRES.2011.10.021.
Teng, J. *et al.* (2015) 'How does bias correction of regional climate model precipitation affect modelled runoff?', *Hydrology and Earth System Sciences*, 19(2), pp. 711–728. doi: 10.5194/HESS-19-711-2015.
Thorndahl, S. *et al.* (2017) 'Weather radar rainfall data in urban hydrology', *Hydrology and Earth System Sciences*, 21(3), pp. 1359–1380. doi: 10.5194/HESS-21-1359-2017.
Tilford, K. A., Fox, N. I. and Collier, C. G. (2002) 'Application of weather radar data for urban hydrology', *Meteorological Applications*, 9(1), pp. 95–104. doi: 10.1017/S135048270200110X.
Tramblay, Y. *et al.* (2016) 'Evaluation of satellite-based rainfall products for hydrological modelling in Morocco', *https://doi.org/10.1080/02626667.2016.1154149*, 61(14), pp. 2509–2519. doi: 10.1080/02626667.2016.1154149.
Valery, A. (2010) 'Modélisation précipitations – débit sous influence nivale Elaboration d ' un module neige et évaluation sur 380 bassins versants', p. 405. Available at: http://www.cemagref.fr/webgr/Download/Rapports_et_theses/2010-VALERY-THESE.pdf.

Valéry, A., Andréassian, V. and Perrin, C. (2014a) '"As simple as possible but not simpler": What is useful in a temperature-based snow-accounting routine? Part 1 - Comparison of six snow accounting routines on 380 catchments', *Journal of Hydrology*, 517, pp. 1166–1175. doi: 10.1016/j.jhydrol.2014.04.059.
Valéry, A., Andréassian, V. and Perrin, C. (2014b) '"As simple as possible but not simpler": What is useful in a temperature-based snow-accounting routine? Part 2 - Sensitivity analysis of the CemaNeige snow accounting routine on 380 catchments', *Journal of Hydrology*, 517, pp. 1176–1187. doi: 10.1016/j.jhydrol.2014.04.058.
Vandewiele, G. L., Xu, C. Y. and Huybrechts, W. (1991) 'Regionalisation of physically-based water balance models in Belgium. Application to ungauged catchments', *Water Resources Management*, 5(3–4), pp. 199–208. doi: 10.1007/BF00421989.
Vaze, J. *et al.* (2011) 'Conceptual Rainfall–Runoff Model Performance with Different Spatial Rainfall Inputs', *Journal of Hydrometeorology*, 12(5), pp. 1100–1112. doi: 10.1175/2011JHM1340.1.
Velasquez, P., Messmer, M. and Raible, C. C. (2020) 'A new bias-correction method for precipitation over complex terrain suitable for different climate states: A case study using WRF (version 3.8.1)', *Geoscientific Model Development*, 13(10), pp. 5007–5027. doi: 10.5194/GMD-13-5007-2020.
Viglione, A. *et al.* (2013) 'Comparative assessment of predictions in ungauged basins - Part 3: Runoff signatures in Austria', *Hydrology and Earth System Sciences*, 17(6), pp. 2263–2279. doi: 10.5194/hess-17-2263-2013.
Vousdoukas, M. I. *et al.* (2016) 'Projections of extreme storm surge levels along Europe', *Climate Dynamics*, 47(9–10), pp. 3171–3190. doi: 10.1007/S00382-016-3019-5.
Vu, M. T., Raghavan, S. V. and Liong, S. Y. (2012) 'SWAT use of gridded observations for simulating runoff - A Vietnam river basin study', *Hydrology and Earth System Sciences*, 16(8), pp. 2801–2811. doi: 10.5194/HESS-16-2801-2012.
Wang, L. P. *et al.* (2015) 'Singularity-sensitive gauge-based radar rainfall adjustment methods for urban hydrological applications', *Hydrology and Earth System Sciences*, 19(9), pp. 4001–4021. doi: 10.5194/HESS-19-4001-2015.
Wang, N. *et al.* (2020) 'Evaluating satellite-based and reanalysis precipitation datasets with gauge-observed data and hydrological modeling in the Xihe River Basin, China', *Atmospheric Research*, 234, p. 104746. doi: 10.1016/j.atmosres.2019.104746.
Willkofer, F. *et al.* (2018) 'The impact of bias correcting regional climate model results on hydrological indicators for Bavarian catchments', *Journal of Hydrology: Regional Studies*, 19, pp. 25–41. doi: 10.1016/J.EJRH.2018.06.010.
Willmott, C. J. (1981) 'On the Validation of Models', *Physical Geography*, 2, pp. 184–194. Available at: https://www.scirp.org/(S(i43dyn45teexjx455qlt3d2q))/reference/ReferencesPapers.aspx?ReferenceID=1432873 (Accessed: 24 November 2021).
Xie, P. *et al.* (2007) 'A Gauge-Based Analysis of Daily Precipitation over East Asia', *Journal of Hydrometeorology*, 8(3), pp. 607–626. doi: 10.1175/JHM583.1.
Xie, P. *et al.* (2017) 'Reprocessed, Bias-Corrected CMORPH Global High-Resolution Precipitation Estimates from 1998', *Journal of Hydrometeorology*, 18(6), pp. 1617–1641. doi: 10.1175/JHM-D-16-0168.1.
Xu, X. *et al.* (2019) 'Evaluation of variability among different precipitation products in the Northern Great Plains', *Journal of Hydrology: Regional Studies*, 24. doi: 10.1016/J.EJRH.2019.100608.
Yang, B. *et al.* (2013) 'Uncertainty quantification and parameter tuning in the CAM5 Zhang-McFarlane convection scheme and impact of improved convection on the global circulation and climate', *Journal of Geophysical Research: Atmospheres*, 118(2), pp. 395–415. doi:

10.1029/2012JD018213.

Yang, X. *et al.* (2018) 'Runoff prediction in ungauged catchments in Norway: Comparison of regionalization approaches', *Hydrology Research*, 49(2), pp. 487–505. doi: 10.2166/nh.2017.071.

Yang, X., Magnusson, J. and Xu, C. Y. (2019) 'Transferability of regionalization methods under changing climate', *Journal of Hydrology*, 568(October), pp. 67–81. doi: 10.1016/j.jhydrol.2018.10.030.

Yapo, P. O., Gupta, H. V. and Sorooshian, S. (1996) 'Automatic calibration of conceptual rainfall-runoff models: sensitivity to calibration data', *Journal of Hydrology*, 181(1–4), pp. 23–48. doi: 10.1016/0022-1694(95)02918-4.

Yasutomi, N., Hamada, A. and Yatagai, A. (2011) 'Development of a Long-term Daily Gridded Temperature Dataset and Its Application to Rain / Snow Discrimination of Daily Precipitation', *Global Environmental Research*, 15(2011), pp. 165–172.

Young, A. R. (2006) 'Stream flow simulation within UK ungauged catchments using a daily rainfall-runoff model', *Journal of Hydrology*, 320(1–2), pp. 155–172. doi: 10.1016/j.jhydrol.2005.07.017.

Yu, P. S. and Yang, T. C. (2000) 'Using synthetic flow duration curves for rainfall-runoff model calibration at ungauged sites', *Hydrological Processes*, 14(1), pp. 117–133. doi: 10.1002/(SICI)1099-1085(200001)14:1<117::AID-HYP914>3.0.CO;2-Q.

Zubieta, R. *et al.* (2015) 'Impacts of satellite-based precipitation datasets on rainfall-runoff modeling of the Western Amazon basin of Peru and Ecuador', *Journal of Hydrology*, 528, pp. 599–612. doi: 10.1016/j.jhydrol.2015.06.064.

APPENDIX A. GR4H – GR4H CEMANEIGE RESULT SELECTION

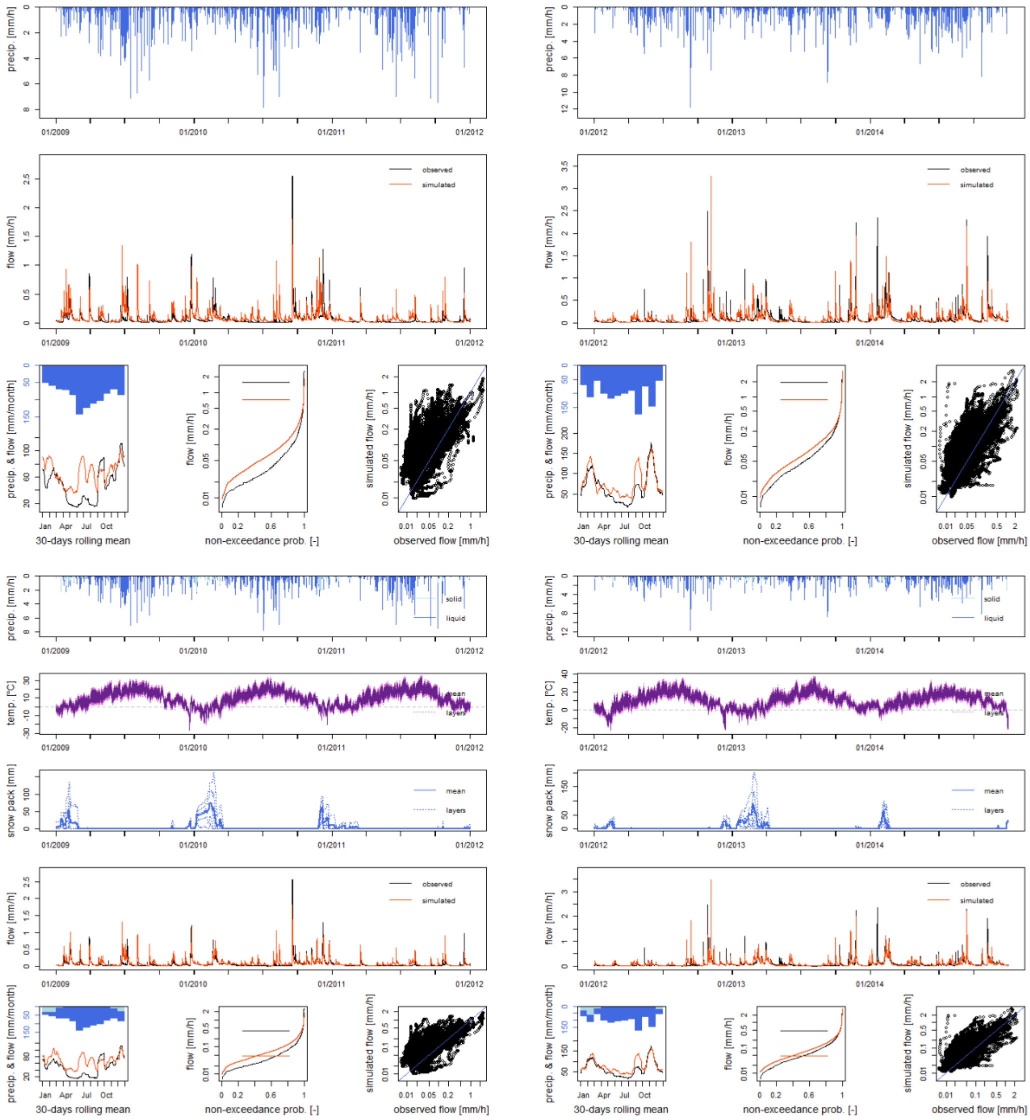

Figure 20: Exported results (conf. 4, GR4H (top)-GR4H CemaNeige (bottom), calibration (left) and validation (right) period) for the Bolska watershed

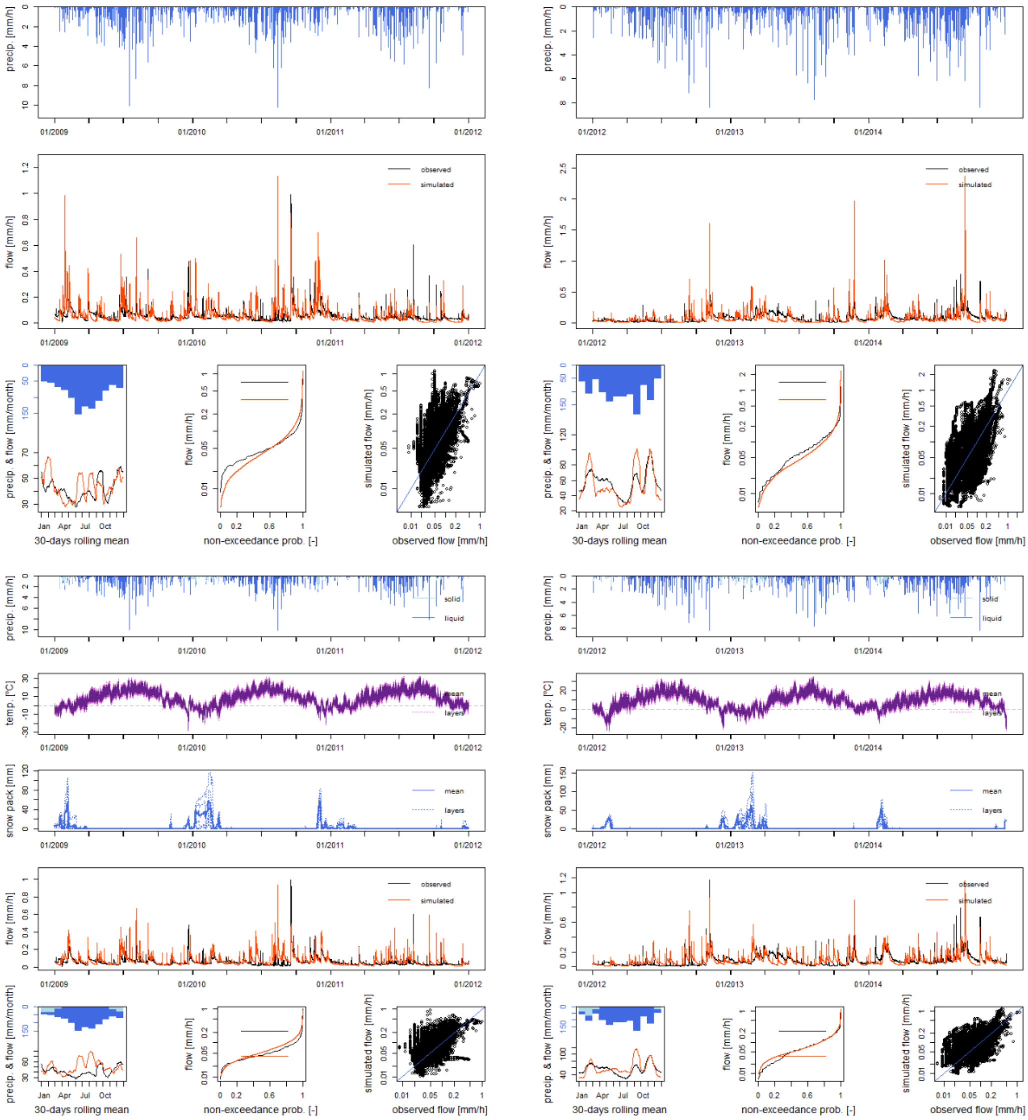

Figure 21: Exported results (conf. 2, GR4H (top)-GR4H CemaNeige (bottom), calibration (left) and validation (right) period) for the Dravinja watershed

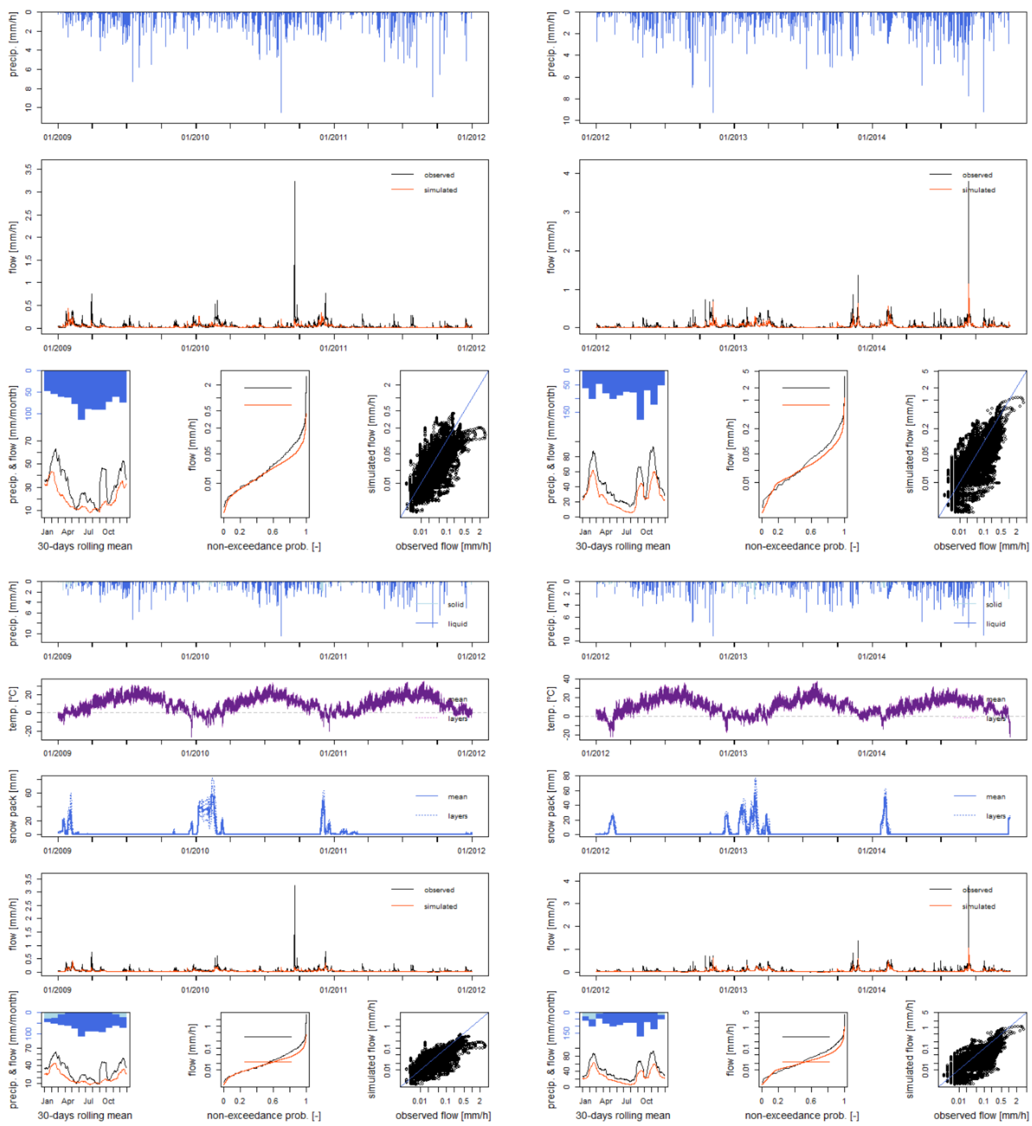

Figure 22: Exported results (conf. 7, GR4H (top)-GR4H CemaNeige (bottom), calibration (left) and validation (right) period) for the Voglanja watershed

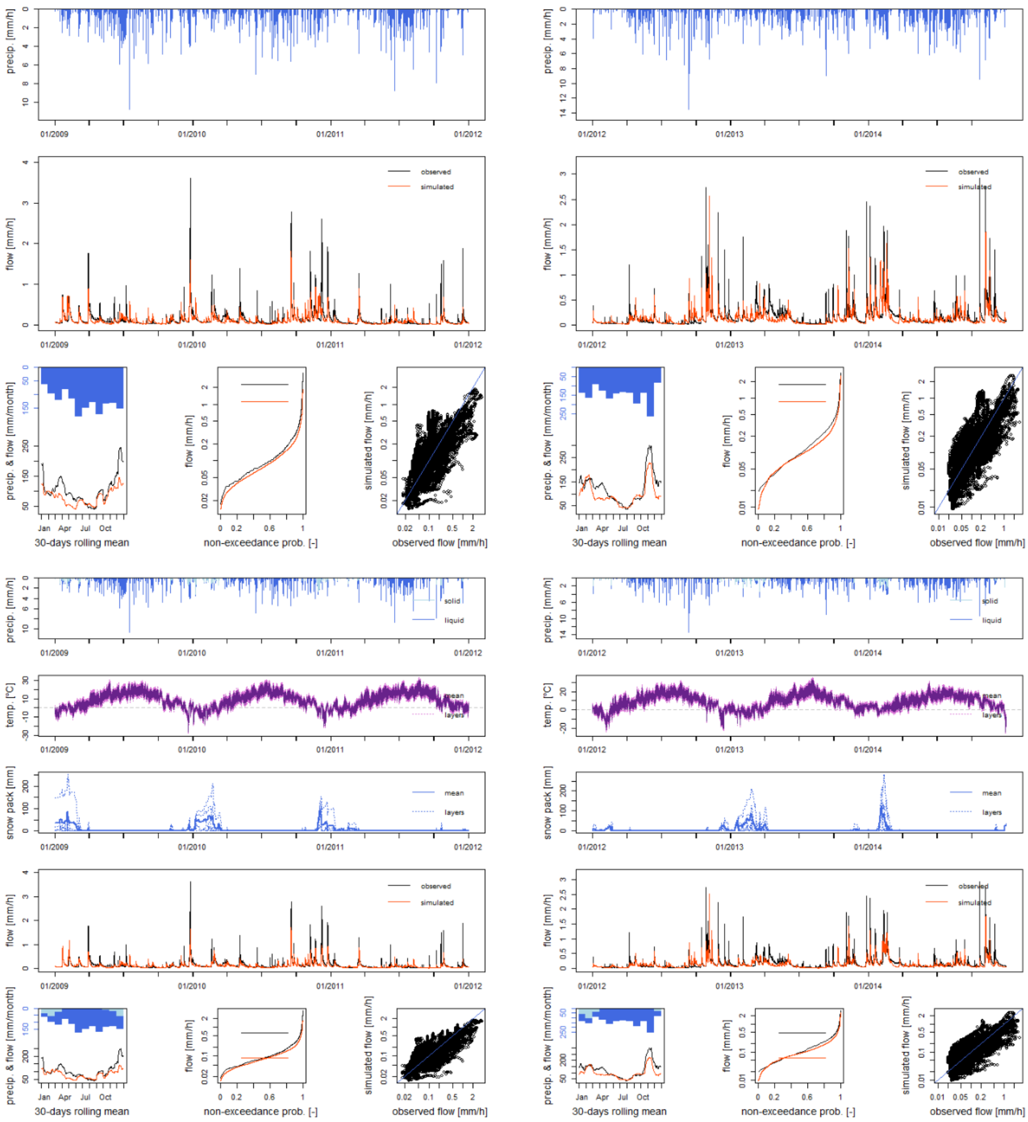

Figure 23: Exported results (conf. 5, GR4H (top)-GR4H CemaNeige (bottom), calibration (left) and validation (right) period) for the Selška Sora watershed

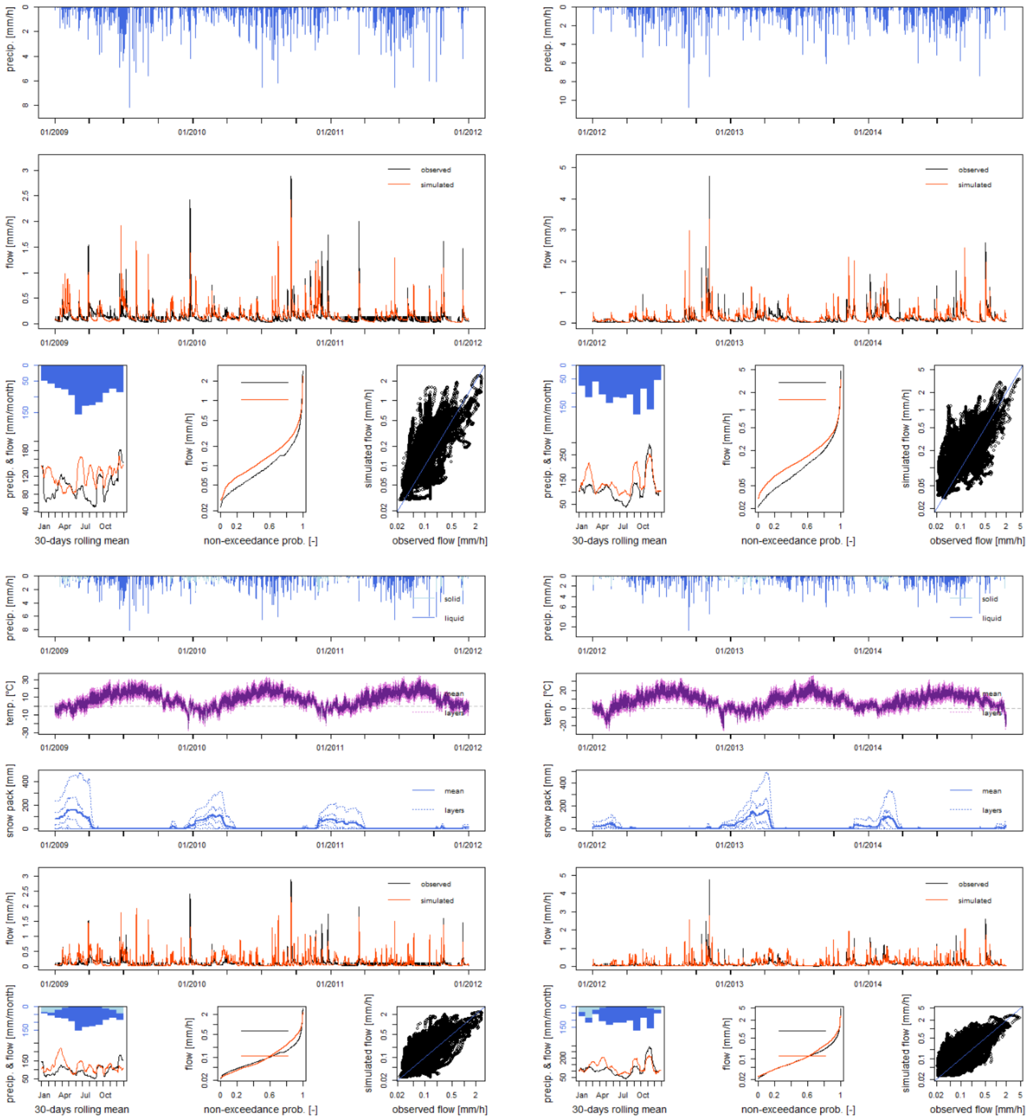

Figure 24: Exported results (conf. 1, GR4H (top)-GR4H CemaNeige (bottom), calibration (left) and validation (right) period) for the Savinja watershed

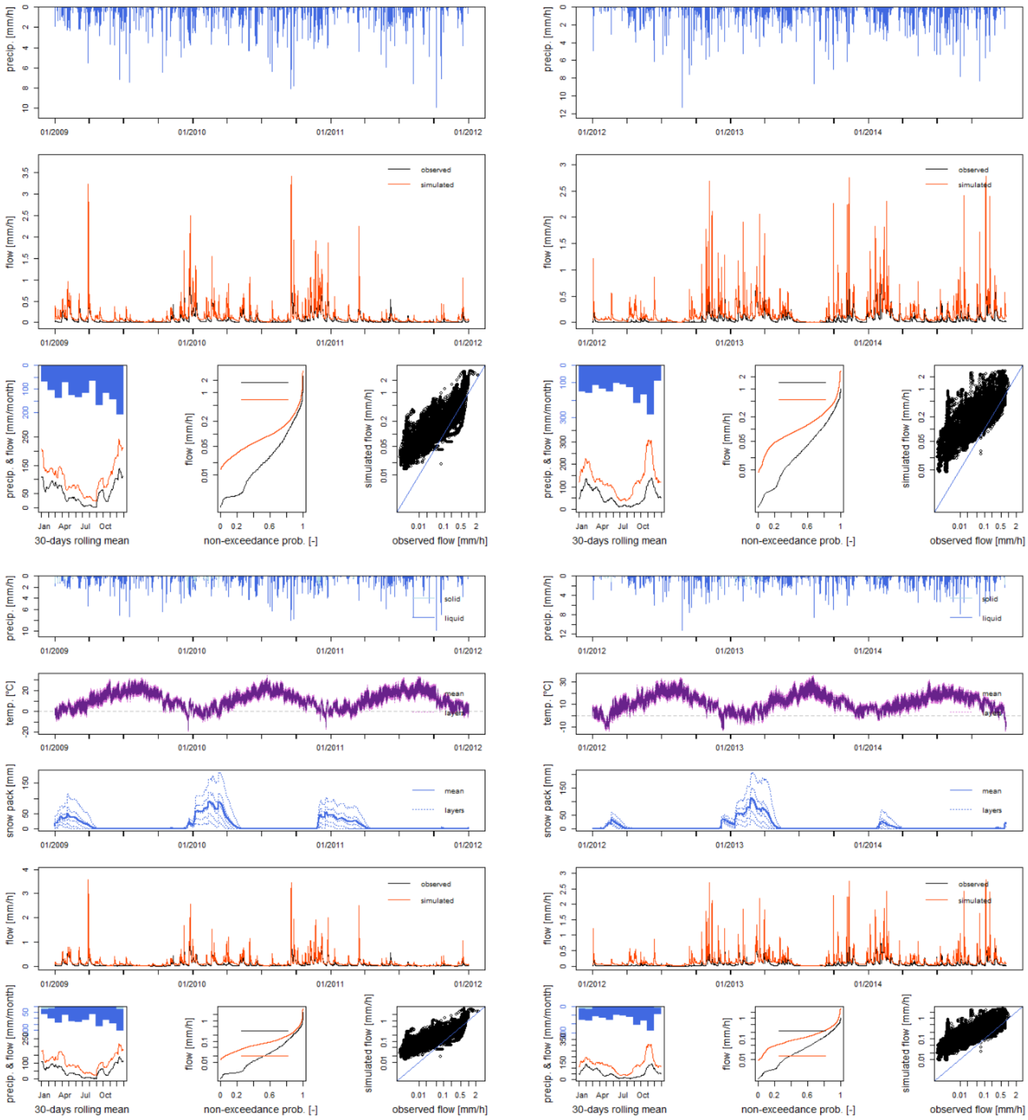

Figure 25: Exported results (conf. 6, GR4H (top)-GR4H CemaNeige (bottom), calibration (left) and validation (right) period) for the Rižana watershed

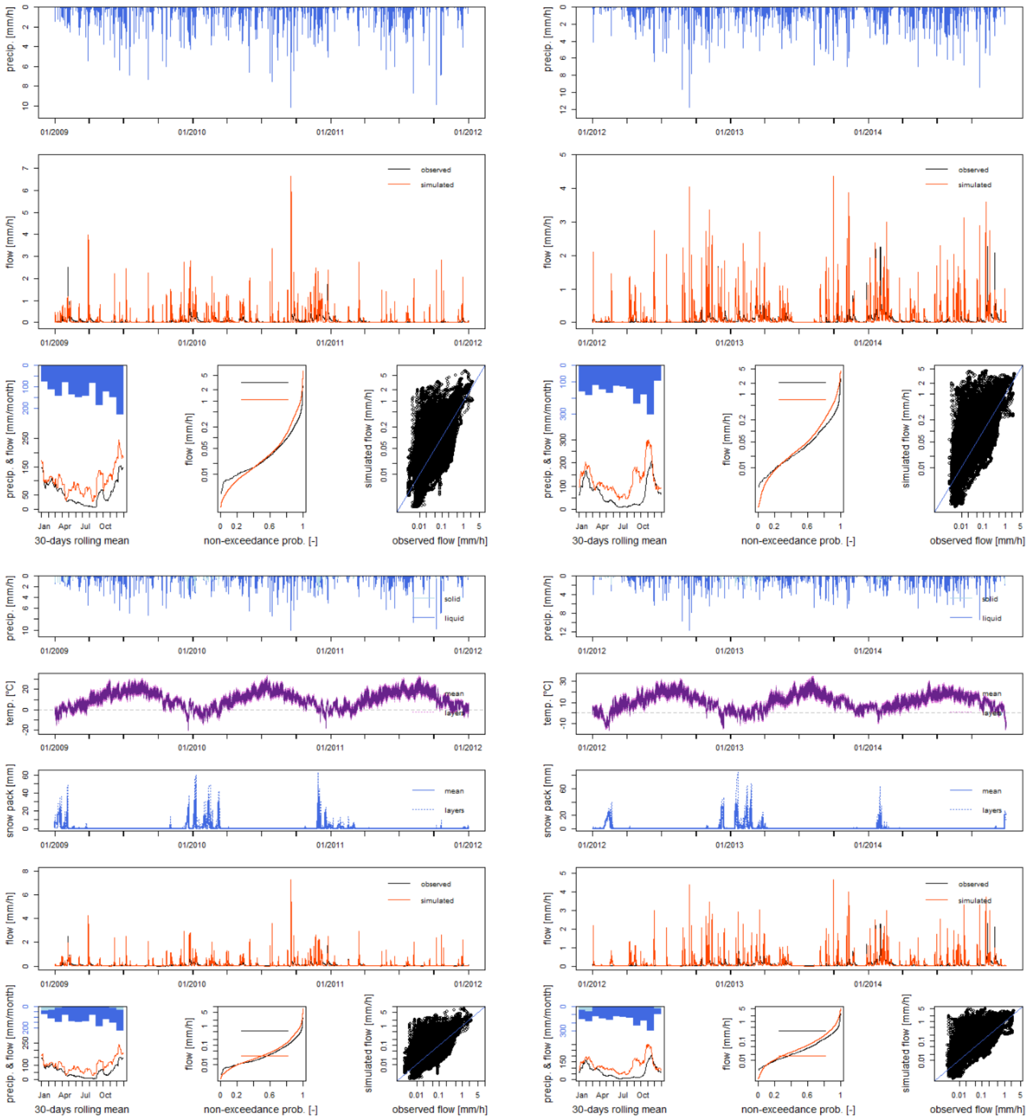

Figure 26: Exported results (conf. 3, GR4H (top)-GR4H CemaNeige (bottom), calibration (left) and validation (right) period) for the Reka watershed

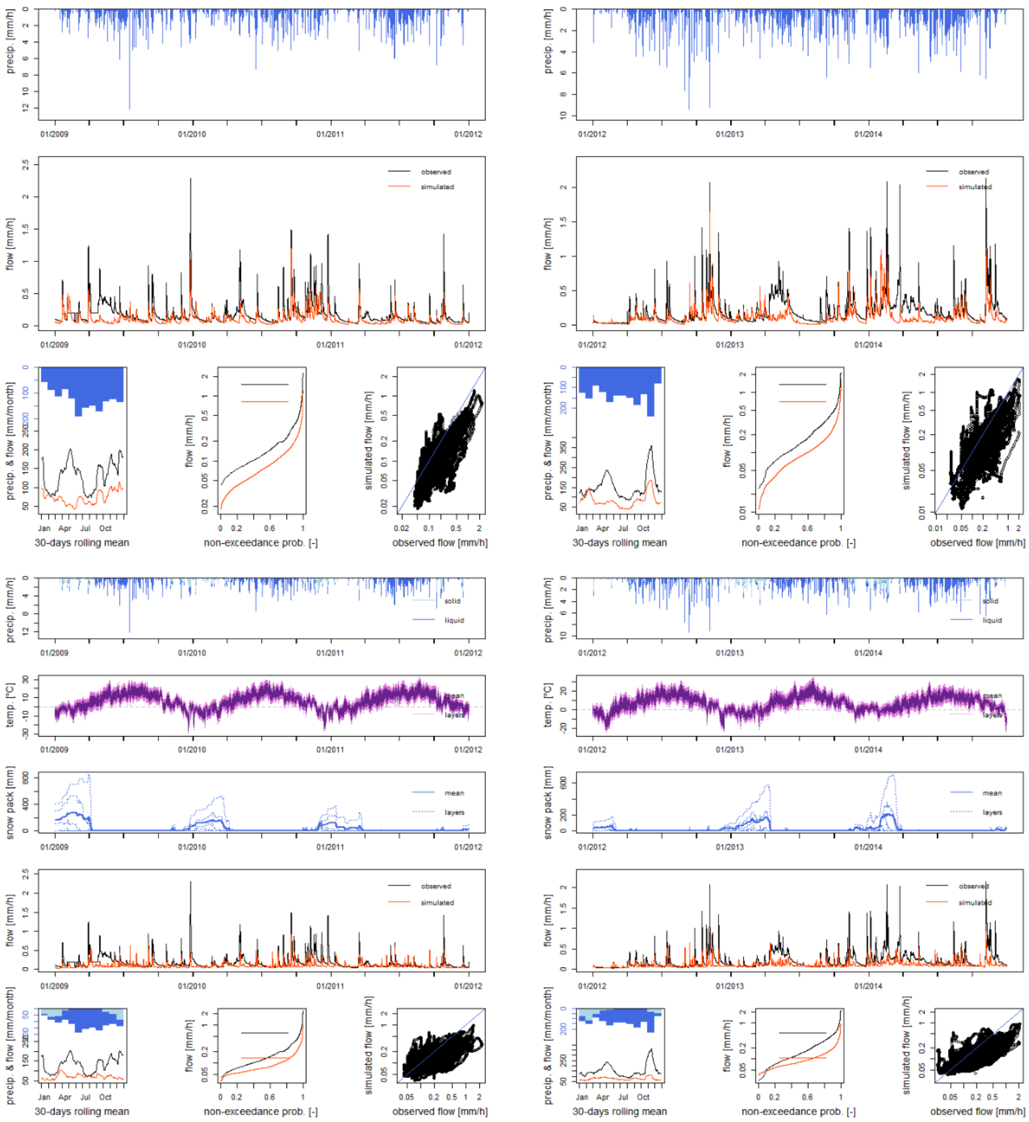

Figure 27: Exported results (conf. 1, GR4H (top)-GR4H CemaNeige (bottom), calibration (left) and validation (right) period) for the Radovna watershed

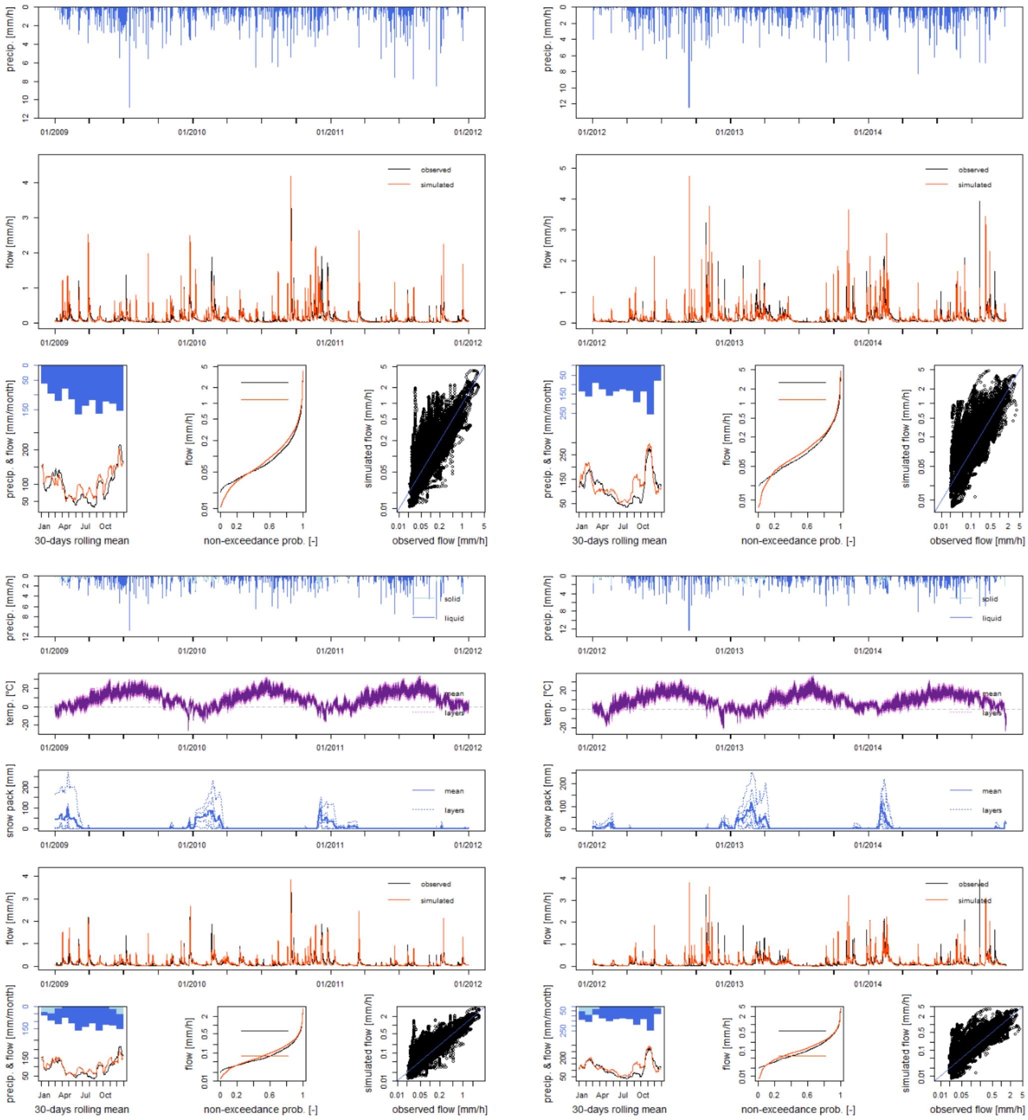

Figure 28: Exported results (conf. 4, GR4H (top)-GR4H CemaNeige (bottom), calibration (left) and validation (right) period) for the Poljanska Sora watershed

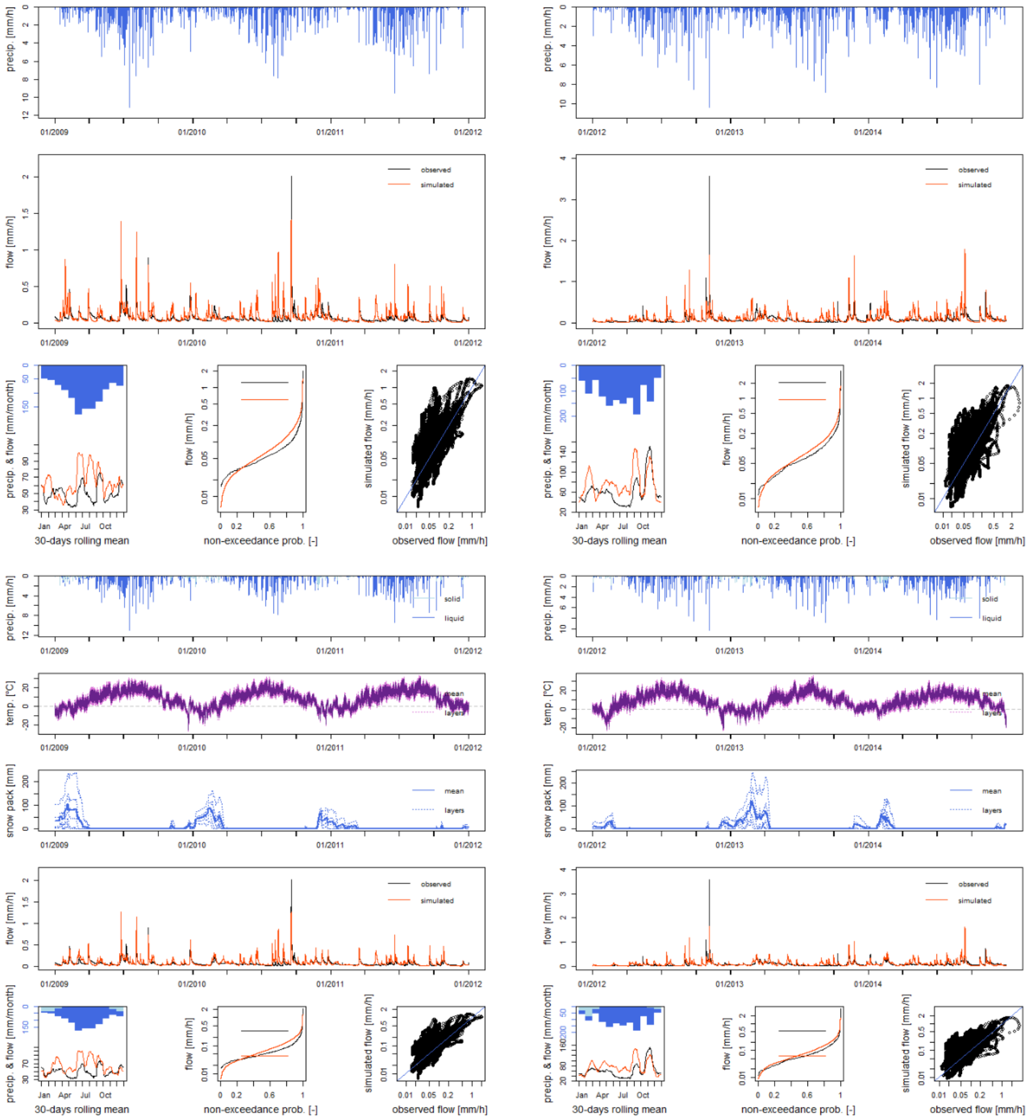

Figure 29: Exported results (conf. 7, GR4H (top)-GR4H CemaNeige (bottom), calibration (left) and validation (right) period) for the Mislinja watershed

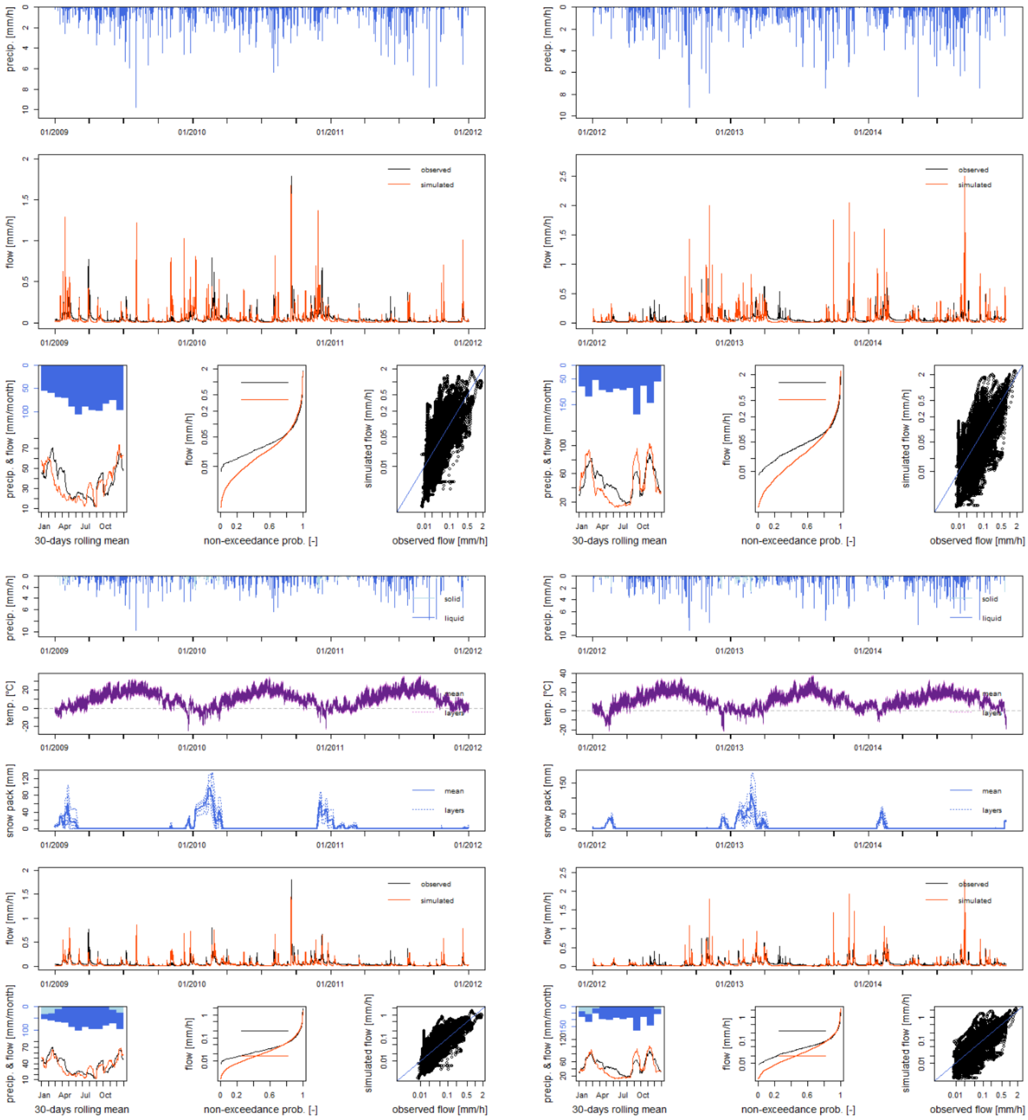

Figure 30: Exported results (conf. 3, GR4H (top)-GR4H CemaNeige (bottom), calibration (left) and validation (right) period) for the Mirna watershed

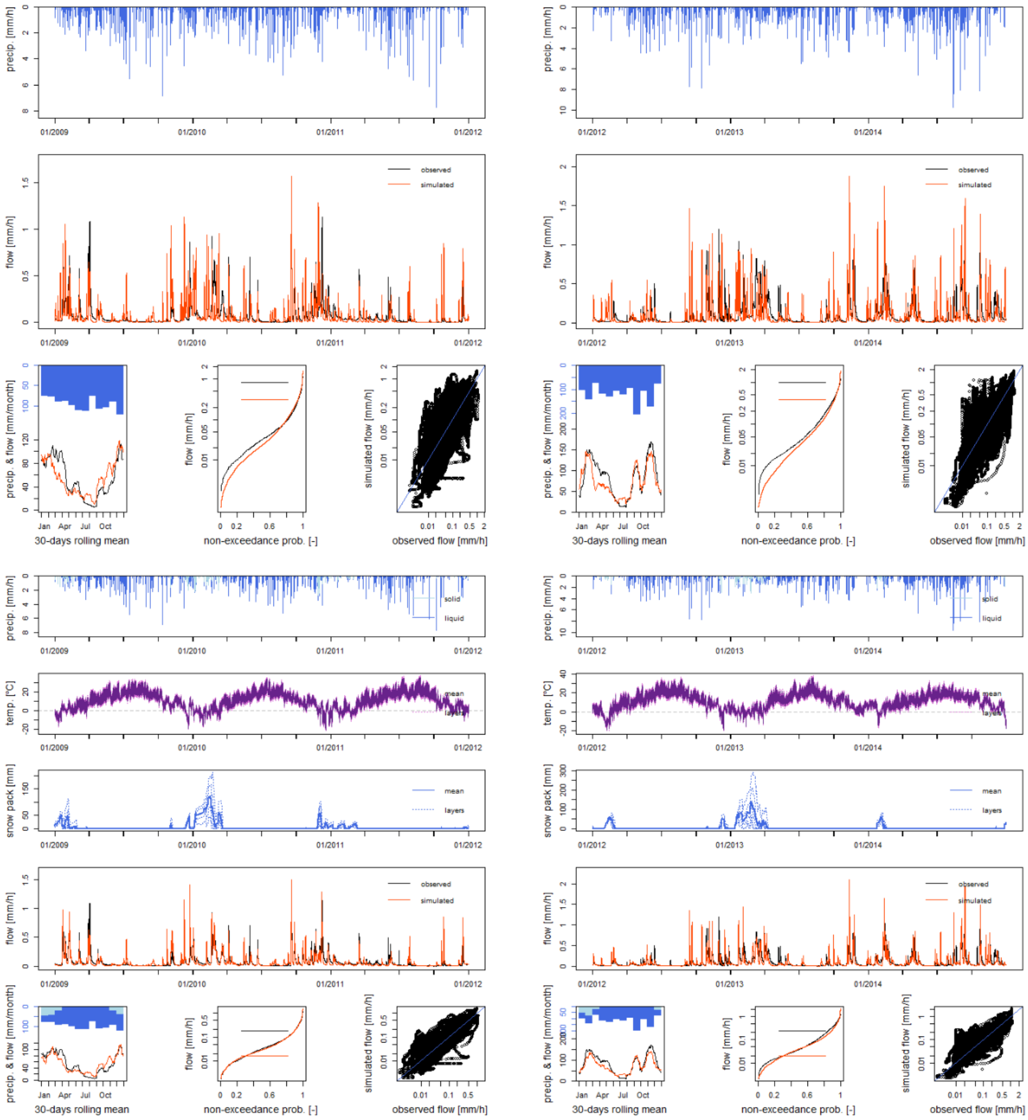

Figure 31: Exported results (conf. 5, GR4H (top)-GR4H CemaNeige (bottom), calibration (left) and validation (right) period) for the Lahinja watershed

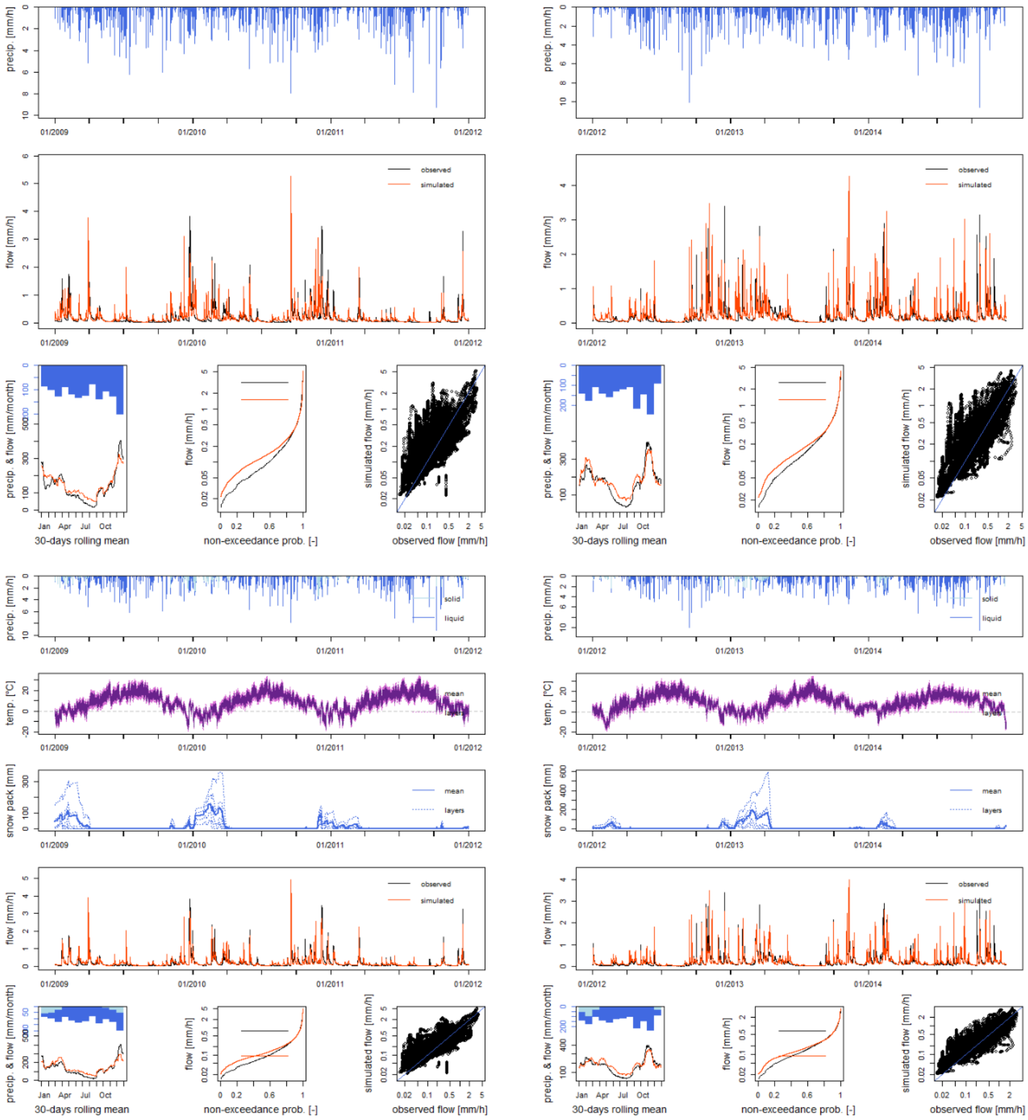

Figure 32: Exported results (conf. 2, GR4H (top)-GR4H CemaNeige (bottom), calibration (left) and validation (right) period) for the Kolpa watershed

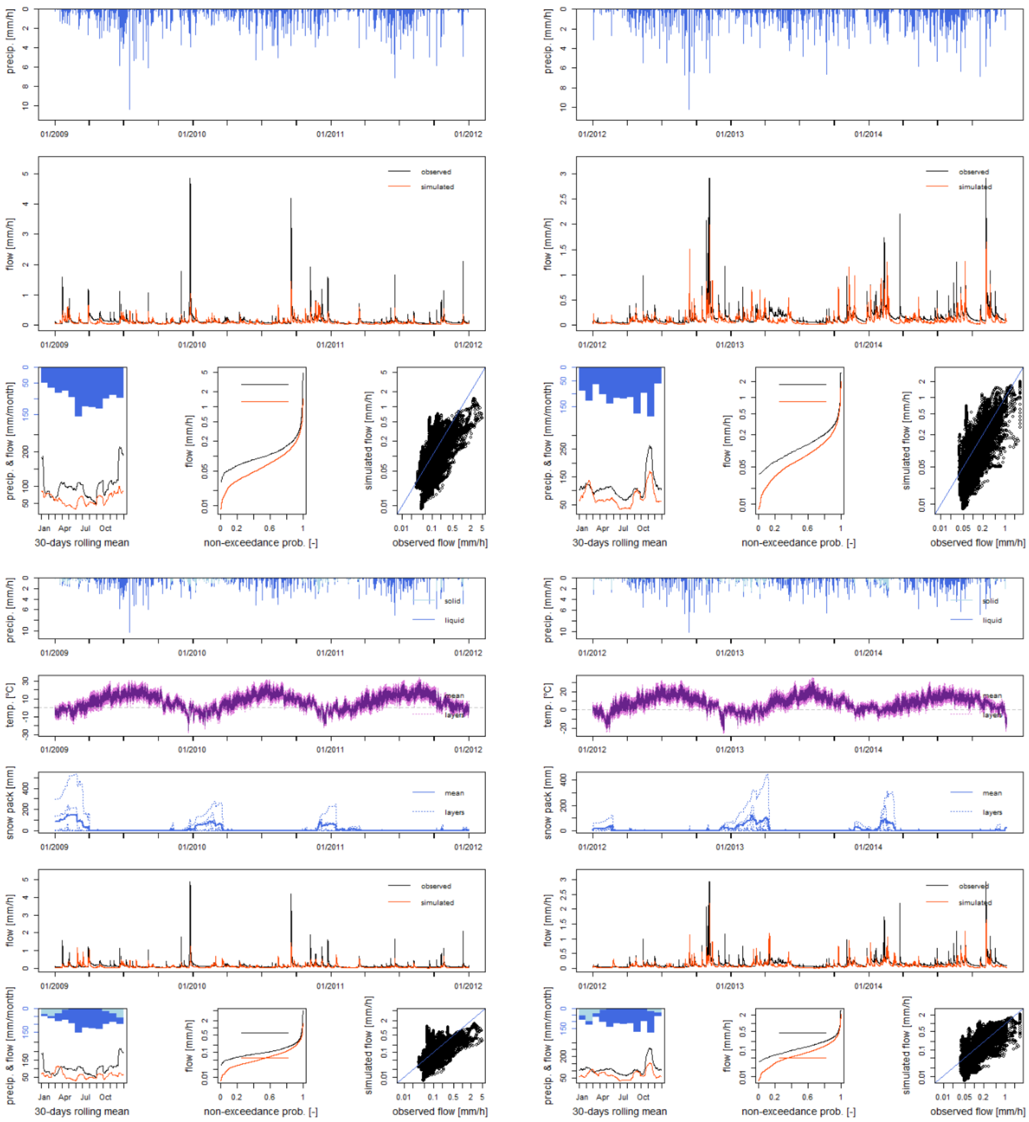

Figure 33: Exported results (conf. 6, GR4H (top)-GR4H CemaNeige (bottom), calibration (left) and validation (right) period) for the Kokra watershed

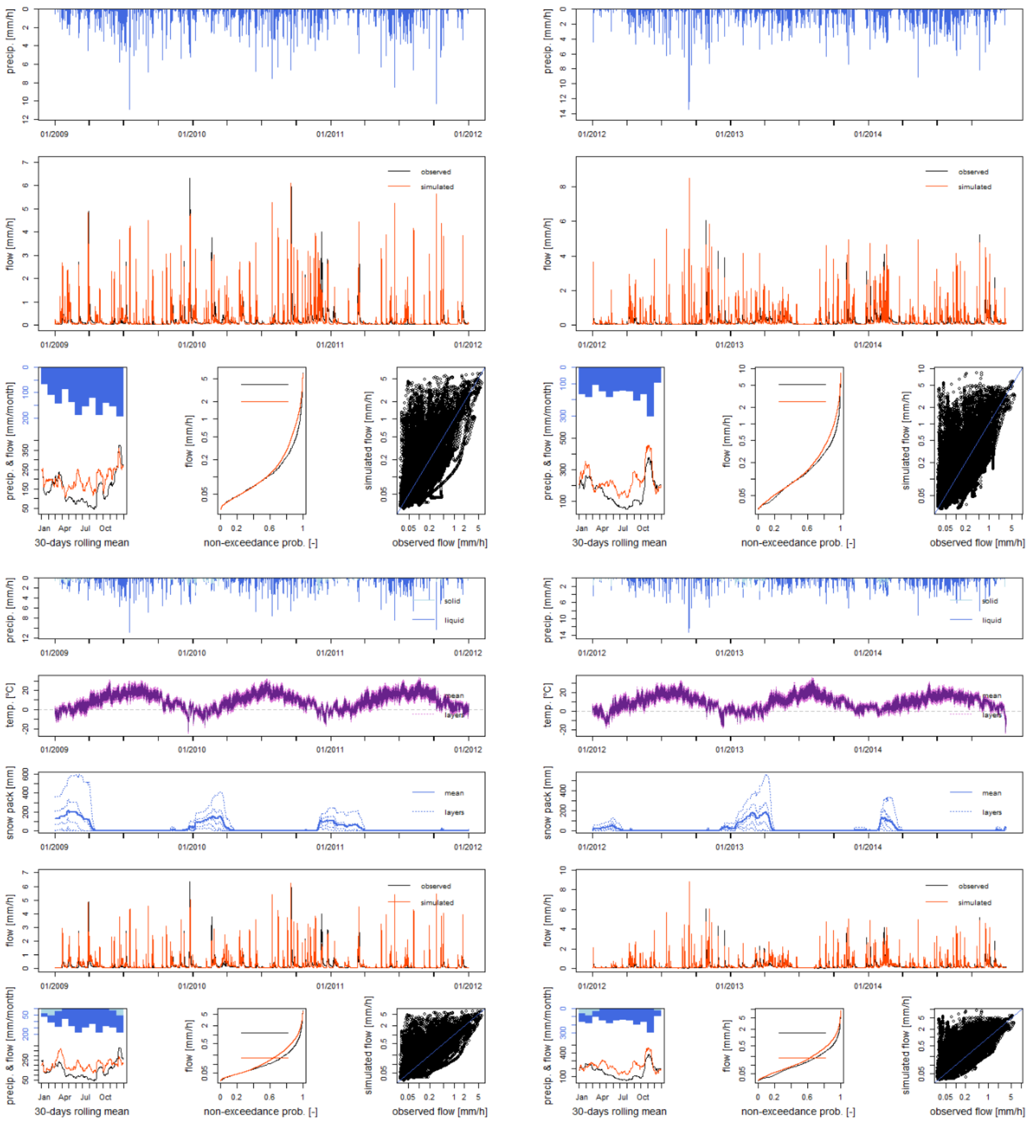

Figure 34: Exported results (conf. 4, GR4H (top)-GR4H CemaNeige (bottom), calibration (left) and validation (right) period) for the Idrijca watershed

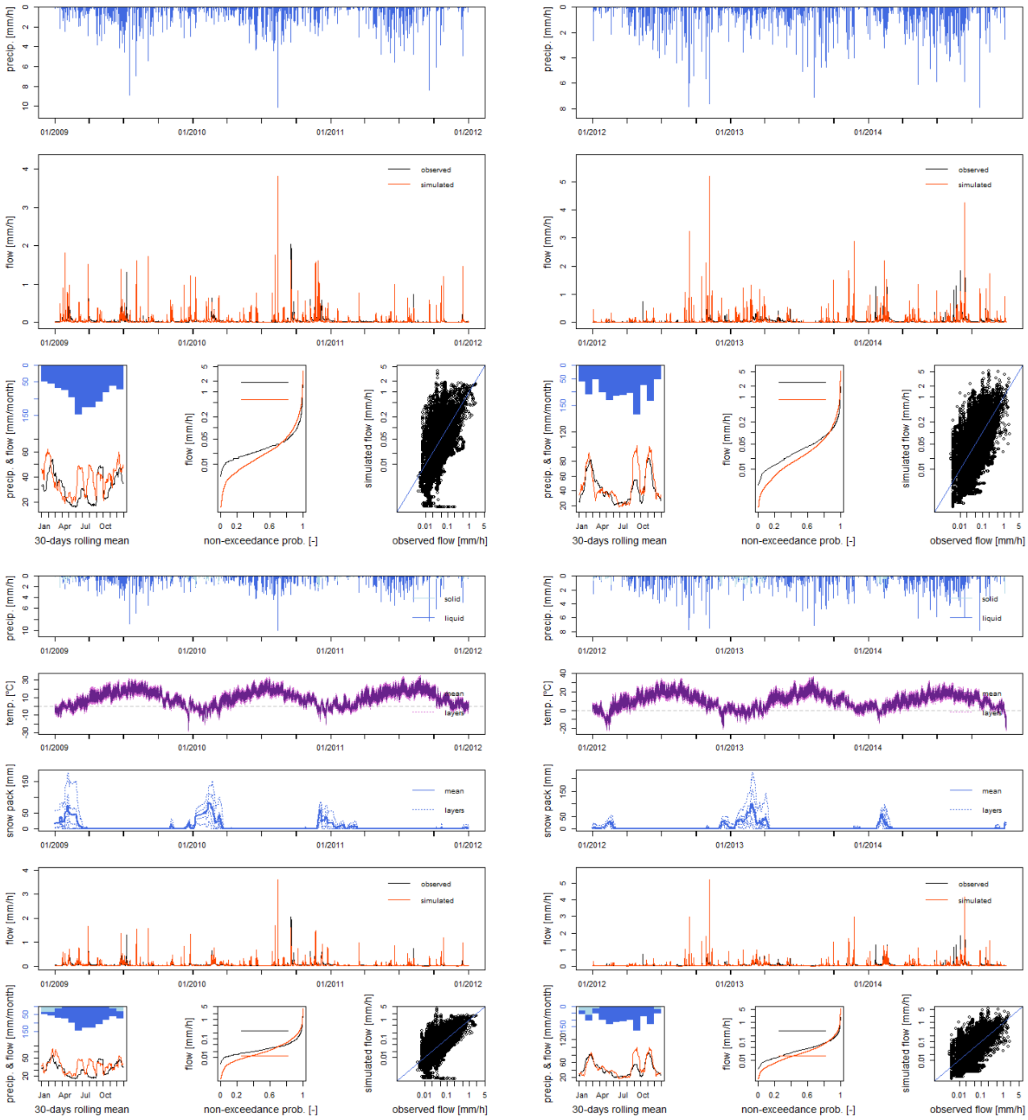

Figure 35: Exported results (conf. 1, GR4H (top)-GR4H CemaNeige (bottom), calibration (left) and validation (right) period) for the Hudinja watershed

APPENDIX B. WATERSHED DISCHARGES – ALL CONFIGURATIONS

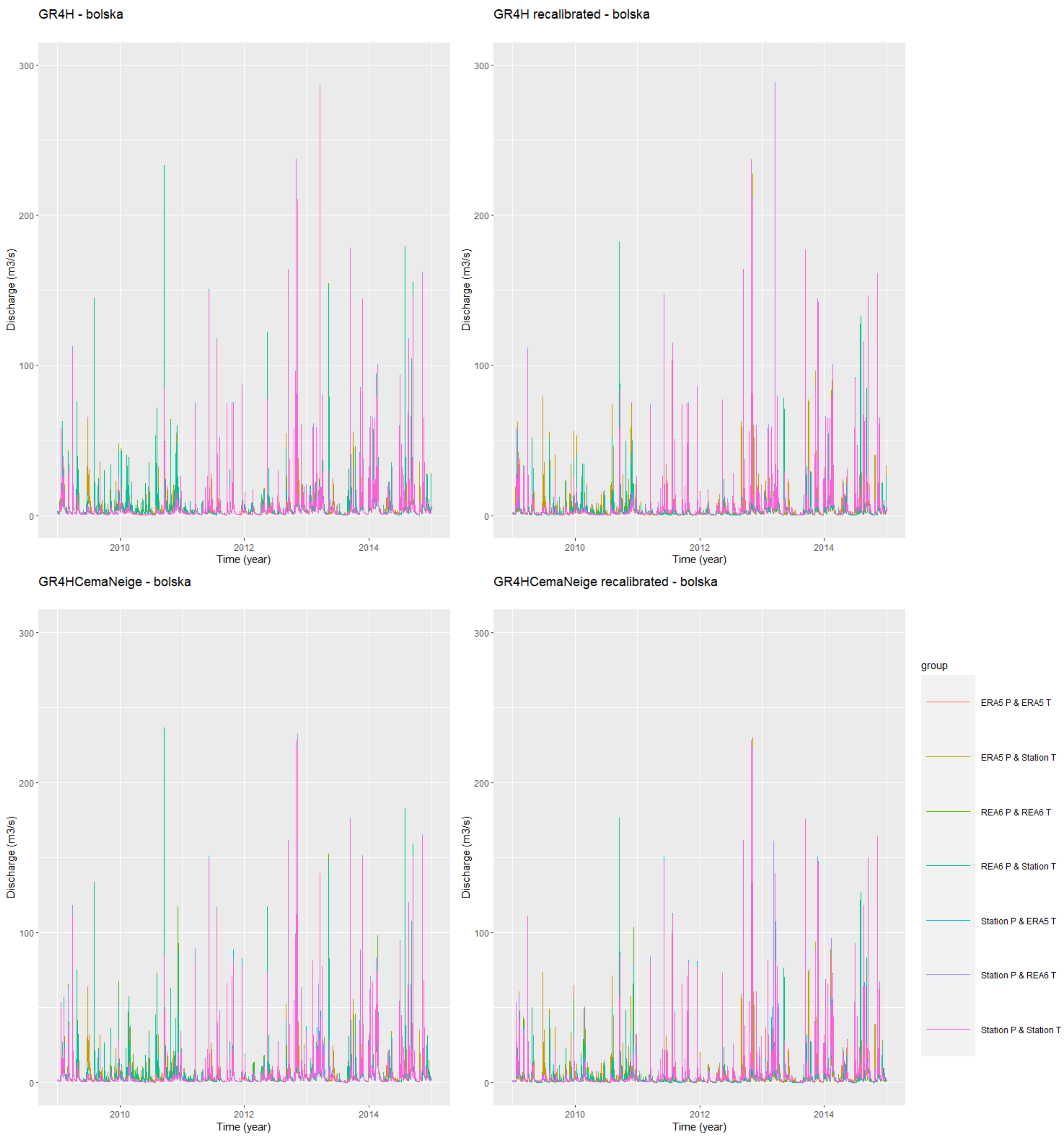

Figure 36: Discharge time series derived from the 7 data configurations - Bolska catchment

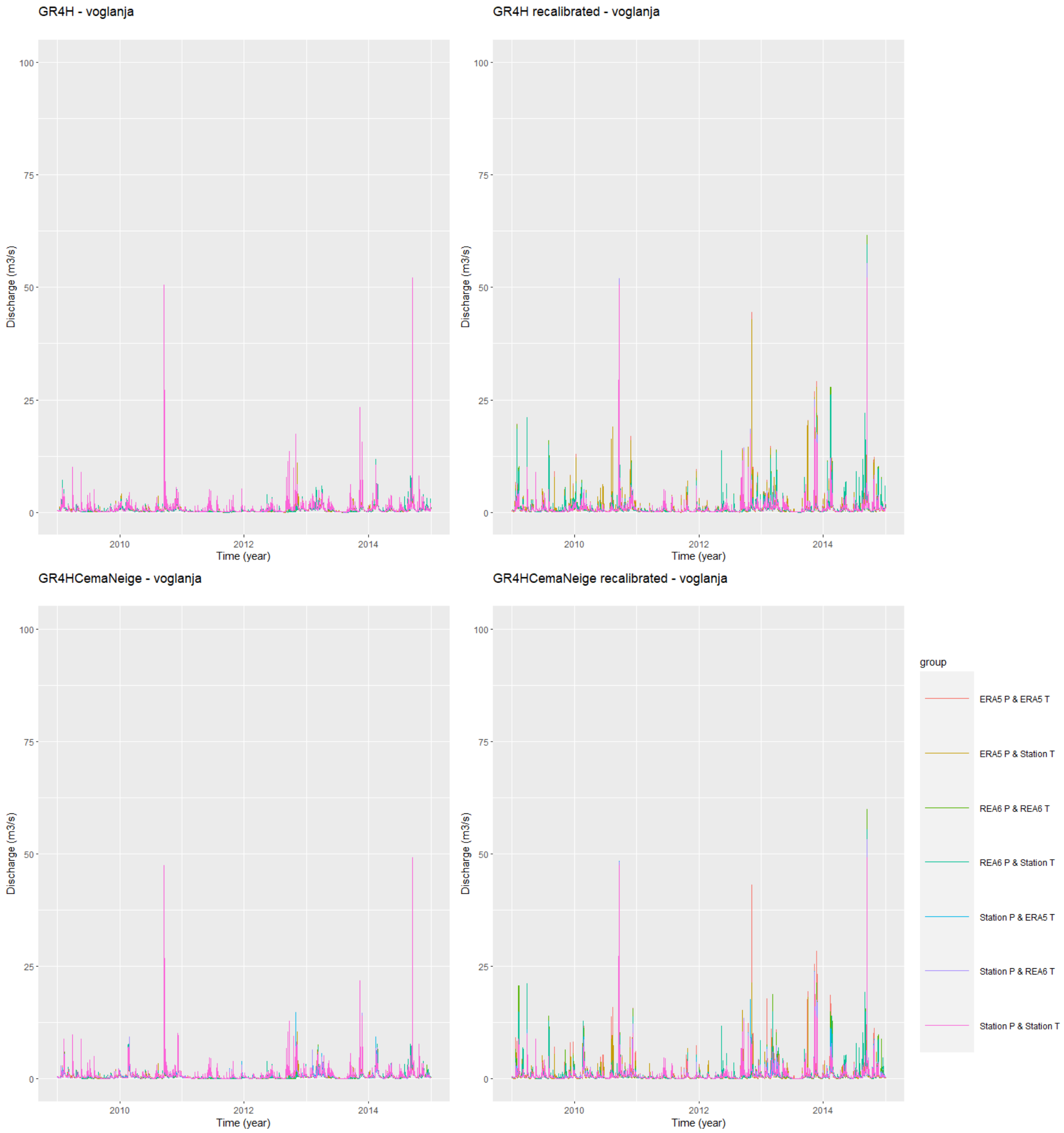

Figure 37: Discharge time series derived from the 7 data configurations - Voglanja catchment

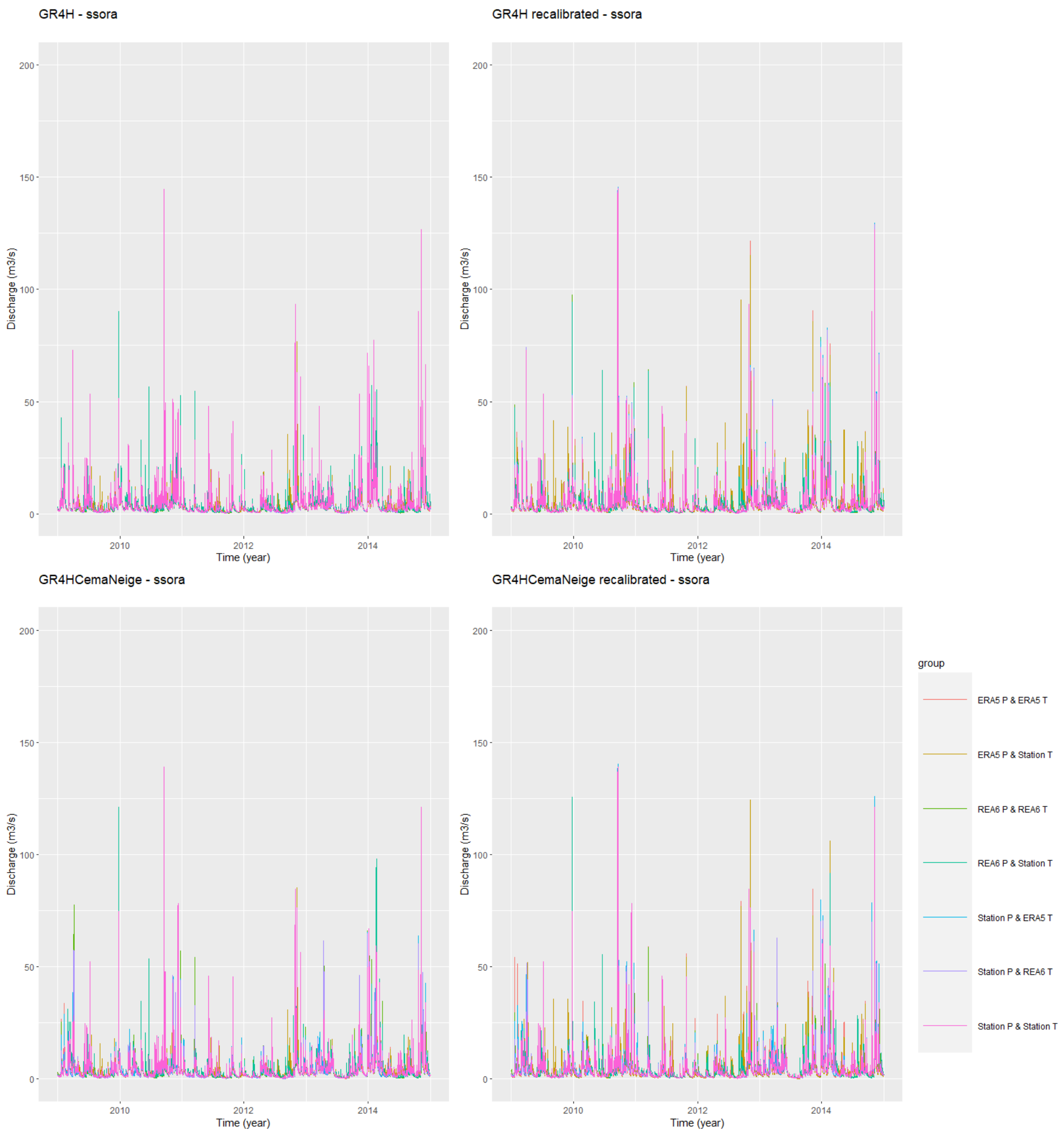

Figure 38: Discharge time series derived from the 7 data configurations - Selška Sora catchment

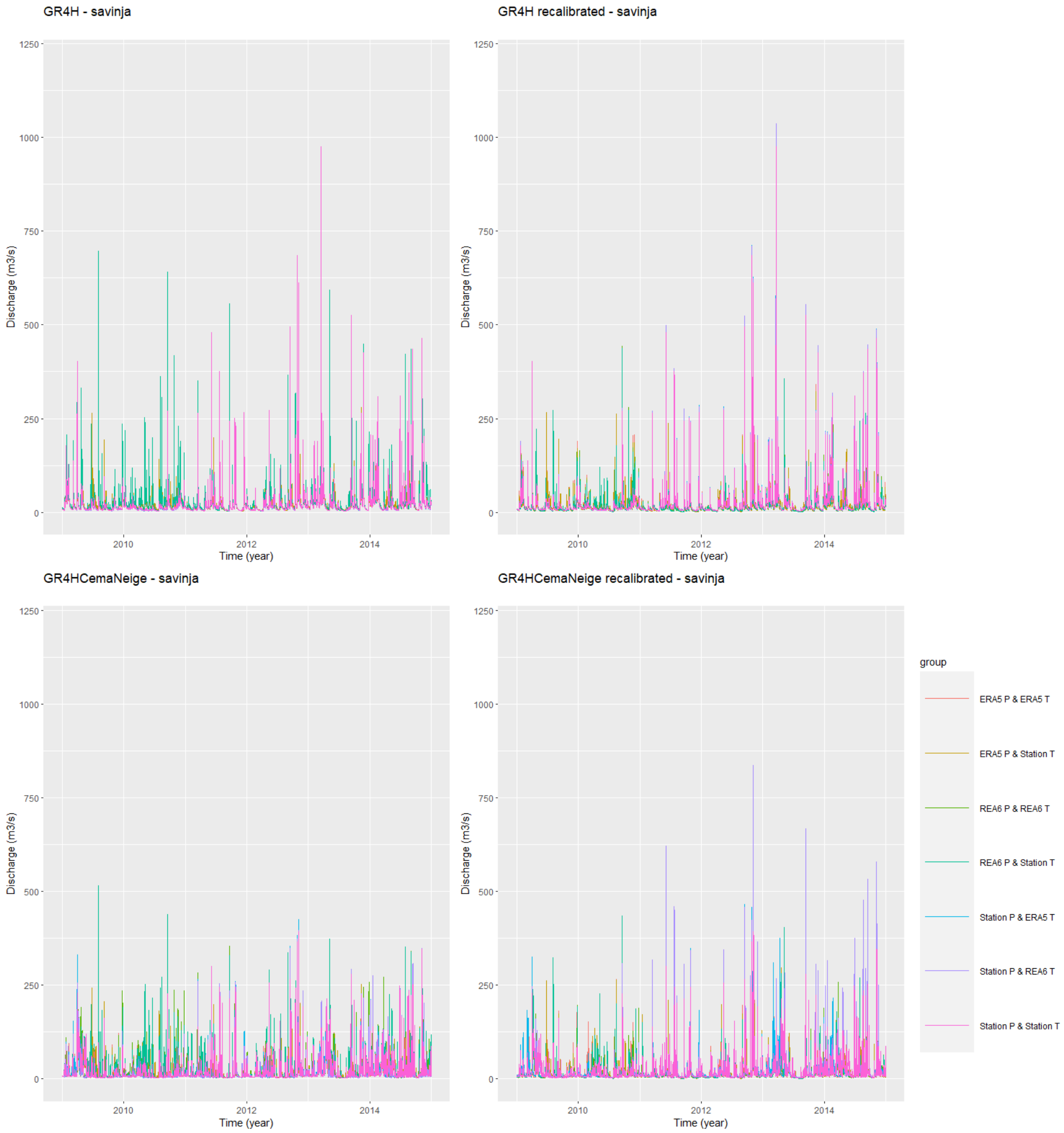

Figure 39: Discharge time series derived from the 7 data configurations - Savinja catchment

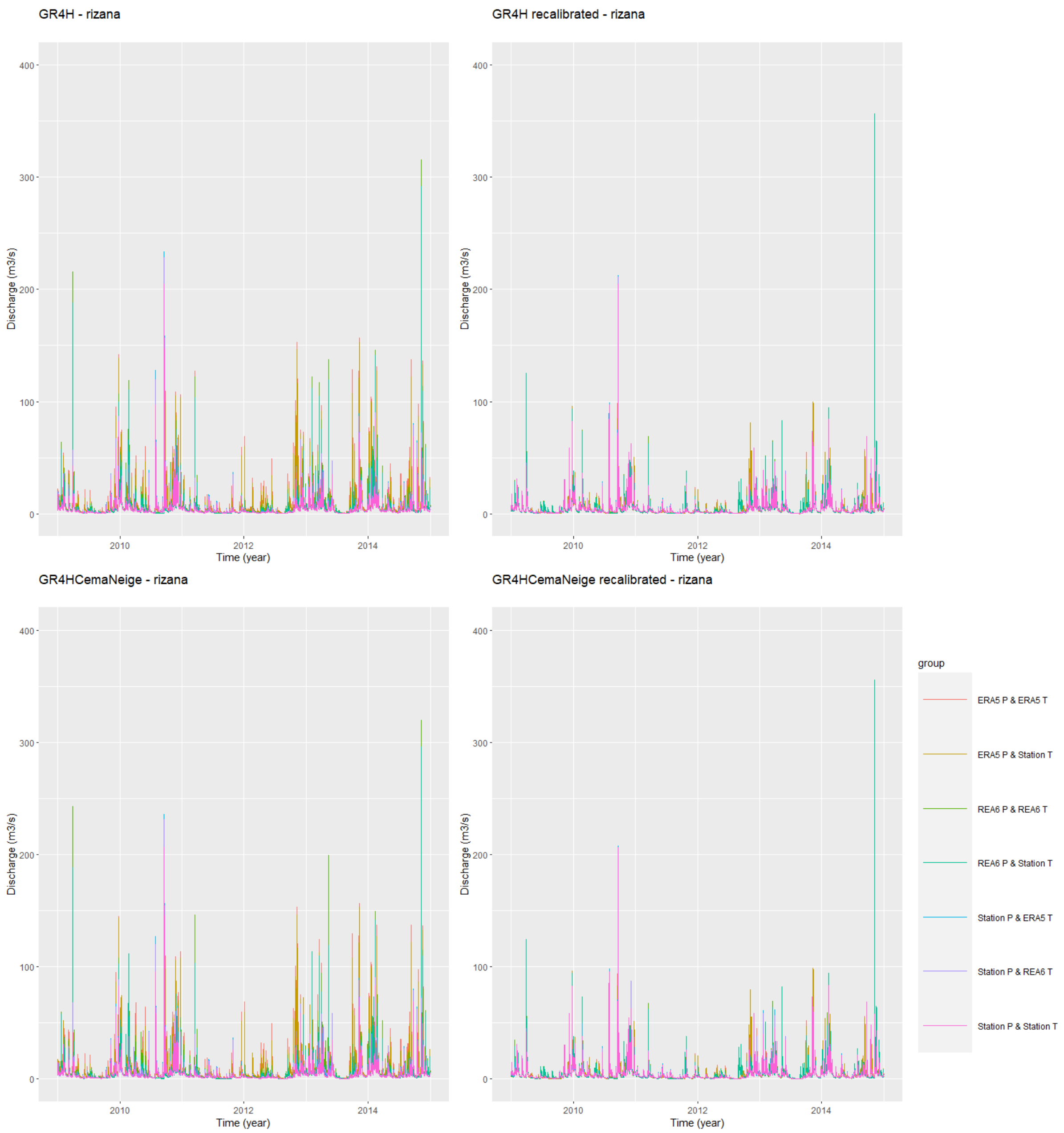

Figure 40: Discharge time series derived from the 7 data configurations - Rižana catchment

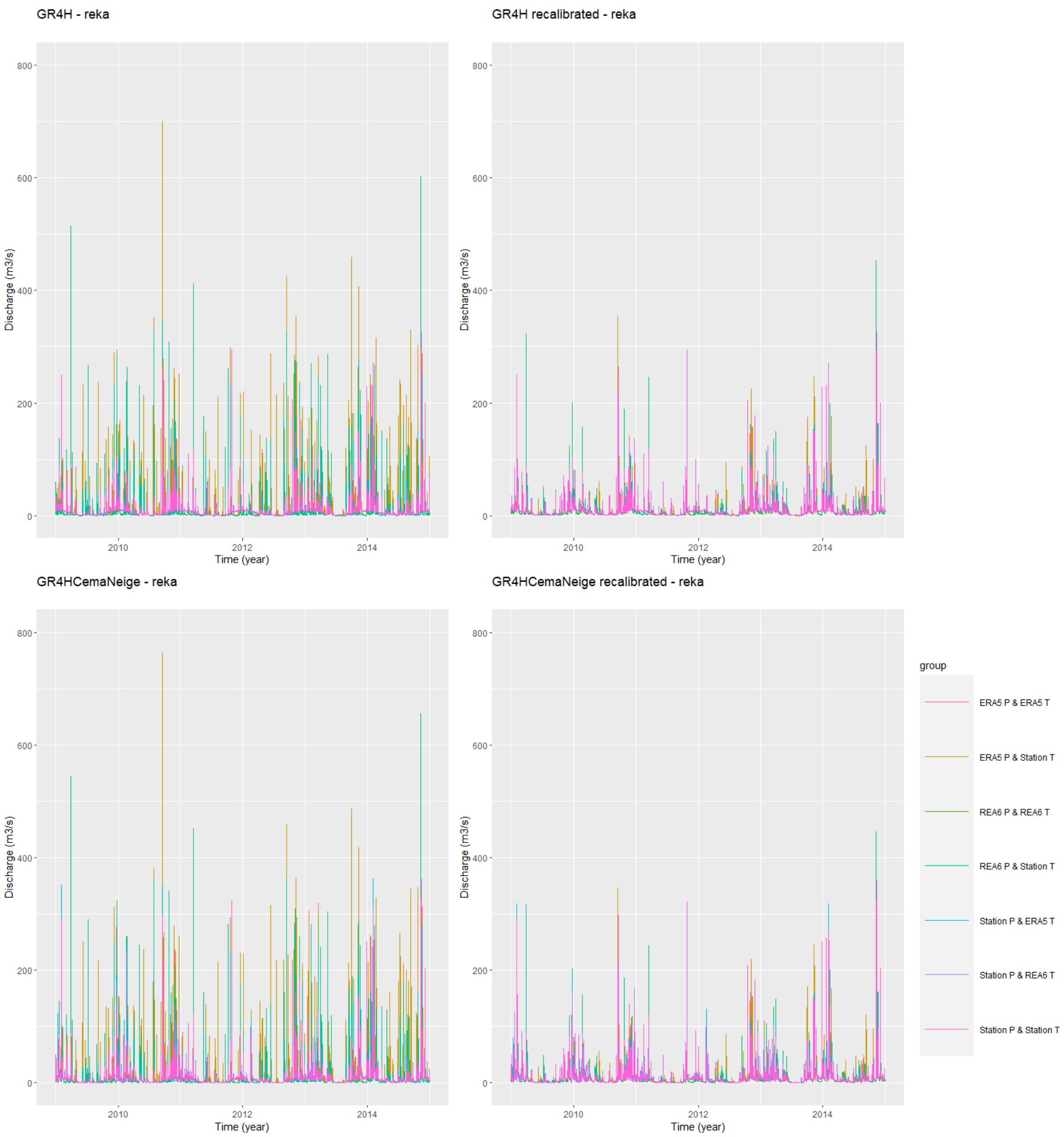

Figure 41: Discharge time series derived from the 7 data configurations - Reka catchment

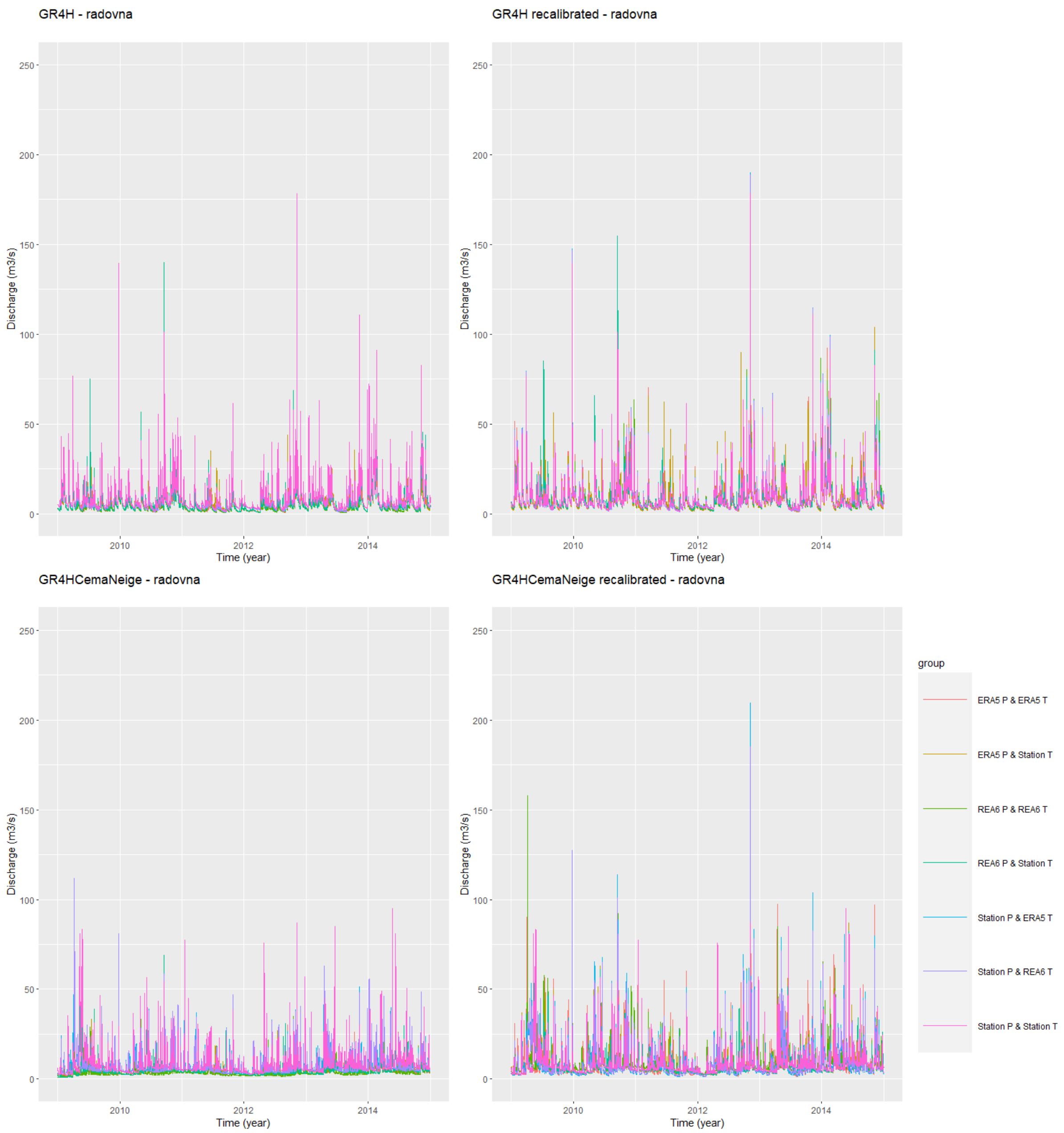

Figure 42: Discharge time series derived from the 7 data configurations - Radovna catchment

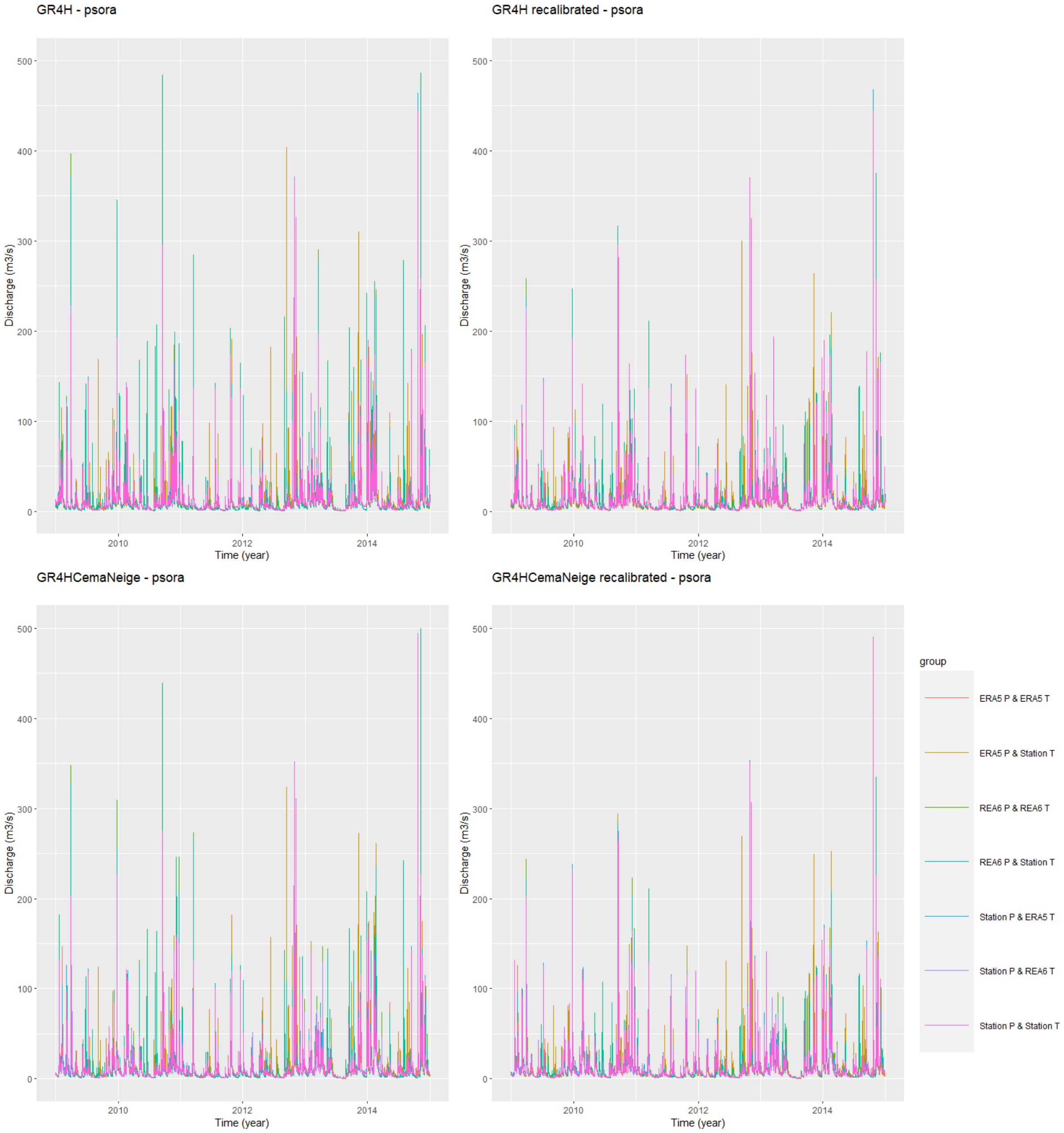

Figure 43: Discharge time series derived from the 7 data configurations – Poljanska Sora catchment

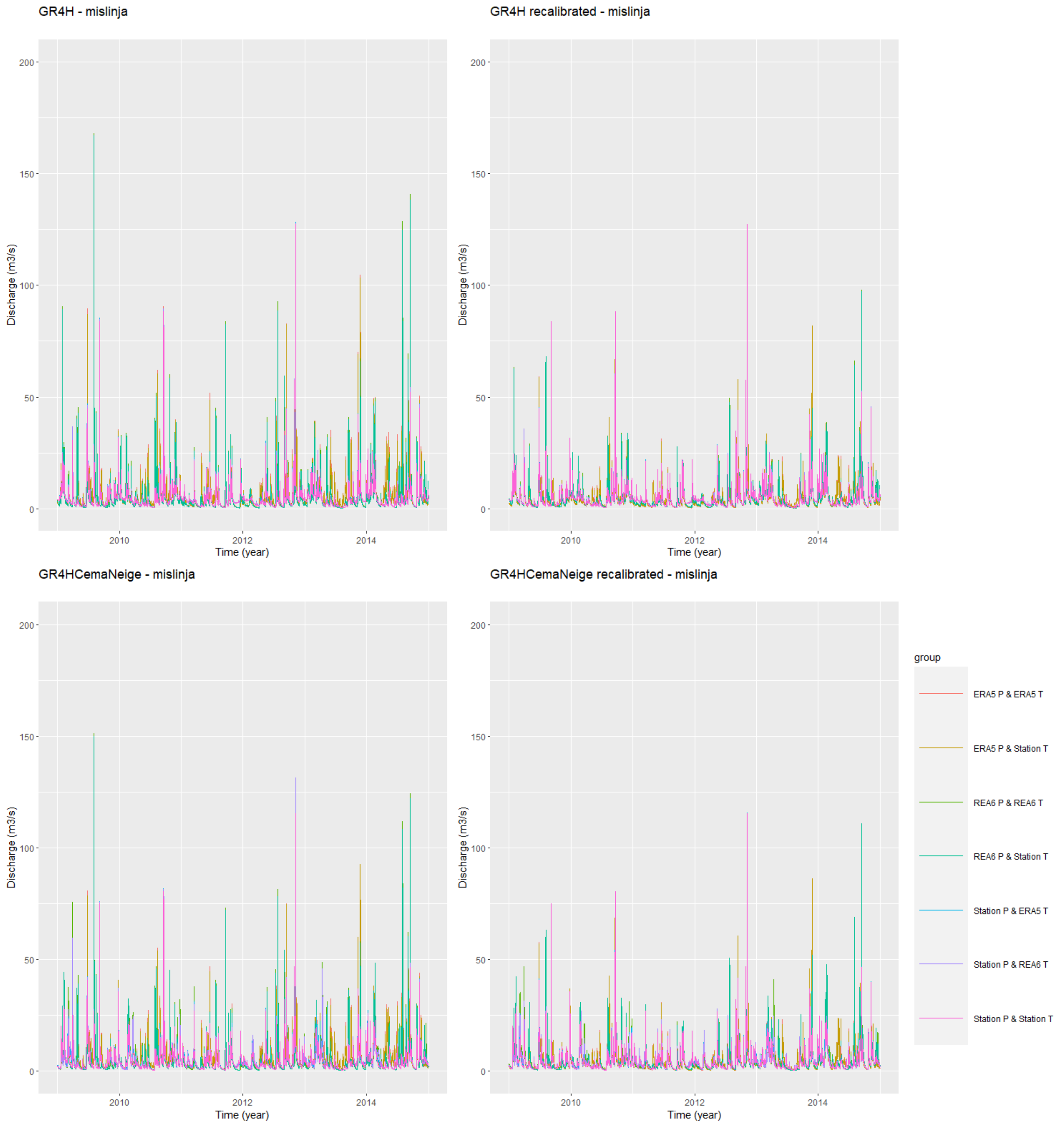

Figure 44: Discharge time series derived from the 7 data configurations - Mislinja catchment

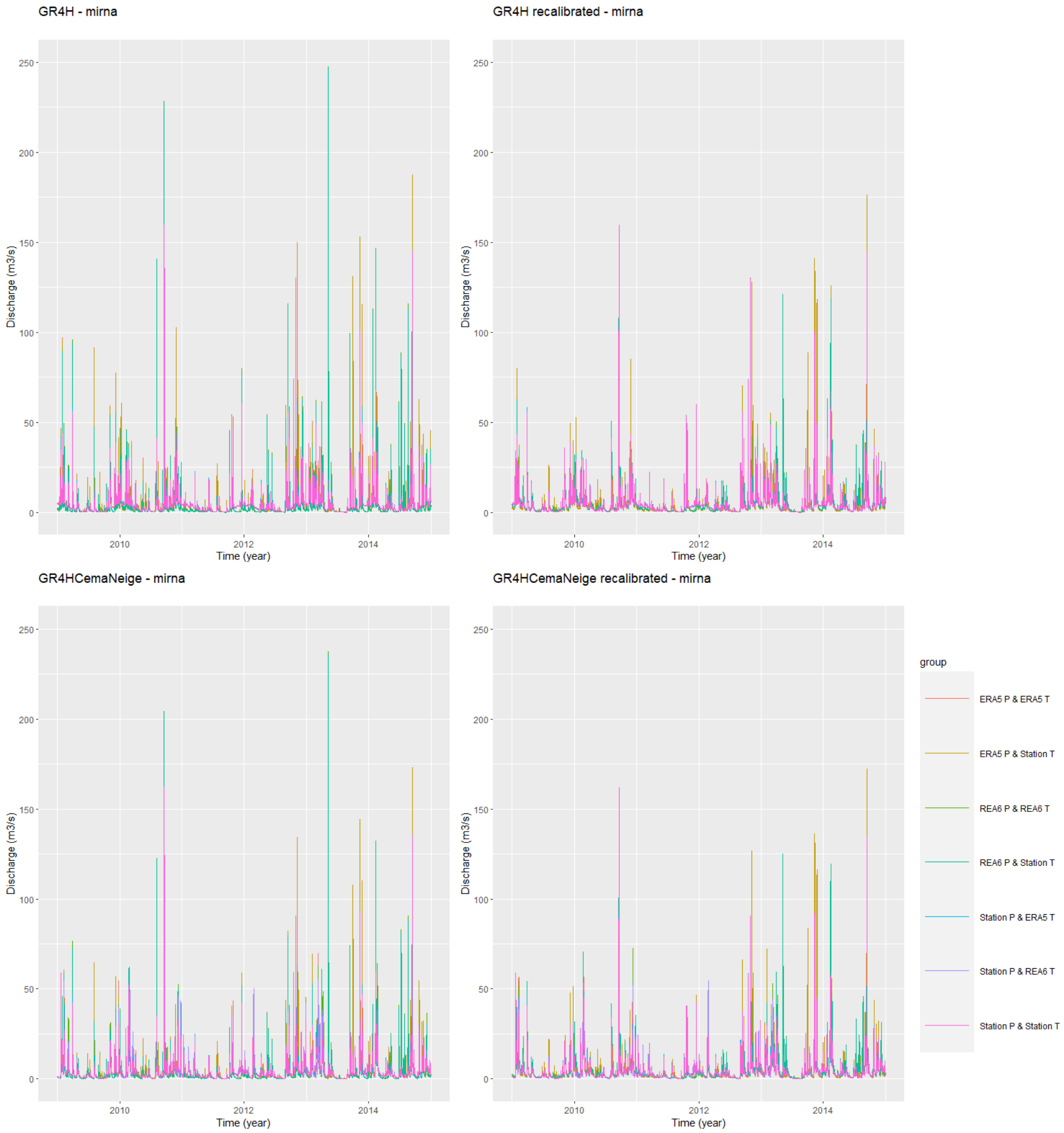

Figure 45: Discharge time series derived from the 7 data configurations - Mirna catchment

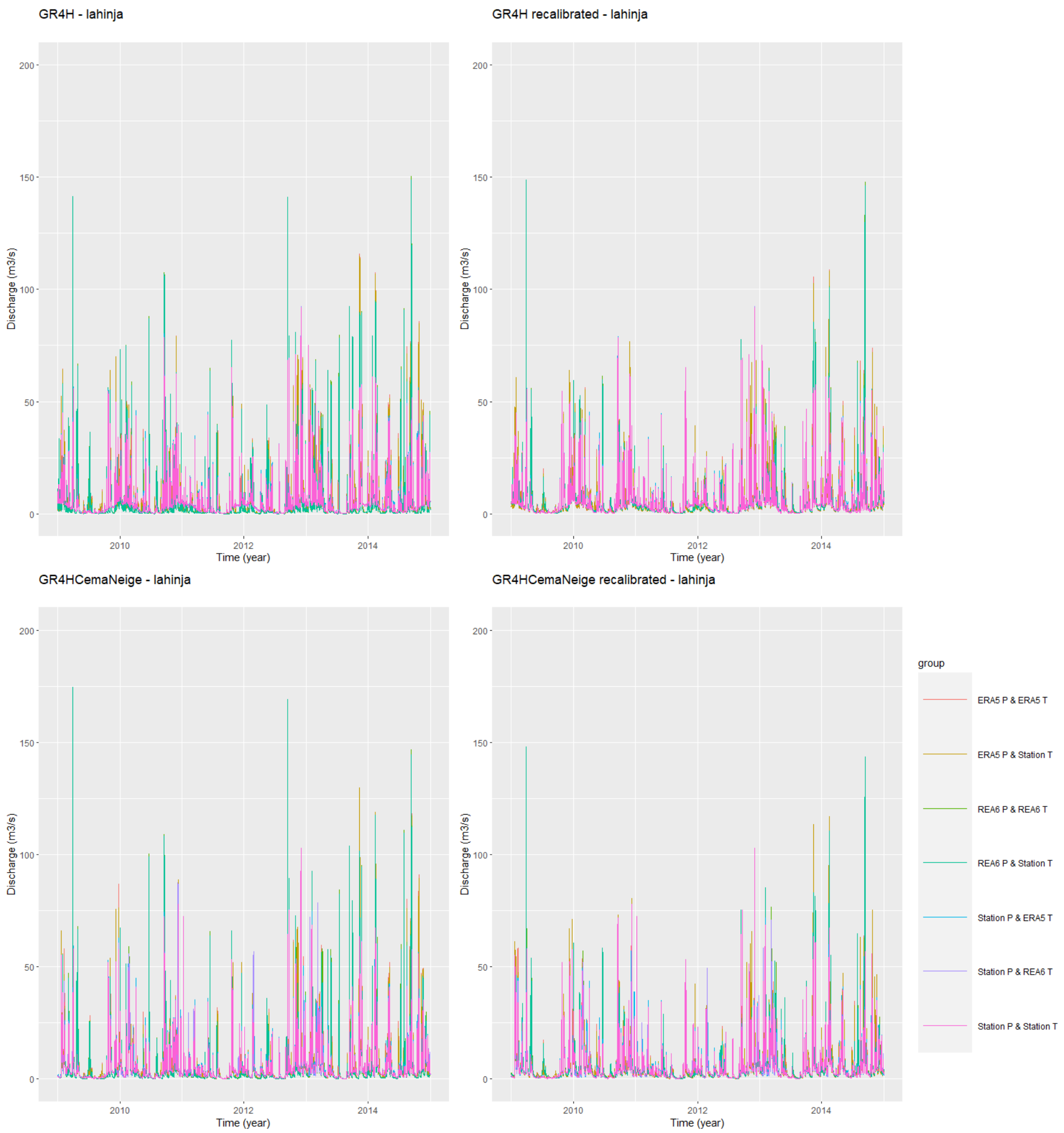

Figure 46: Discharge time series derived from the 7 data configurations - Lahinja catchment

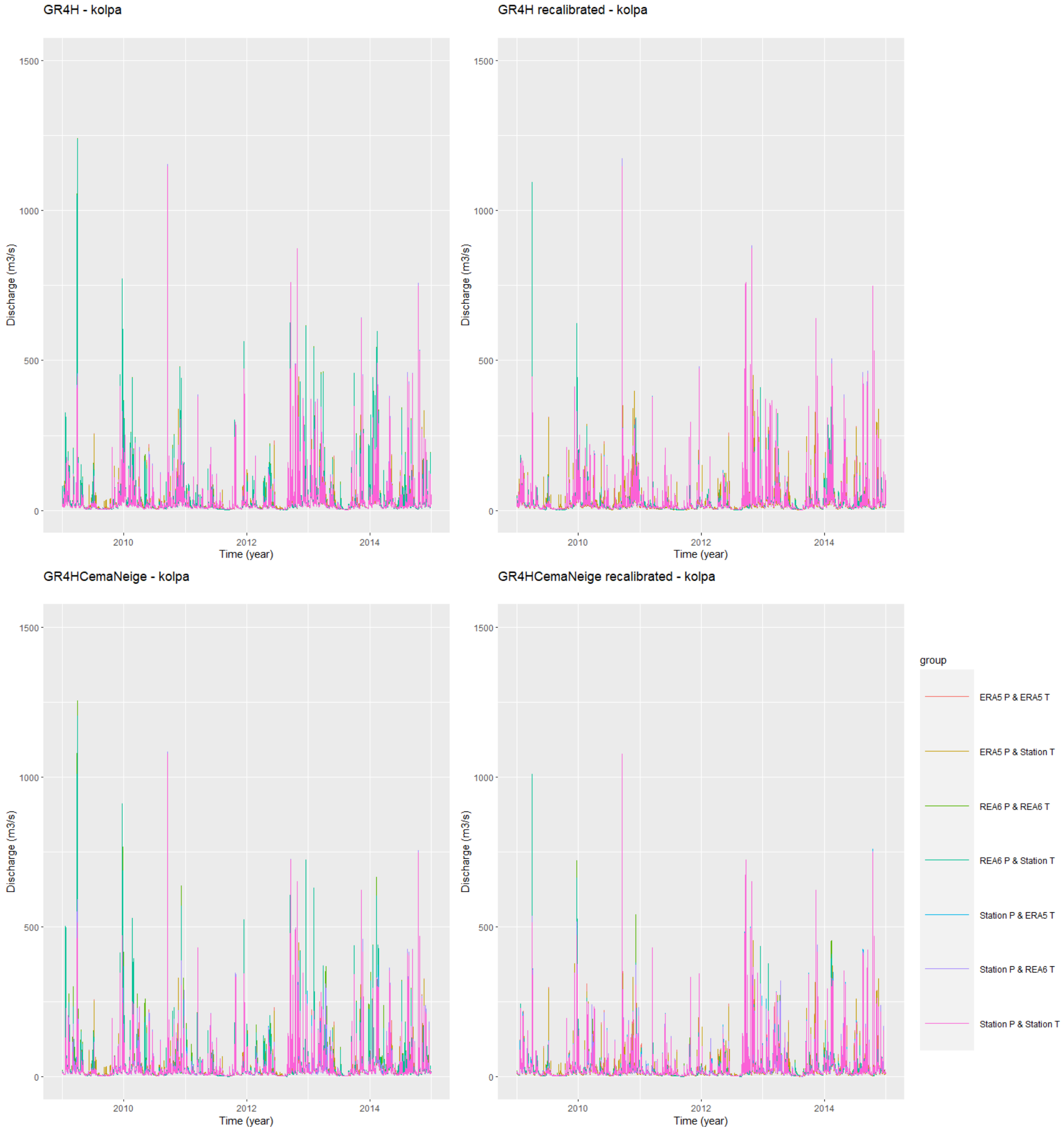

Figure 47: Discharge time series derived from the 7 data configurations - Kolpa catchment

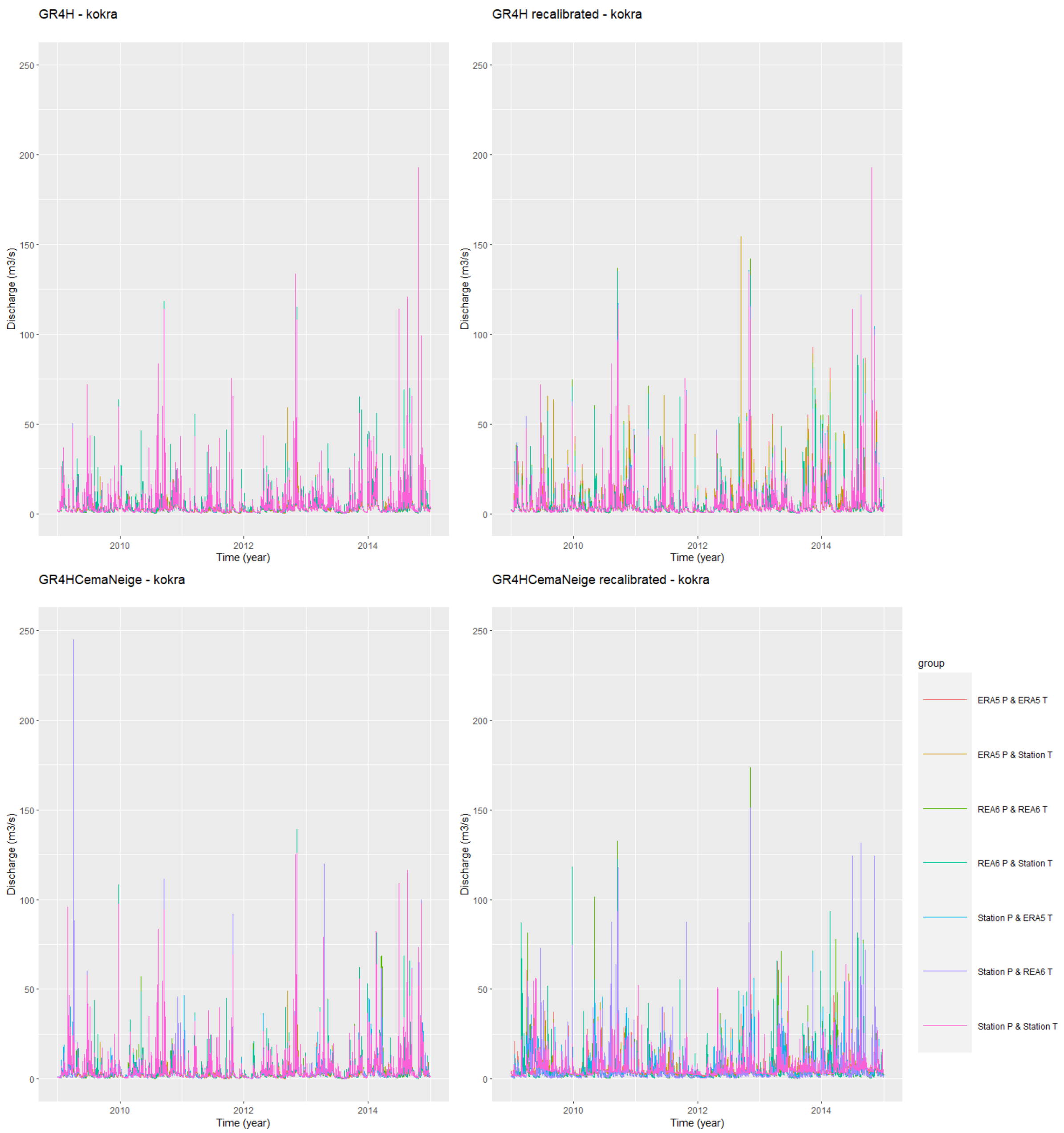

Figure 48: Discharge time series derived from the 7 data configurations - Kokra catchment

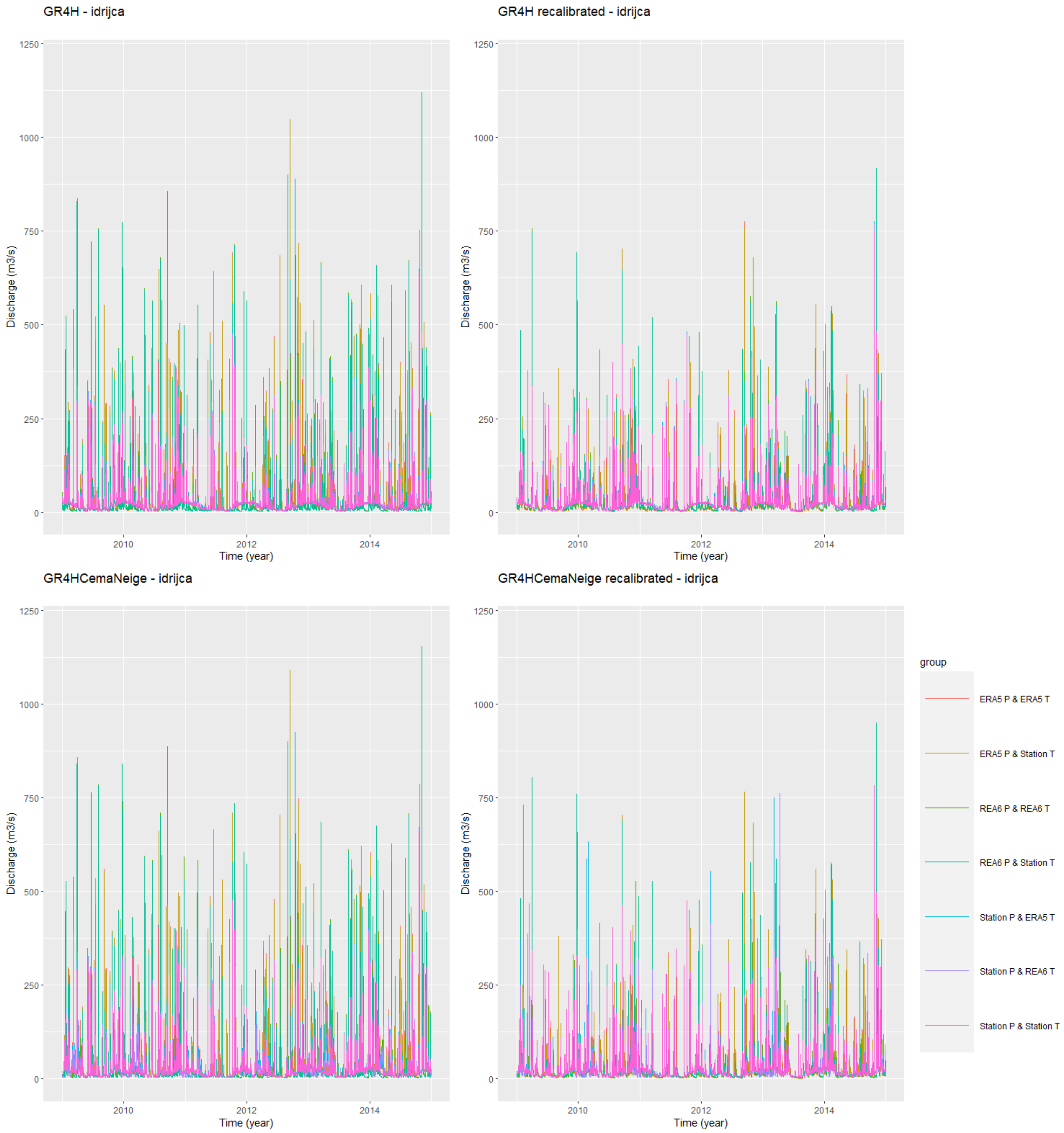

Figure 49: Discharge time series derived from the 7 data configurations - Idrijca catchment

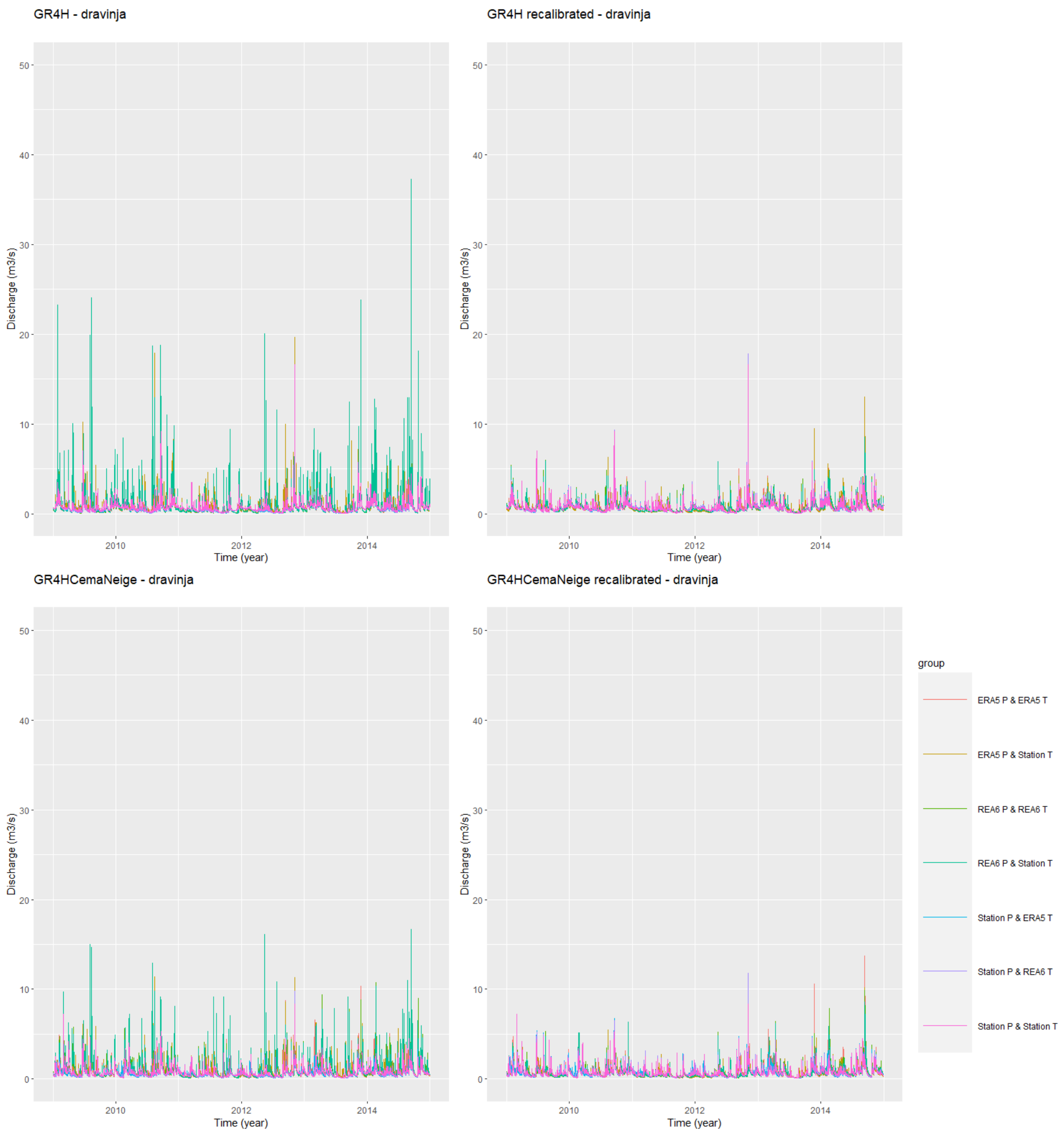

Figure 50: Discharge time series derived from the 7 data configurations - Dravinja catchment

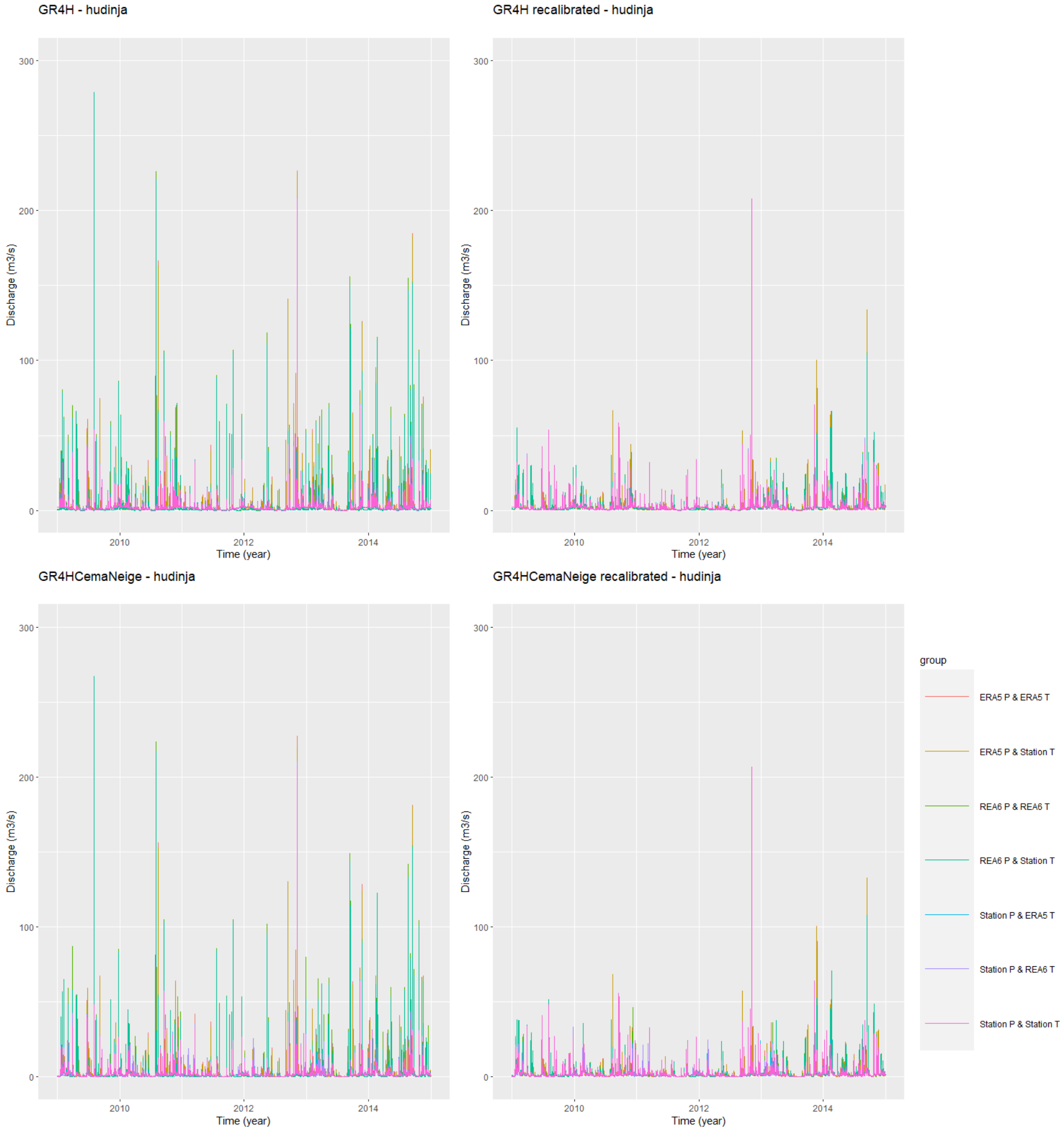

Figure 51: Discharge time series derived from the 7 data configurations - Hudinja catchment